Project:

AERO-UA

(Grant Agreement number 724034)

"Strategic and Targeted Support for Europe-Ukraine Collaboration in Aviation Research"

Funding Scheme: Coordination and Support Action
Call: H2020-MG-2016-2017
Date of the latest version of ANNEX I: 15/7/2016

D3.4 Final report on pilot projects in aerostructures

Project Coordinator (PC):	Mr. Giles BRANDON Tel: +352 26394233 Email: giles.brandon@intelligentsia-consultants.com
PC Organization Name:	Intelligentsia Consultants
Lead Partner for Deliverable:	TECPAR / ITWL
Deliverable Due Date:	30/9/2019
Deliverable Issue Date:	4/9/2019

Document History

(Revisions – Amendments)

Version and date	Changes
1.0 – 30/8/2019	First version
1.1 – 4/9/2019	Second version following review by consortium partners

Dissemination Level		
PU	Public	**X**
PP	Restricted to other program participants (including the EC Services)	
RE	Restricted to a group specified by the consortium (including the EC Services)	
CO	Confidential, only for members of the consortium (including the EC)	

The overall aim of the AERO-UA project is to stimulate aviation research collaboration between the EU and Ukraine through strategic and targeted support. AERO-UA is focused solely on Ukraine, because the country has a huge aerospace potential but a low level of aviation research collaboration with the EU. Ukraine's aerospace sector spans the full spectrum of systems and components development and production with OEMs, Tier 1 and 2 suppliers, aeroengine manufacturers, control systems manufacturers, R&D institutions, aeronautic universities, and SMEs. This is also reflected in the sector's important contributor to the country's economy (e.g. aircraft production of €1,9 billion in 2011).

Ukrainian aerospace organisations possess unique know-how that can help Europe address the challenges identified in the ACARE SRIA / Flightpath 2050 Report. Furthermore, following the signing of the Agreement for the Association of Ukraine to Horizon 2020 in March 2015, Ukrainian organisations are eligible to participate in Clean Sky 2 and H2020 Transport on the same funding terms as those from EU member states. Equally, genuine commercial opportunities exist for European aviation organisations to help modernise Ukraine's aerospace sector.

The AERO-UA project will achieve its overall aim via four high-level objectives:

1. Identifying the barriers to increased EU-UA aviation research collaboration;
2. Providing strategic support to EU-UA aviation research collaboration;
3. Supporting EU-UA aviation research knowledge transfer pilot projects; and
4. Organising awareness-raising and networking between EU-UA stakeholders.

The AERO-UA consortium is comprised of key EU and UA aviation organisations that will implement WPs closely mapped to the high-level objectives. The consortium will be supported by an Advisory Board involving Airbus, DLR, Min. Education and Science of Ukraine, Ukrainian State Air Traffic Services Enterprise and retired Director of EADS Jean-Pierre Barthélemy.

Table of Contents

1. Introduction

The task relating to the pilot projects between EU-UA partners in the field of aerostructures (Task 3.1) was part of WP3, “EU-UA aviation research knowledge transfer pilot projects” of the AERO-UA “Strategic and Targeted Support for Europe-Ukraine Collaboration in Aviation Research” project.

This work package provides targeted support for EU-UA collaboration in aviation research in the form of knowledge transfer pilot projects to be implemented by the AERO-UA partners. The pilot projects are structured around three key areas relevant to the challenges of ACARE SRIA / Flightpath 2050: **Aerostructures**, Aeroengines and Aerospace Manufacturing.

The task includes the organisation of short-term visits between the EU and UA partners, in order to exchange knowledge, receive training and/or conduct feasibility studies. Where possible, these visits are combined with project meetings and events.

Based on the results of the pilot projects, such as the feasibility studies prepared, it is expected the AERO-UA partners will continue to cooperate either by applying for larger scale research projects or preparing joint publications or presentations.

2. Pilot Project 3.1a: Advanced design of aerospace composite structures

According to the AERO-UA Grant Agreement (description of action), the main goal of this pilot project is to exchange knowledge and training between the EU and UA partners concerning:

- Advanced mechanics of composite materials and structures on micro- and macro-level
- Analytical design and FEM simulation approaches applicable for integral composite structures

UoM's relevant expertise includes FEM-based failure, fatigue and damage tolerance analysis of composite structures, and design of light weight multifunctional structures. Meanwhile, the UA partners – in particular KhAI and NASU - have experience of analytical-based optimization of composite structures strength, stiffness and buckling performances at early design stages, design of hybrid metal-to-composite joints using micro-fasteners concept and thin-wall airframe structures repair using CFRP composite patches of optimal geometry.

The knowledge exchange is expected to involve:

- Composite material and composite structure mechanics (micro- and macro-scale)
- Fast and accurate design and simulation methods applied for composites
- Failure, fatigue and damage tolerance analysis of composite structures
- Innovative experimental methods for micro-scale and macro-scale analysis
- Composite design for future components and structures
- Joining of composite structures (conventional mechanical joints, hybrid joints)
- Stress-strain state, failure initiation and propagation in joints
- FEM modelling of aerospace composite structures
- Virtual design of airframe structures for the entire life cycle

The training is expected to cover:

- Modelling of fatigue behaviour, damage initiation and crack propagations in composite structures
- Multi-scale modelling of composite materials and composite structures
- Design allowables and numerical modelling of airframe structures and joints
- Design of components, tools and facilities for efficient and economic production"

Project consortium members participating in Pilot Project 3.1a:

- **University of Manchester, Aerospace Research Institute (UoM)**
  - Structural design analysis and optimisation
- **National Aerospace University – Kharkiv Aviation Institute (KhAI)**
  - Multifunctionality (Mechanical and electrical behaviour) of composites
- **Public Joint Stock Company FED (FED)**
  - Multifunctionality (Mechanical and electrical behaviour) of composites
- **National Academy of Sciences of Ukraine, Frantsevich Institute for Problems of Material Science & Pisarenko Institute for Problems of Strength (NASU)**
  - Multifunctionality (Mechanical and electrical behaviour) of composites
- **Technology Partners Foundation (TECPAR) / Air Force Institute of Technology (ITWL)**
  - Test case and validation

Milestones achieved M1 – M18:

- Identification of test case
- Preliminary model
- Final selection of analysis types to be performed

- Multifunctional testing
- Modelling of electrical conductivity
- Full model analysis of the provided test case
- Optimisation leading to design changes
- Implementing SHM results for design changes

Milestones achieved M19 - M36:

- Disseminating the results

2.1 Background to the pilot project

A key purpose of Pilot Project 3.1a is to perform Finite Element (FE) design analysis of aerospace composite structures to accelerate product innovation. In this regard, carefully selected case studies were performed / conducted to analyse the design parameters at various (micro and macro) scales for multifunctional composites and improved airframe light weight structures which can be incorporated into pilot projects 3.1b and 3.3b.

Within the pilot project two topics are being investigated, both involving the use of Finite Element Method (FEM).

Topic 1: Polymers reinforced by complex fibre architectures for multifunctionality – electrical conductivity and strength ("PLATFORM")

One selected topic of the pilot project is to develop and validate strategies for Finite Element Model (FEM) simulation of Multifunctional Composites (MFCs). This topic investigated achieving multifunctionality in composite materials by designing complex fibre architectures (woven, weft-knitted, etc.) with novel combinations of reinforcement fibre materials and strategies for simulating the multifunctional composite. In multi-functionality, a combination of mechanical characteristics and electric and thermal conductivity was the main consideration. Combined microstructure and structural simulation were performed by KhAI on complex fibre architecture reinforced polymer composites, provided by NASU (Frantsevich Institute for Problems of Material Science), and tested by NASU (Pisarenko Institute for Problems of Strength).

Polymer composite materials based on carbon fabrics of various weaving schemes have found wide application in the aerospace industry. In terms of specific strength and stiffness, carbon composites are significantly superior to metals, but they have a significantly lower electrical conductivity, which must be taken into account in designing structural elements subjected to direct and indirect effects of lightning strike. At present, there are many ways to increase the electrical conductivity of composite materials and structures made of them, such as the use of carbon fibres with increased electrical conductivity, the introduction of conductive layers in the form of metal nets into the composite structure, modification of the matrix material using conductive nanoparticles, and others. The use of these methods makes it possible to create multifunctional composite materials possessing the necessary combination of mechanical and electrical characteristics.

Carbon fabrics with 3D knitting architecture have some advantages over traditional reinforcement materials, such as high manufacturability, high resistance to out-of-plane loading and also increased transversal electrical conductivity, which allow for effective dissipation and transfer of electrical charge caused by lightning strike. This type of reinforcement materials is more suitable for providing multifunctional properties of structure by selecting appropriate fabric architecture, filament type and modification of matrix material to increase their conductive properties.

The development of such materials requires the availability of reliable methods for determining their mechanical, thermal and electrical properties. At present, the determination of the electrical characteristics

of composites is based mainly on the use of experimental methods that provide reliable results but at the same time are not effective for choosing the optimum architecture of material when a large number of variants are required. Obviously, the availability of reliable simulation methods will allow for solving the problem of creating multifunctional composite materials more effectively.

Pilot project 3.1a is focused on the development of methods of design and producing of multifunctional composite materials based on the use of carbon fabrics with 3D architecture and conductive polymer matrix. The first stage of work concerned development of a reliable method for prediction of mechanical and electrical properties of composites with 3D reinforcement, enabling the selection of the knitting scheme with the optimal combination of material properties.

Pilot Project 3.1a has assumed the working name of 'PLATFORM' (Polymers reinforced by complex fibre architectures for multifunctionality).

Topic 2: Simulation informed by Structural Health Monitoring (SHM) acquired data ("SINDBAD")

This topic investigates designing composite structures, i.e. a UAV model by FEM simulation techniques that are enhanced by in-situ measured strain of data acquired through SHM technologies (principally continuous fibre optic strain measurement).

It has been decided that Pilot Project 3.1b [composites SHM] could be used as the case study for this topic and the SINDBAD topic will be incorporated in Pilot Project 3.1b.

2.2 Knowledge exchanged

The following is a list of significant meetings and visits that have progressed Pilot Project 3.1a (composites design):

- Kick-off meeting (11th & 12th October 2016), Hamburg
- Meeting between KhAI and UoM (10th December 2016), as part of British Council in Ukraine funded visit of KhAI to UoM, Manchester
- Teleconference (27th March 2017)
- AERO-UA Project Meeting and tour of Antonov (19th & 20th April 2017), Kyiv
- UoM representative visits to NASU institutes: Frantsevich Institute for Problems of Materials Science, Pisarenko Institute for Problems of Strength, Paton Electric Welding Institute (21st April 2017), Kyiv
- Teleconference (6th June 2017)
- Working meeting hosted at UoM (3rd & 4th July 2017), Manchester
- AERO-UA Project Meeting (29th May & 1st June 2018), Kharkiv
- "Composites in Action" workshop (18th – 25th November 2018), Manchester
- AERO-UA Project Meeting (24th – 26th April 2019), Zaporizhia
- AERO-UA Final Project Meeting (1st & 2nd September 2019), Athens

The majority of the effort under Pilot Project 3.1a [composites design] has been devoted to identifying specific skills and interests of each partner as well as a challenging project to come to a consensus between project partners as to a specific topic, scope of work, and work share which will yield sufficient research output to generate at least one journal publication and one conference attendance.

Topic 1: Polymers reinforced by complex fibre architectures for multifunctionality – electrical conductivity and strength ("PLATFORM")

Samples of two types of carbon fabric were produced by the Frantsevich Institute for Problems of Material Science at NASU and provided to KhAI for the manufacture of samples for mechanical testing and electrical measurements. Specimens for tensile tests in the weft direction and specimens for electrical conductivity measurement in both warp and weft directions were fabricated with the vacuum infusion method (Fig. 1).

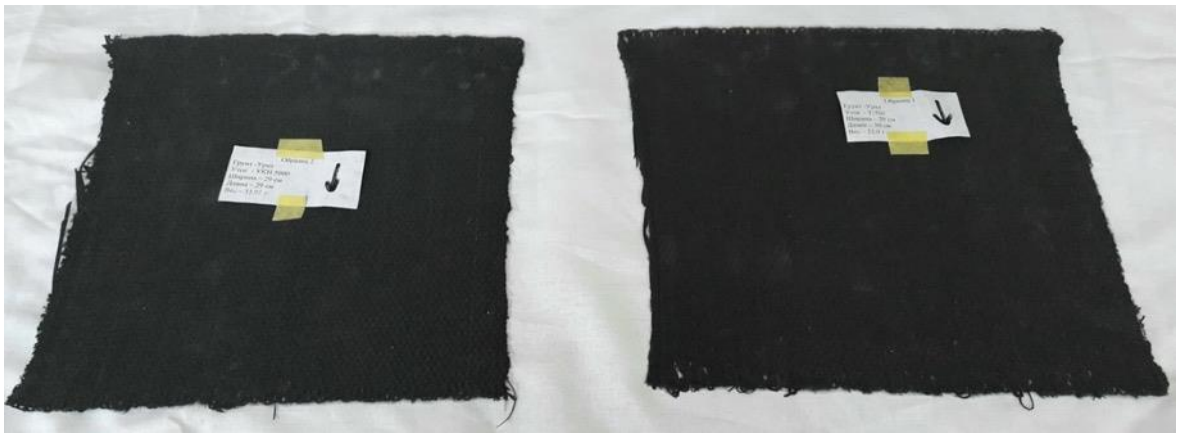

Figure 1. Produced plate made of carbon 3d-fabric

Pilot project 2: Simulation informed by Structural Health Monitoring (SHM) acquired data

UoM has received a model of airframe structure for investigation from TECPAR / ITWL and the model will be used for design analysis.

2.3 Training provided

The participants of the AERO-UA Pilot Projects 3.1a, 3.1b, and 3.3b working meeting on July 34 2017 at the University of Manchester or in Warsaw were:

No.	*Name*	*Organisation*
1	Prof Mojtaba Moatamedi	Aerospace Research Institute (UoM)
2	Dr Adam Joesbury	Aerospace Research Institute (UoM)
3	Dr Matthieu Gresil	i-Composites Lab (UoM)
4	Prof Prasad Potluri	Northwest Composites Centre (UoM)
5	Prof Constantinos Soutis	Aerospace Research Institute (UoM)
6	Dr Lina Smovziuk	National Aerospace University (KhAI)
7	Dr Fedir Gagauz	National Aerospace University (KhAI)
8	Dr Valeriy Fadeyev	Public Joint Stock Company (FED)
9	Dr Krzysztof Dragan	Technology Partners Foundation (TECPAR) / Air Force Institute of Technology (ITWL)
10	Dr Michal Dziendzikowski	Technology Partners Foundation (TECPAR) / Air Force Institute of Technology (ITWL)
11	Dr Iryna Bilan *(via Skype)*	Frantsevich Institute for Problems of Material Science (NASU)

2.4 Scientific results

Topic 1: Polymers reinforced by complex fibre architectures for multifunctionality – electrical conductivity and strength ("PLATFORM")

For simulation of mechanical and electrical behaviour of 3D reinforced plastics a CAD-model of fabric was built using passport data about knitting scheme (see Fig. 2). Filaments of "background" and weft were modelled as solid bodies with average cross-section size.

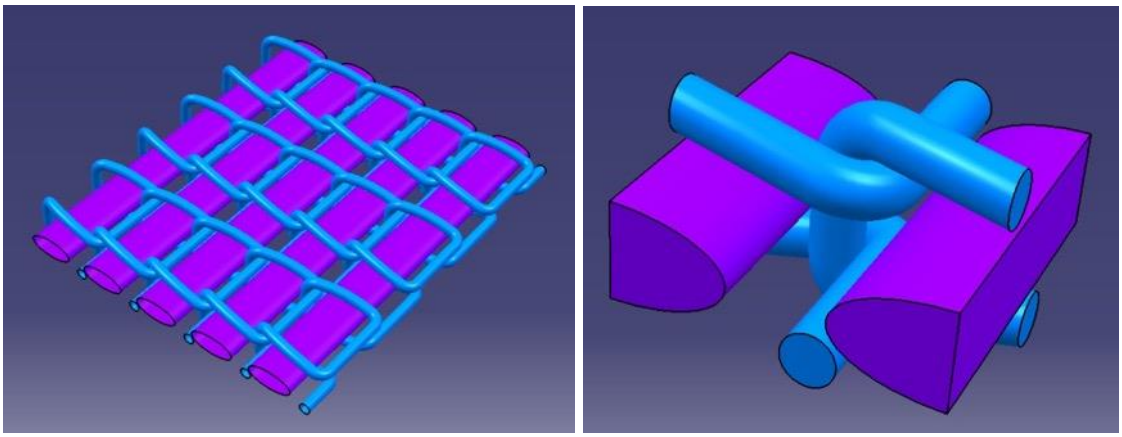

(a) (b)

Figure 2. CAD model of 3d-fabric (a) and representative element (b)

For further simulation of mechanical and electrical behaviour of 3D reinforced composites it was necessary to take into account deformation of fabric during processing that causes a change of material thickness from about 1,53 to 0,98 mm. In order to solve this problem, the process of deformation of the fabric under vacuum pressure was simulated using FEM (Fig.3). The filaments of the fabric were modelled as elastic bodies with transverse and shear moduli of elasticity tending to zero. After simulation deformed mesh was imported in CAD system to create CAD-models of deformed materials.

The obtained CAD-models of 3D reinforced plastic representative elements were used for simulation of the material's mechanical properties and electrical conductivity using unit-cell approach with FEM in Abaqus system.

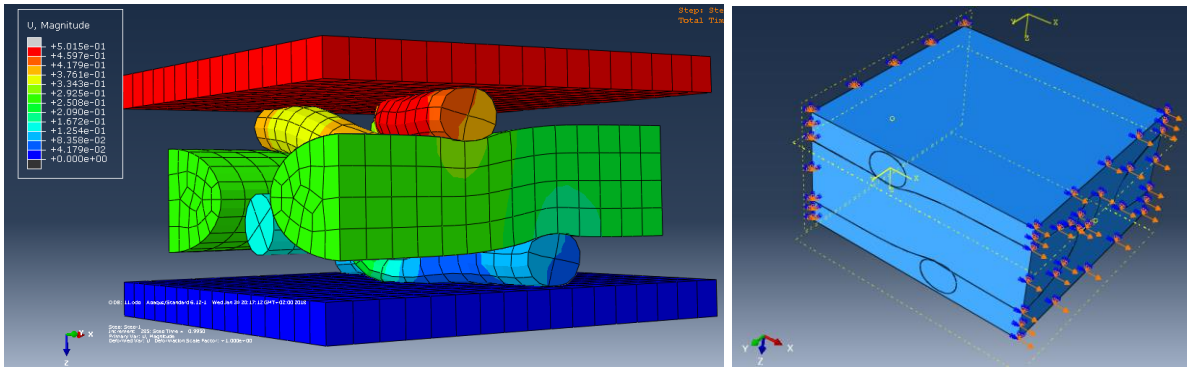

(a) (b)

Figure 3. Simulation of 3D fabric deformation under vacuum pressure (a) and resulting CAD-model for simulation (b)

For determination of filaments mechanical and electrical properties in all directions with account of local fibre volume fraction, known relations of micromechanics of composite materials and percolation theory were used. As a result numerical values of elasticity moduli and failure stresses in warp and weft directions, Poisson ratios, and also electrical resistivity of 3D reinforced plastics were obtained.

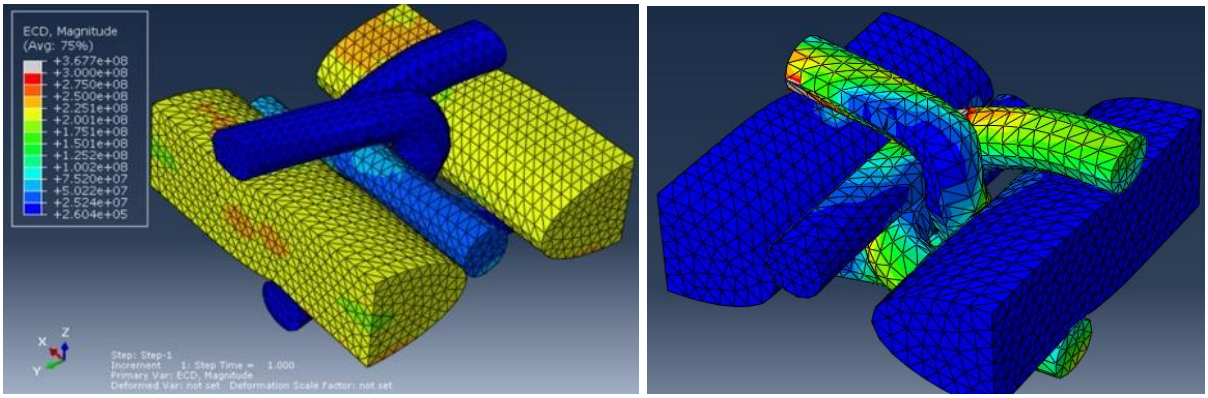

Figure 4. Electric current density in weft and warp direction of 3D fabric cell

Mechanical tensile tests were performed using a universal tensile machine. A video extensometer system Mercury-RT was used for determination of specimens strains during loading (Fig. 5). As a result of testing elasticity moduli and failure stresses of materials made of two types of 3D fabrics were obtained.

Figure 5. Mechanical testing of specimens

Electrical resistivity of materials was measured with an RLC-meter under current frequency 1 kHz. Ends of specimens were clamped between brass bushes to achieve better electrical contact (Fig. 6). Electrical resistivity of materials made of two types of 3D fabrics was obtained during the experiment.

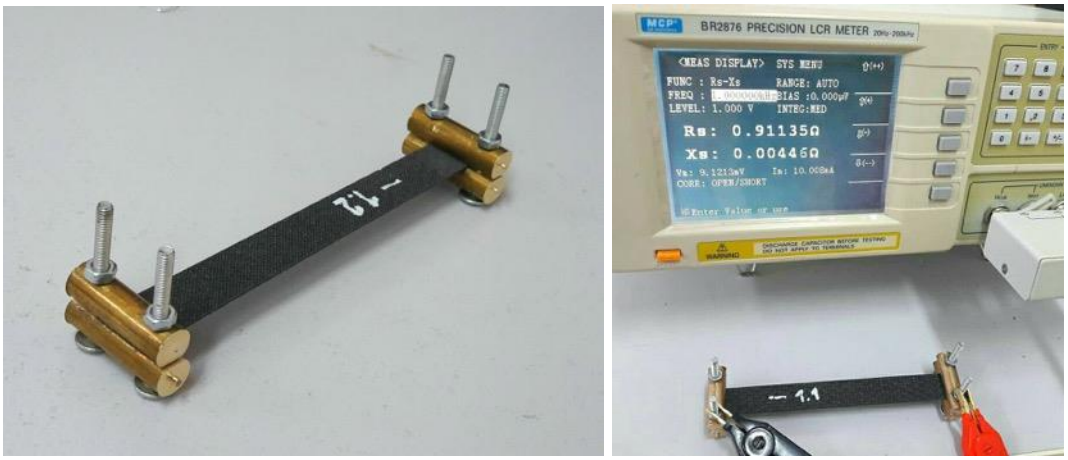

Figure 6. Electrical resistivity measurement

During analysis of the obtained results, the reliability of the proposed method for predicting the properties of materials reinforced with 3D fabrics was evaluated. The mechanism of material failure was analysed and this analysis forms the basis of the recommendations for modifying the fabric parameters to increase the strength of the material given.

Topic 2: Simulation informed by Structural Health Monitoring (SHM) acquired data ("SINDBAD")

The airframe structure model provided by TECPAR / ITWL could not be utilised in this project due to compatibility issues. For this reason, efforts on this pilot project were focused on Topic 1.

2.5 State-of-the-art comparison

UoM's relevant expertise includes FEM-based failure, fatigue and damage tolerance analysis of composite structures, and design of light weight multifunctional structures. Meanwhile, the UA partners – in particular KhAI and NASU - have experience of analytical-based optimization of composite structures strength, stiffness and buckling performances at early design stages, design of hybrid metal-to-composite joints using micro-fasteners concept and thin-wall airframe structures repair using CFRP composite patches of optimal geometry.

A SWOT analysis was completed for this pilot project, to identify the internal strengths and weaknesses in relation to simulation and manufacture of multifunctional composite materials, and to assess potential external opportunities and threats. These are detailed below:

Internal **S**trengths:

- Experts on FE simulation and experimental measurement of multifunctionality in composites, such as electrical/thermal conductivity, are available in both EU and UA
- Experimental facilities are available in UA for assessment of multifunctionality introduced in composite materials
- Advanced modelling techniques have been developed at UoM for design and assessment of lightweight multifunctional composite structures

Internal **W**eaknesses:

- UoM and UA do not have a proven track record in the simulation of advanced scenarios related to multifunctional materials
- Internal collaboration is not currently taking place
- Compatibility of computational tools is a limitation to internal and external collaboration on research projects focused on advanced simulation

External **O**pportunities:

- UA capability puts them in a good position to collaborate with EU and worldwide
- Potential to build a taskforce/workforce for advanced design and simulation of multifunctional composites
- Potential for collaboration and support from UA on design processes in future aerospace

External **T**hreats:

- Lack of government or private funds in UA for development of design processes
- No interest in industry-academic collaboration
- Data sharing within some sectors (e.g. defence, military) on advanced design processes can be problematic due to security factors

2.6 Dissemination

This work has been disseminated within the consortium and at the “Composites at Action” workshop that took place in Manchester in November 2018.

3. Pilot Project 3.1b: Aerospace composite structural health monitoring system

According to the AERO-UA Grant Agreement (description of action), the main goal of this pilot project was to conduct a feasibility study of an aerospace composite structural health monitoring system using a network of embedded sensors – developed by TECPAR / ITWL – for application in Ukrainian aircraft. The project examined issues such as: composite structure manufacturing, determination of failure mode detection and optimisation of technology for embedding sensors in the composite material structure at TRL 5 and higher.

Embedding sensors in a composite structure can increase the reliability of its operation. However, it may adversely affect the structural properties of the composite. The project addressed these issues by developing manufacturing technology guidelines for smart composite structures with self-diagnostic capabilities. Furthermore, the feasibility of preparing a technology demonstrator, e.g. a Ukrainian aerospace composite structure containing an embedded sensor network for structural health monitoring, was considered.

Project consortium members participating in pilot project 3.1b:

- **Technology Partners Foundation (TECPAR) / Air Force Institute of Technology (ITWL)**
  - Coordination, development of the PZT guided waves, passive SHM system development
- **University of Manchester, Aerospace Research Institute (UoM)**
  - SHM of composites monitoring based on FBG sensors
- **National Aerospace University – Kharkiv Aviation Institute (KhAI)**
  - FOS and Sensors integration with composite structure
- **National Academy of Sciences of Ukraine, Paton Electric Welding Institute PEWI (NASU-PEWI)**
  - Acoustic Emission for damage detection, active system development

Milestones achieved until M18:

- Definition of the project participants' list.
- Formulation and agreement between the contributing partners of the tasks to be performed within the feasibility study.
- Partners' agreement to prepare the State of the Art portion of the feasibility study in selected areas.
- Preparation of partners' input for the project meeting held in Kiev (April 19-20, 2017).
- Preparation of involved partners' input for a working meeting of Task 3.1 pilot projects, which was held at the University of Manchester (July 3-4, 2017); during the meeting objectives for the SHM study for composites structures were defined (facility tour included a short presentation of the SHM capabilities).
- Preparation and delivery of the State of the Art.
- Contribution of the Merging Partners to the State of the Art description, discussion and agreement on the final version of the document.
- Preparation of the partners' input for the project meeting held in Kharkiv (May 30 – June 1, 2018).

Milestones achieved in the period M19 - M36:

- Discussion on the common case study to be followed by the involved Partners (TECPAR/ITWL, PEWI, KhAI, UoM) – M19-M20.
- Preparation for the workshop "Composites in Action" – M19-M25 (UoM).

- Preparation of specimens for the pilot study (KhAI) – M20-M23):
  - a set of specimens with and without embedded PZT sensors for shear tests;
  - a set of specimens with and without embedded PZT sensors for bending tests;
  - a set of specimens with embedded PZT sensors for SHM capabilities study (TECPAR and UoM);
  - a set of specimens for acoustic emission tests (PEWI).
- Conduction of acoustic emission tests on first set of specimens (PEWI) – M22-M26;
- Conduction of shear tests of specimens with and without embedded PZT sensors (KhAI) – M22-M26;
- Collection of data from the embedded PZT specimens during tests with introduction of artificial damage (TECPAR) – M24-M25.
- Organization and participation in the “Composites in Action” workshop – M26 (UoM);
- Experiments on the specimens by UoM/TECPAR/ITWL using guided waves – M29-M34.
- Experiments on the specimens by PEWI using acoustic emission method – M29 – M34.
- Preparation by Partners of input for the project meeting (M29-M30) held in Zaporizhia (April 24 – April 26, 2019).
- Bending tests of specimens with and without embedded PZT sensors by UoM – M29 – M32.
- Numerical simulations of structure behaviour with embedded PZT sensors by KhAI - M29 – M34 (KhAI).
- Preparation of the summary of the results and feasibility study report – M33-M36 (all of the Partners).
- Draft of the paper preparation containing results of the pilot project – M33-M36 (all of the Partners).
- Preparation of presentations for 9th International EASN conference, September 3 – 6, 2019, Athens – M33-M36 (all of the Partners).
- Preparation by Partners of input for the final project meeting (M35-M36) held in Athens (September 1, 2019).

3.1 Background to the pilot project

One of the **basic technical challenges** of our time is ensuring a high **safety level with minimal costs** of operation of machines and the civil infrastructure. This is particularly important in the case of transportation, especially in the aerospace industry, as well as in many other industries, e.g. in the energy sector, where the loss of structural integrity can cause severe injuries or death of many people or high material losses.

Currently, in order to prevent the development of damage to critical level, especially in the case of aircraft or critical infrastructure in the power, petrochemical or mining industries, various non-destructive testing (NDT) methods are used. Besides methods based on visual assessment of the surface of the inspected structure, e.g. with use of liquid penetrants or magnetic powders indicating surface discontinuities, the most commonly used NDT techniques are: ultrasonic testing (UT), eddy current testing (ET) and thermographic testing (TT). UT and TT methods can be used in particular for the detection and evaluation of subsurface damage, e.g. debonding or delamination of composite structures.

Non-destructive inspections are crucial for the current system of ensuring the safety and reliability of aircraft and industrial infrastructure [1,2]. However, their use is associated with some limitations, e.g. the inspected object needs to be removed from service for the time of the inspection. Furthermore, most advanced NDT methods are time consuming which contributes significantly to operational costs, especially for the inspection of components of complex geometry or hard to access hot-spots. In some cases, their

use causes a danger to the health of persons performing the inspection, e.g. for inspections of wind turbine blades, other power or petrochemical infrastructure.

In order to reduce operating costs, as well as to increase safety, extensive research has been carried out worldwide on the development of Structural Health Monitoring (SHM) systems. SHM systems are supposed to work autonomously and provide continuous assessment of the structural integrity. A variety of sensors and measurement methods have been applied for SHM thus far [38]. Changing the philosophy – from periodic NDT inspections to continuous structural integrity monitoring – would greatly improve safety, especially for hard-to-access critical hot-spots or elements subjected to high loads or operated in an aggressive environment. Ultimately, SHM systems will become components of the so-called Health and Usage Monitoring Systems (HUMS) which will allow to assess the remaining lifespan of a structure, taking into account its individual operating conditions, e.g. loads spectrum of wind turbine blades and structural components of aircraft, as well as their current condition. This could reduce the number of unscheduled inspections and overhauls which increase the maintenance costs.

There is no single, universal method allowing for detection and assessment of damage of any kind [1, 39]. Therefore, SHM systems are developed based on different kinds of transducers and signal analysis methods, in order to enhance their efficiency in detection of damage of a given type. Within the Aero-UA project, different SHM technologies were involved, based on expertise and capabilities of the project partners.

3.2 Knowledge exchanged

The following knowledge was shared among the partners by the mid-point of the project:

Partner	***Knowledge shared***
Paton Electric Welding Institute at NASU (UA)	*Acoustic Emission (AE) based SHM*
TECPAR / ITWL (PL), UOM (GB)	*PZT sensors for SHM applications*
KhAI (UA)	*Technology of FBG sensors integration with composite structures*

3.2.1 Acoustic Emission for evaluation of structural state – new generation equipment for AE based SHM – contributor: E. O. Paton Electric Welding Institute at NASU (UA)

Background of SHM introduction in Ukrainian industry

The idea of development and introduction of systems of continuous monitoring of technical state of chemical production facilities of the OJSC Odessa Port Plant (OPP) emerged as far back as 1990. By this time, construction and mastering of design capacities of all the plant facilities was completed. The main purpose of the plant is to manufacture and export reloading of chemical products of its own production and products of other chemical enterprises in Ukraine and Russia. At the same time, the plant was successfully operating two large-capacity ammonia production units, and later, in connection with the need for expansion of production volume due to favourable world chemical products market and the plant's good geographical location, three such units, two units for carbamide production, and complexes for ammonia, carbamide and methanol reloading were built. The ammonia reloading complex included four large-capacity storage tanks with a total design storage capacity of 120,000 tons of liquid ammonia. These were exactly the structures where development and introduction of systems of continuous monitoring of technical state of OPP objects began in 2001 to ensure their safe operation took place.

By the end of the 1980s, social pressure appeared to fundamentally improve the ecological condition of the regions by closing potentially hazardous chemical enterprises. Odessa held a referendum on closing

such productions in OPP. Considering that this was already after the accidents at Chernobyl NPP and Jonava “Azot, Ltd.” (Lithuania) with destruction of isothermal liquid ammonia storage tanks with a capacity of 10,000 tons, the OPP issue became even more serious. Even though the safety and reliability of plant operation was ensured by application of modern equipment and technologies, strict observation of technological modes of operation of the main production units and reloading complexes, timely performance of overhauling and scheduled maintenance, compliance with labour protection standards and requirements, in the referendum it was decided to close the hazardous productions at OPP.

The plant’s management managed to reach a compromise variant: the plant was not closed, but the frequency of filling the liquid ammonia tanks storage had to be reduced twofold compared to the design value, which drastically affected the rhythm of reloading complex operation, leading to disruption of operation of the liquid ammonia suppliers, and to downtime of ammonia-carriers waiting for loading. However, even with reduced storage capacity, it remained Europe’s largest liquid ammonia storage facility, located 18 km from Odessa with its 1 mln inhabitants and 8 km from the city of Yuzhnii. This fact, as well as continuous traffic of transport ships with liquid ammonia in Black Sea waters, required a closer consideration of the issue of ensuring OPP safe operation.

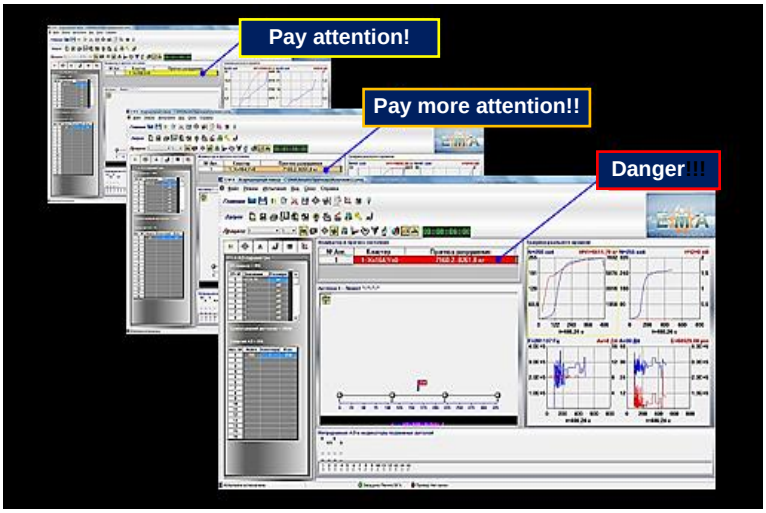

a

Readings of indicator in display upper left corner	Personnel actions
Green band	**Standard operation mode**
Yellow band	**First warning** Attention! At appearance of predicted breaking pressure and it exceeding the working pressure by more than 50% - continue operation
Orange band	**Second warning** At predicted breaking pressure exceeding the working pressure by more than 50% and less – stop operation
Red band	**Emergency situation** Stop operation! After appearance of prolonged intermittent sound signal – urgent load relief

b

Figure 7. Indication on monitoring equipment screen with presentation of the main parameters, characterizing the storage material state (a), and personnel actions at different readings of hazard indicator (b)

It became necessary to develop and introduce such a system of monitoring the technical condition of technological equipment, and, primarily, large-capacity isothermal liquid ammonia storages, which would enable application of instrumental methods of continuous monitoring for absence of propagating defects in the material and welds of equipment, detection of initiating defects, monitoring their propagation, as well as simultaneous calculation of safe residual operating life of facilities for ammonia production and storage. For this purpose, the experience of enterprises and organizations from Ukraine, Russia, Germany, Italy, Finland, USA and Japan on application of methods of non-destructive testing and diagnostics at critical industrial facilities was studied. The approaches to ensuring reliable and safe service of operating structures and constructions were developed in the most comprehensive manner by domestic scientists led by the E. O. Paton Electric Welding Institute of the NAS of Ukraine in a new scientific direction: real-time diagnostics and prediction of structure failure. It was necessary to conduct the required retrofitting and introduce the developed technology at OPP.

The solution to the problem became possible with development of the Acoustic Emission method and instrumentation and modern advances in the field of electronics, computer engineering and information technologies. The EMA-3 diagnostic system was developed at the E. O. Paton Electric Welding Institute together with Hungarian specialists who developed an algorithm, allowing determination of breaking load of structure materials already at an insignificant level of the current load. Depending on material grade, this level can be equal to 20% of breaking load level. Moreover, analysing the material state and having in the data base information on the initial level of this state, the system assesses the structure's residual life.

Fig. 7(a) shows three images of the EMA-3 system monitor screen, formed during structure operation. It is interesting to note the presence of rectangular signal indicators, changing their colour successively from green to red, located in the screen's upper left corner, and informing the operator about the stages of fracture development and their criticality for the monitored structure (Fig. 2(b)). Signal indicators in "Fracture prediction" line give the ranges of anticipated breaking loads, calculated already at the first stages of structure loading and at each next warning. Continued application of load allows the system to acquire a sufficient scope of information so as to precisely define the breaking load and calculate the material residual life. For greater clarity, warnings about the hazard of further loading of structures in keeping with the Table are displayed on the monitor screen (Fig. 7(b)).

Thus, the EMA-3 system can answer the main questions of interest:

1. At what load the structure will fail.
2. For how long the structure will preserve its serviceability with the defects found at the moment of monitoring.

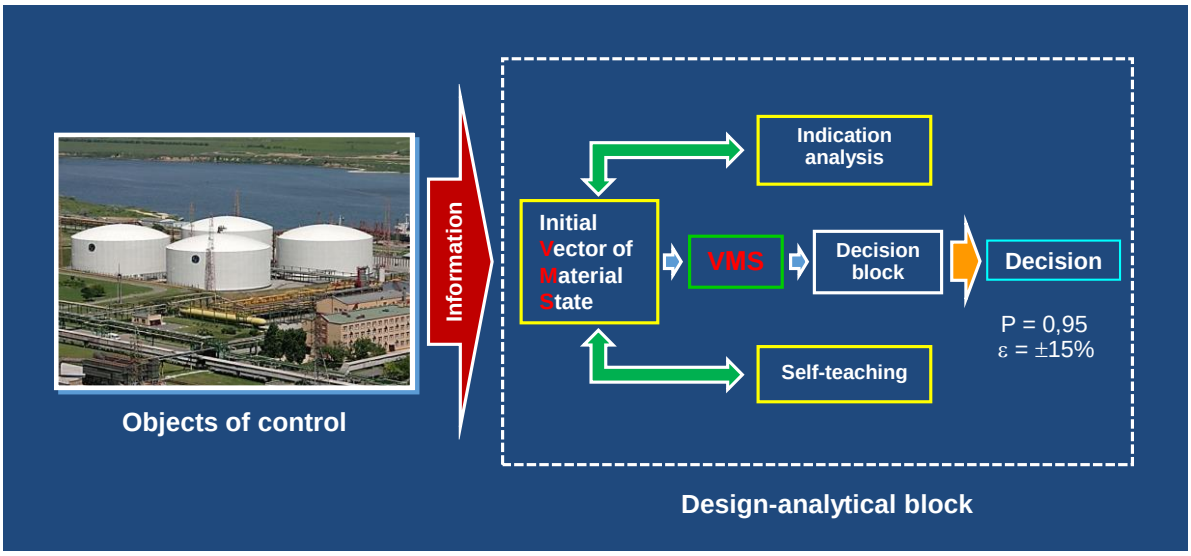

Figure 8. Block-diagram of adaptive image recognition system at structure state assessment

Operation of software and respective program packages (SW and PP) of this kind of systems is based on the principles of the theory of image recognition, when the indications of fracture processes running in materials are formed into the vector of material state (VMS) (Fig. 8). Its further comparison with the training vector and correction of both of them when entering additional data into decision module, allows for generating a system decision on structure material state and predicting this state for the period of time for which the structure will preserve its serviceability. A simple schematic of material state recognition contains two main blocks – transducer and classifier.

Instruments and programs realizing AE technology

In order to implement the technology presented above, instrumentation and special software have been developed, which provide the information, required for further analysis and applying on its basis the theory of structure state recognition at the present moment and its prediction for a certain time interval. Application of modern measuring instrumentation and powerful computer equipment allows realization, with application of this software, of an advanced information AE technology and ensuring its efficient operation. We will consider these subjects in greater detail.

Review materials on software for AE diagnostic systems EMA were first published in 2005 [20]. In particular, basic capabilities of the software for prediction of breaking loads and residual life were described. By that time, technical parameters of monitoring hardware and software, including the prediction, had been confirmed by Ukrmetrteststandard service (former TsSM of Gosstandart of Ukraine). Since then, upgrades and expansion of software capabilities have been successively performed, based on experience of practical application of the systems, interaction with users and taking into account the world experience.

With the development of new programs, expansion of the capabilities of current software version, cardinal change of basic capabilities and their visual presentation in the program, the version number has changed. Publications [21, 22, 33] deal with the most important features of EMA program version 3.9 and concurrent supplementary programs used at periodical inspection and continuous monitoring of industrial facilities.

Note that, similarly to previous versions, the EMA-3.9 program was developed in Microsoft Visual Studio 6 environment to the requirements of Windows SDK which ensures its performance on the basis of all the currently available 32-bit Microsoft operating systems for PC, starting with Windows 95 and ending with Windows 10, as well as 64-bit ones. The program is device-independent and supports application of AE measuring systems of different manufacturers. Also envisaged is the so-called batch data processing mode that allows analysing any format-compatible data derived with application of this or third-party software in AE systems of various types.

Numbering of Version 3.9 was selected proceeding from the fact that 4th generation equipment for AE diagnostics is currently at the stage of final modification and testing. After complete integration of software with the above-mentioned equipment, the upgraded program will receive a new number. Improvements and upgrades made after EMA-3.5 presentation in 2005 make this a fundamentally new software product, as many of the most important internal data processing algorithms and their external visual presentation have changed.

Development of the Internet enabled solving the problem of remote control of monitoring systems, remote assessment of the state of operating structures and prompt decision-making in emergencies. More than 10 years of experience of operation of diagnostic systems with such capabilities, showed that they can form the basis for initiating the next stage of work in the field of ensuring structure safety, the stage of controlling their service parameters. The primary step in the sequence of stages to ensure the reliability of structures and equipment in operation is their continuous monitoring, obtaining a continuous flow of information about their state.

Reference [22] sets out in detail the requirements of AE monitoring systems, which should be incorporated into the software and hardware system, controlling the operation of industrial facilities based on the data on their state obtained during monitoring. These requirements were used for development and current testing, in particular at OPP, of new fourth generation of EMA system instruments, developed, similarly to the previous one, together with Hungarian specialists, who possess substantial experience in this area, acquired over several decades.

New developments of AE instrumentation incorporate the most recent advances in the field of electronics and computer engineering. The instruments are smaller and lighter, support the most modern data transfer interfaces, and have a higher reliability due to the absence of mobile components. The system flexibility, based on connecting several instruments, was increased. Earlier, the number of jointly operating measuring modules was not more than two, with the maximum total number of channels standing at no more than 64. Now two main types of instruments, having 4 and 16 AE channels, respectively (Fig. 9), can be connected in any sequence, the total number of simultaneously processed AE channels has been increased to 128, and the number of LF channels, transmitting process data, was increased similarly.

Figure 9. New generation instruments EMA-4 based on 4-channel and 16-channel modules AED-404, AED-416

EMA-3.9 system software was upgraded for interaction with new types of equipment. For this purpose, a program interface was implemented for network connection with instruments, obtaining diagnostic information from them, and issuing control commands. As EMA programs were initially designed for processing data from not more than 64 AE channels and 16 LF channels, changes of the inner processed data structure and file format used were required, with parallel optimization of memory, taken up by the transmitted and stored information blocks.

The user interface was also modified with a view to the possibility of displaying data from each AE and LF channel, selecting them in primary or additional processing algorithms, adjusting and configuring simultaneous operation of channels in complex location antennas.

Thus, a fundamental upgrading of EMA-3.9 program was performed after its presentation in 2013. The new software product was called EMA-3.91.

Given below are the main features of the EMA-3.9 and EMA-3.91 programs, providing new capabilities in processing diagnostic information and transition to controlling the operation of industrial facilities. The EMA-3.9 program combines the interfaces of adjustment of the processes of AE data clustering and filtering. The developed clustering algorithm allows selection of any combination of the following indications characterizing the AE signal: coordinate, amplitude, rise time, duration, oscillation number, velocity, frequency, energy and noise level. This enabled a more detailed classification of

detected defects and analysis of AE information as a whole. The obtained AE events can be filtered by the same indicators by which their clustering is performed.

Parameter filtering criteria are set by minimum and maximum values. Simultaneous application of several filtering bands and clustering by the required parameters provides more effective filtering out of process noise and detailed analysis of information. The program enables selection between input parameter filtering, with cutting off of unnecessary information, and filtering performed after event occurrence. Application of these algorithms in practice showed that both the capabilities are useful, but the first should be preferred, as the scope of stored and processed data is reduced, sometimes quite significantly.

Location based on delay matrix enables error minimization and prevention of event coordinates falling into an inadmissible region. The matrix is created on the basis of the pre-determined velocity of sound propagation in the material; at the change of specified velocity automatic recalculation of the matrix is performed, which is then used as the basis for subsequent determination of AE event coordinates.

EMA-3.91 program settings windows contain a new interface with the common table of parameter entering for clustering and filtering (Fig. 10). Changes can be made in real time – both during adjustment and during full-scale testing or continuous AE monitoring.

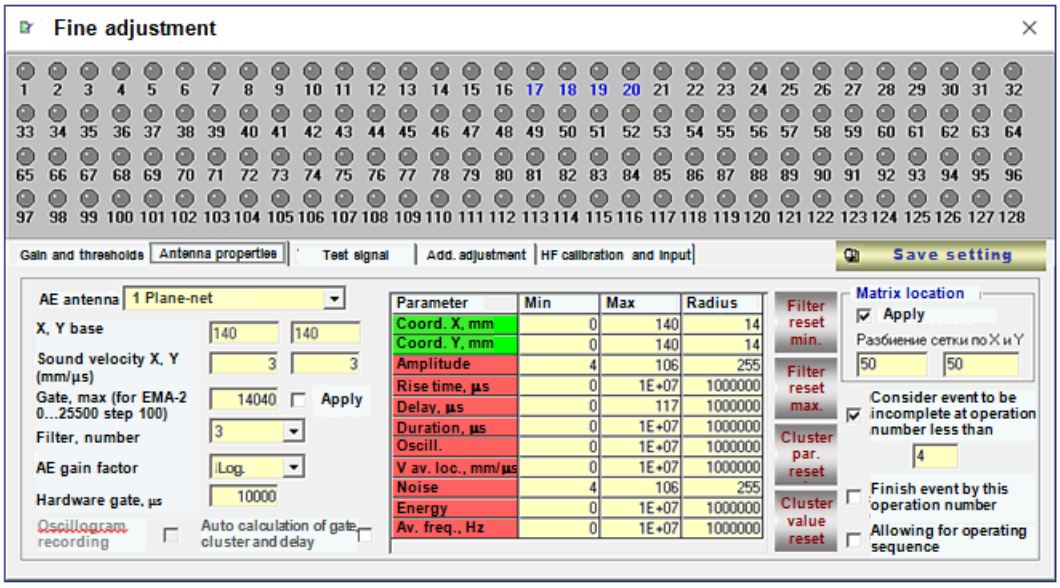

Figure 10. Setting antenna properties in fine adjustment window of EMA-3.9 program: in central part of the window – table with set filtering and clustering parameters, in the upper part – AE activity indicators in 128 AE channels

The "Antenna properties" insert allows for establishing bandpass digital filters for such AE event parameters as duration, oscillation number, time of signal rise to maximum, AE amplitude, average signal frequency, etc. Upper and lower band limits are set. If AE location antenna supports matrix location mode (for linear, planar or cylindrical antennas), matrix parameters in the window can be changed in real time.

One of the features of EMA system software is working not only with acoustic, but also with process information, which is entered into the system in the form of LF parameters: load, pressure, deformation and temperature, etc. Capability of adjustment of the coefficients and calibration functions directly during measurement is implemented. Changes are displayed on real-time graphs, which enables quick selection of the required kind of calibration. In addition, manual entering and extrapolation of LF are provided in the case entering any of the LF parameters into the system by electric or program means is impossible. A possibility of entering current value of LF parameters and their reverse extrapolation during measurement was added. This allows obtaining an LF parameter variation curve of, for instance, current pressure which is either stepped or represented by inclined sections.

There is also the possibility to automatically correct established thresholds of amplitude discrimination after a pre-set time passes (Fig. 11). The above modification is extremely important for the system's autonomous operation during monitoring, as it enables reacting on time to changes of acoustic background without operator intervention.

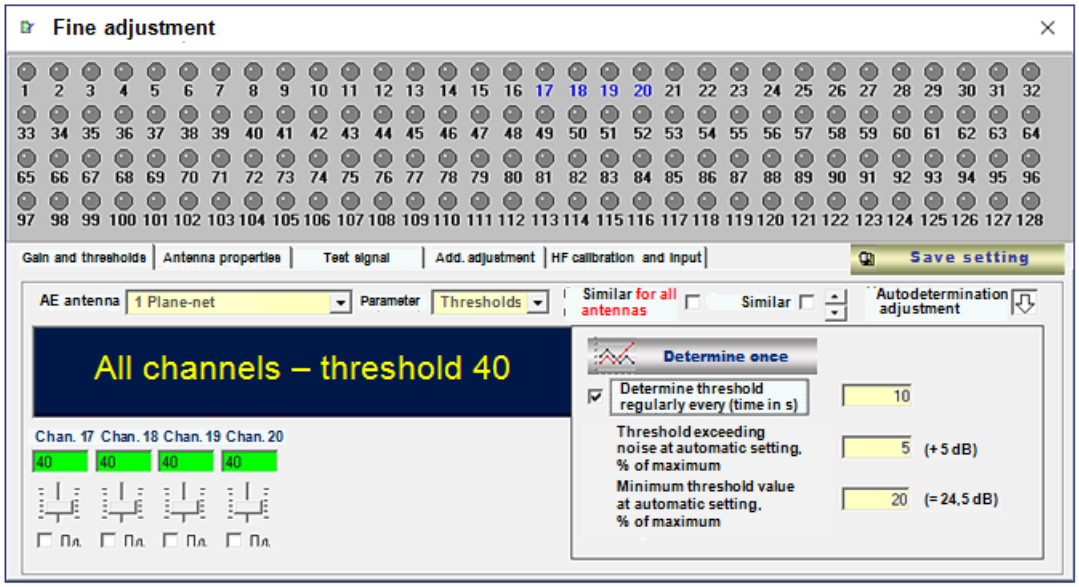

Figure 11. Setting the parameters of automatic determination of thresholds in fine adjustment window of EMA-3.9 program (bottom right)

The information window (Fig. 12) contains a graph showing table data from the information window list. When different content of the list is selected, the graph is automatically updated. Each of the parameters included on the list can be shown on the graph or switched off. The graph type can be point, bar, line, or stepped. Graph position and size are adjustable.

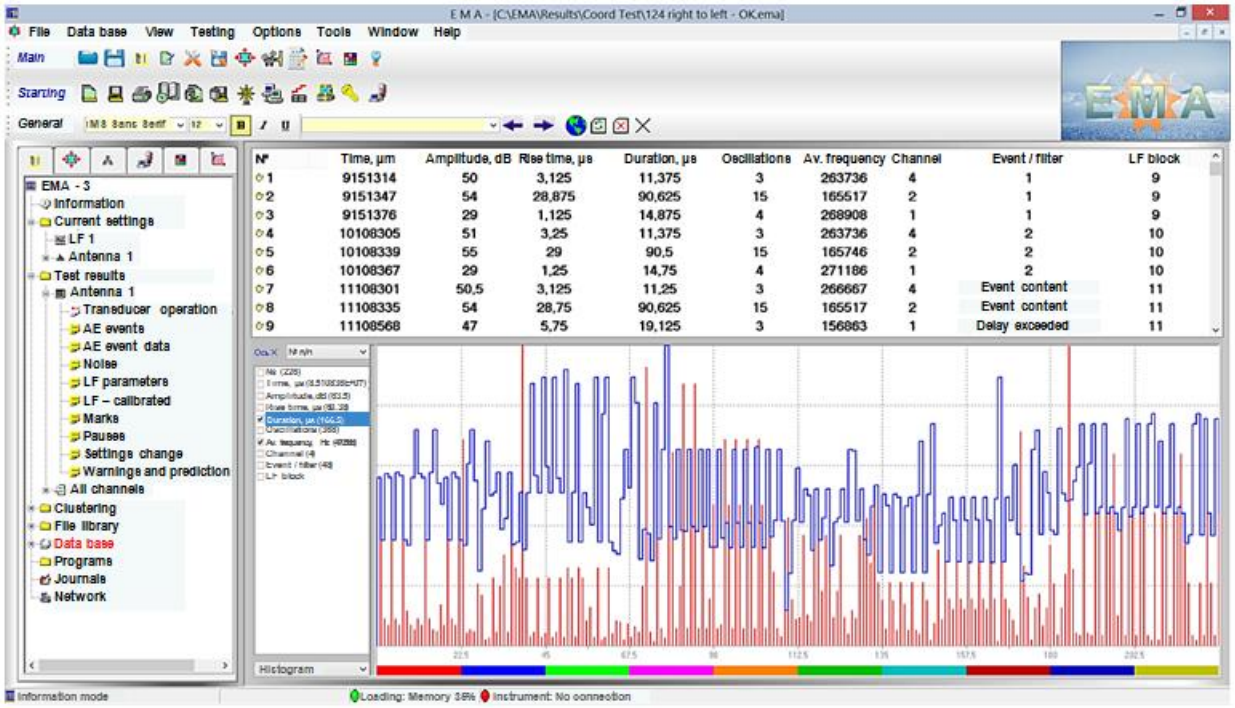

Figure 12. EMA-3.9 program information window with data on transducer operation: in window lower part – the graph, where response time and average frequency are selected as displayed parameters

At table analysis each transducer operation contains information on the AE events to which it referred (if the operation did not refer to any events, the reason for rejection is specified). In the case of rejection of events, the criteria based on which which it was performed are indicated in the appropriate table. Considered possibilities allow an essential expansion of system informativeness and performance of complex comprehensive analysis of obtained data. Moreover, errors made by the operator when setting up the system can be easily detected and corrected.

The location screen (Fig. 13) displays both all the location antennas used during AE monitoring simultaneously, and the required antenna, as desired by the user. To improve visibility, a flash appears in AE generation points.

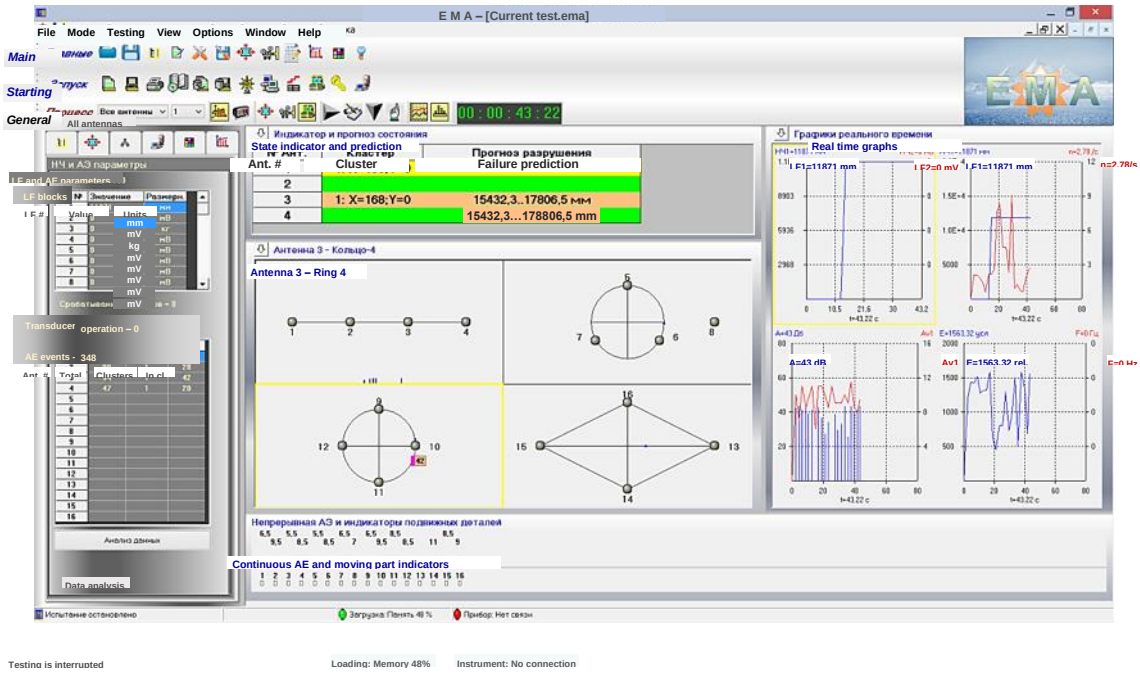

Figure 13. EMA-3.9 program testing window with displaying of 4 location antennas (Screen 1): above location screen – fracture prediction area, left – tables of AE and LF data, right – real-time graphs; below location screen – continuous emission value

The program applies additional methods of data analysis in the graphic form: distribution of AE parameter values by channels and correlation between channels. The data analysis window (Fig. 14, 15) is designed for viewing and additional analysis of obtained AE data, in particular with the capability of automatic real-time updating. Screen 1 (Fig. 13) contains data by clusters and is largely similar to the data in the information window; it enables viewing AE event data by selected antenna clusters and transducer operations associated with them. Screen 2 (Fig. 14) allows for selection and comparison of data in individual AE channels in the form of parameter distribution.

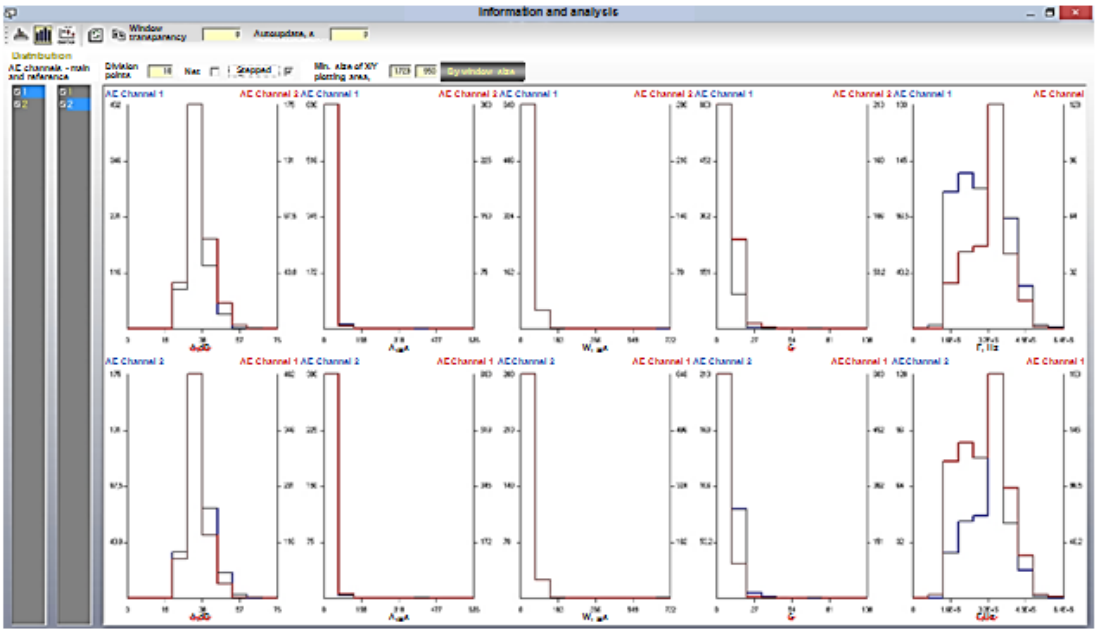

Figure 14. Window of EMA-3.9 program data analysis with graphs of AE data distribution by channels (Screen 2)

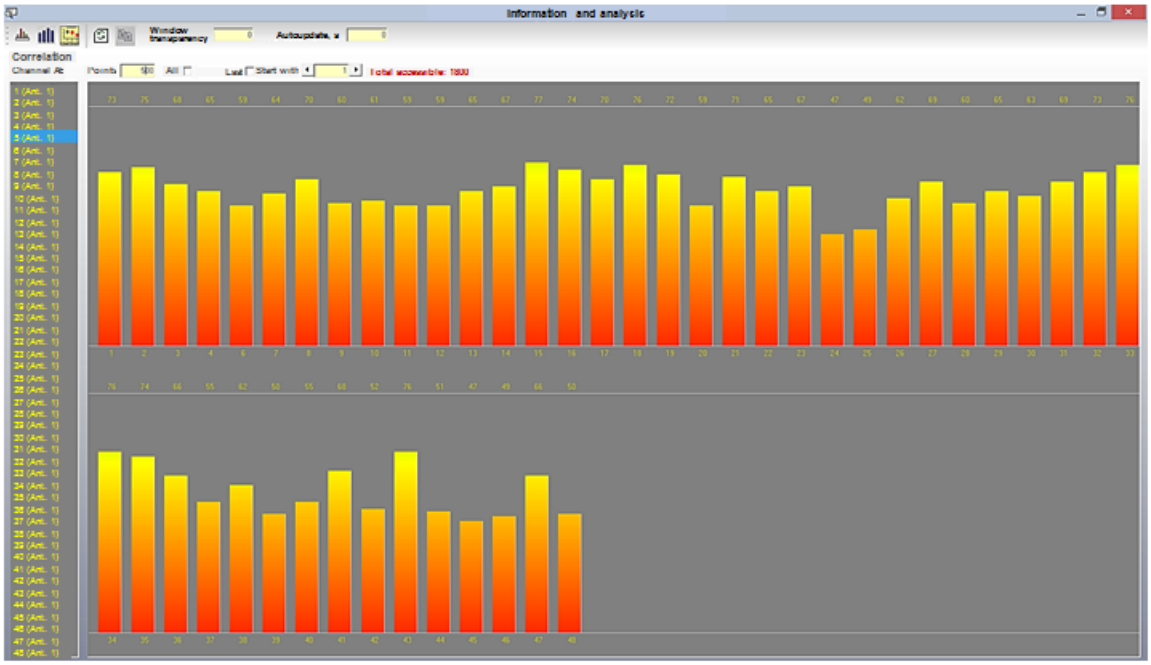

Figure 15. Window of EMA-3.9 program data analysis with graphs of AE noise correlation by channels (Screen 3)

Graph type selection (bar or stepped) and net displaying/hiding are provided.

Screen 3 (Fig. 15) displays a bar graph of the correlation of a specified number of continuous AE data for a selected channel with the other channels.

Experience of EMA system operation in production, in particular, in continuous monitoring mode, showed that automation of repeated and labour-consuming operations is one of the most important objectives. A number of software tools presented above solve some specific automation problems. Unfortunately, it is not always clear in advance what exactly the operations which will have to be automated are, due to the diversity of objects of control, their operating conditions and suggestions made by the staff operating the systems.

For this reason, EMA program Version 3.9 is fitted with built-in system of programming in VBScript language (Fig. 16), which corresponds to the Microsoft specification.

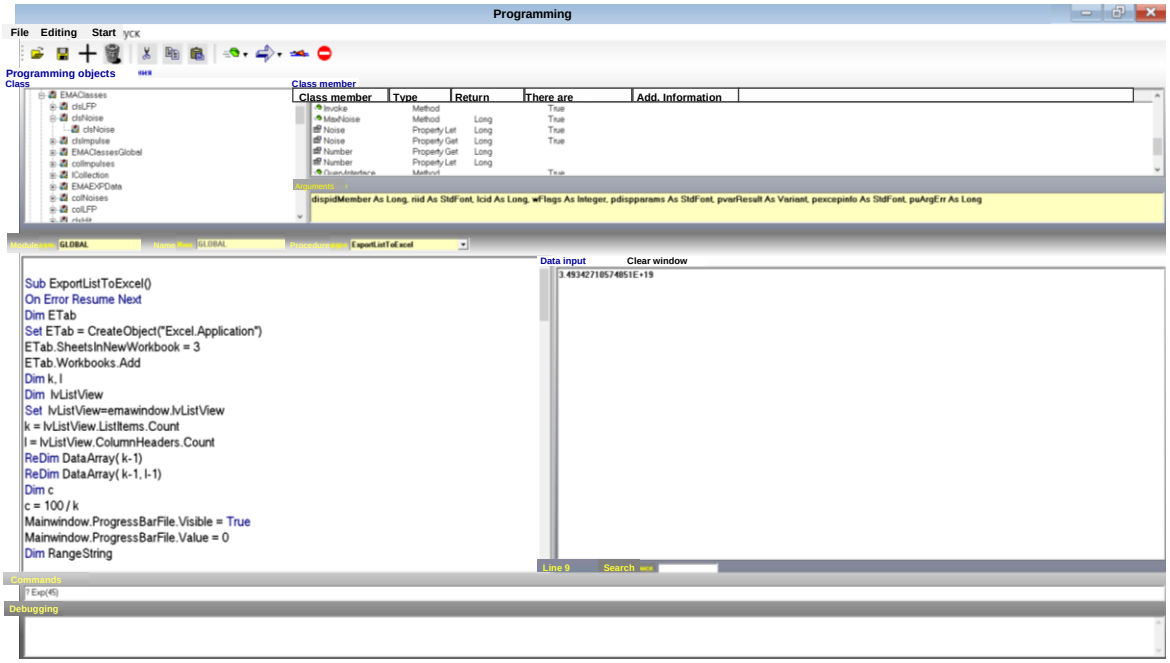

Figure 16. EMA-3.9 programming window: top – object browser; left – code editor; right – output window; bottom – command line and adjustment window

The possibility of further analysis of processed data or of their completely alternative processing is implemented. In particular, it is possible to completely change the algorithm of event formation, their coordinate calculation, displaying features, tabulated and graphic presentation of data, etc. This not only enhances program functionality, but also enables experimenting with data processing, extending the scientific and practical experience gained which will undoubtedly be useful in development of subsequent software versions.

It is noteworthy that a number of the above-mentioned developments and upgrades are the result of close interaction of developers of AE control and monitoring systems of different modifications with their users, performance of joint investigations and analysis of arising comments and suggestions.

Analysis and optimization of methods and algorithms for AE source coordinate location were performed in 2015 with application of new capabilities [22]. Transition to control of complex-geometry objects, particularly with random arrangement of AE transducers, required fast and operative assessment of possible errors at locating AE sources. Previously such assessment was performed experimentally, directly on the object after transducer arrangement, with application of pulsed sounding from a special generator or by Hsu-Nielsen method, based on graphite rod breaking. In EMA system software, verification is performed using automated program virtual testing of location errors for pre-set location antenna configurations (Fig. 17). An undoubted advantage of this checking method is the fact that it can be performed very quickly, and before the start of physical placing of transducers on the object. This way an optimum transducer layout and the most suitable algorithm for AE source coordinate calculation are selected.

The developed system of testing AE source location accuracy allowed for considerable simplification and shortening of the process of AE testing setting up, as well as advance assessment of the reliability of location of AE sources detected during real measurements in certain areas of the object of control. The developed program allows assessment of the range of sound wave velocities for selection of the optimum variant to be used during location that qualitatively improves its accuracy.

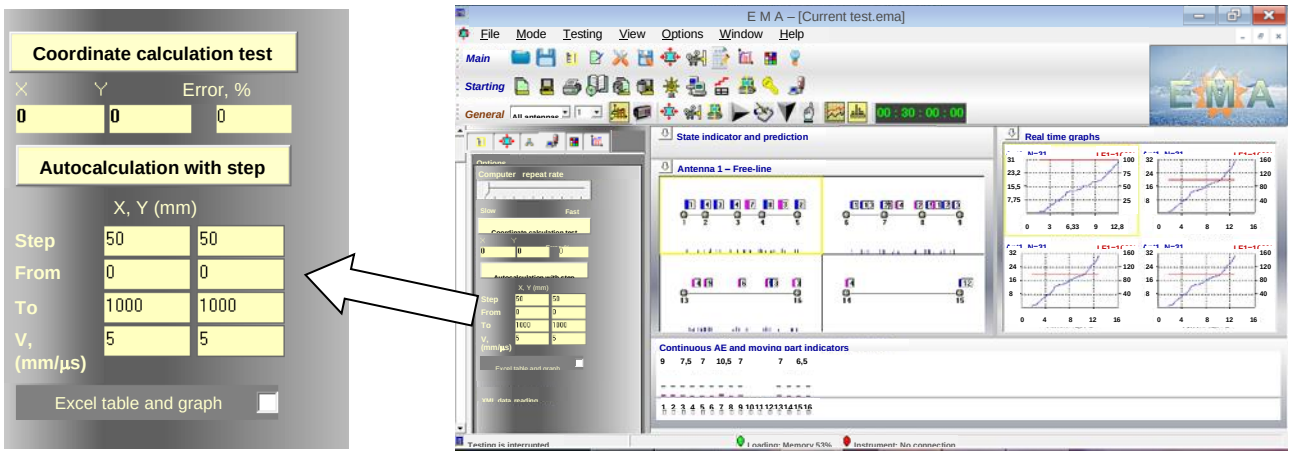

Figure 17. EMA-3.9 program testing window with elements of control of virtual testing of coordinate determination error

Virtual testing allows for quickly checking the currently available or newly created algorithms of AE source location for accuracy and promptly correcting them. It should be noted that the results of such a check were used for correction or complete replacement of location algorithms developed for EMA systems, in cases when virtual testing demonstrated their insufficient accuracy.

The hardware and software tools developed allow for obtaining all the required information from the object of control as initial data for operation of the algorithm of assessment of structure material state at specified conditions of probability of assessment and error. As already mentioned, the following AE parameters can be obtained in real time: signal amplitudes, number of operations and events, event energy, time of signal rise up to maximum, normalized event duration, number of oscillations in the signal and event, frequency characteristics of AE arising in the material; in VMS – also monitored material temperature, stressed state of monitored components and some derivatives of the above parameters, required for completing the full vector.

The above additional analytical tools enable complementing the prediction derived with VMS application, by expanded data on specific processes of damage and fracture propagation in structures. Note that fourth-generation EMA systems also allow performing real-time analysis of AE signal oscillograms.

Safe operation management and normalized intelligent advice

The AE technology developed is incorporated as a component into the production process and the monitoring, integrated into the enterprise computer network, complements the currently available tools of following the current state of objects in production. At OPP, considering the company requirements, the management defined a new task: transition from statement of data obtained during monitoring to their application in controlling safe operation of ammonia reloading complex equipment. Instead of a simple indication of the degree of safety of the current state, automatic recommendations on responding to the hazard were provided. This means deeper integration of monitoring into the production structure with intelligent tools for formulating and making decisions on the possibility of further operation and recommended operating modes.

"Normalized intelligent advice" (NIA) is put into practical use in Reference [22]. In the context of production objectives such advice contains analysis of the situation in the object of control and clear instructions on object operation in this situation. In case of danger, such instructions envisage interrupting the structure loading or even its partial or complete unloading, if required; NIA is formulated automatically and in a short time (several seconds) after appearance of potential danger for the object. NIA issuing is

accompanied by visual and sound warning about the danger, information about the degree of danger and specific section of the object of control which is in danger (Fig. 18).

The advice is formulated in keeping with the Table (Fig. 7(b)), based on analysis of not only the current, but also previous data on the state of the object of control, and it is based on many years' experience of operation of this type of objects and their control by continuous AE monitoring systems. NIA is the base for subsequent realization of automated safety management. Its implementation required extensive practical experience in advanced computer technologies.

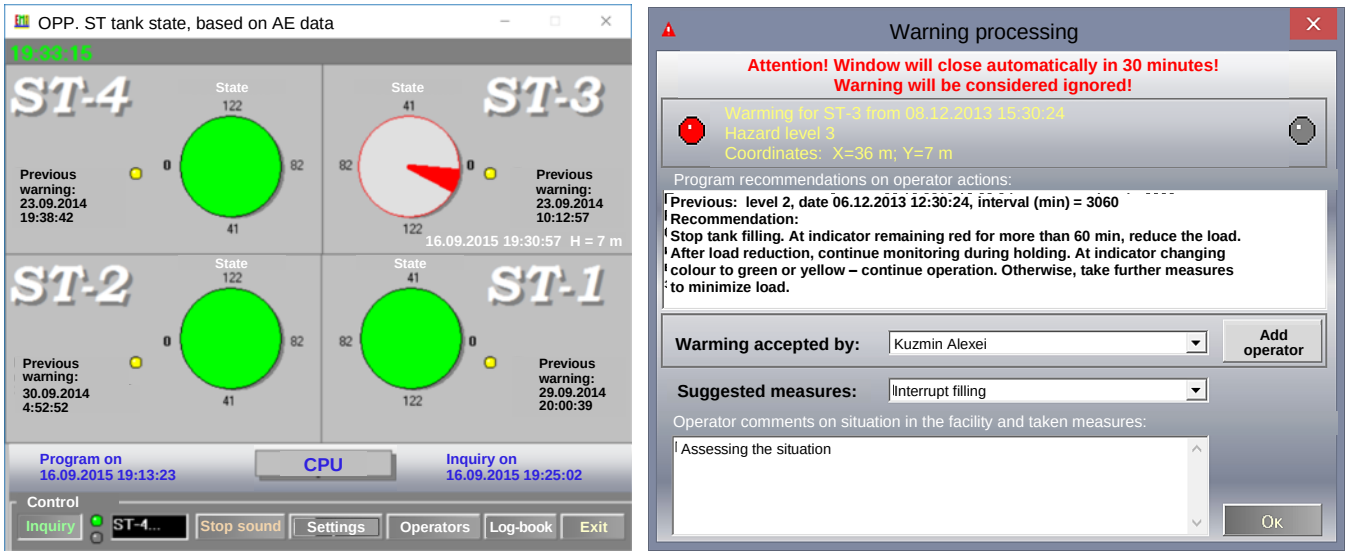

a *b*

Figure 18. User interface of indicator program for operators when monitoring the state of OPP liquid ammonia storages: a – window with state criticality indicator, right upper indicator shows 3rd level warning: "Danger" for one of the sectors of object of control; b – window for warning processing by operator, which includes "Normalized Intelligent Advice" recommendation

The program automatically keeps a log of accepted warnings (Fig. 19), which is filled in only when the "Demand operator reaction to warning" flag is set.

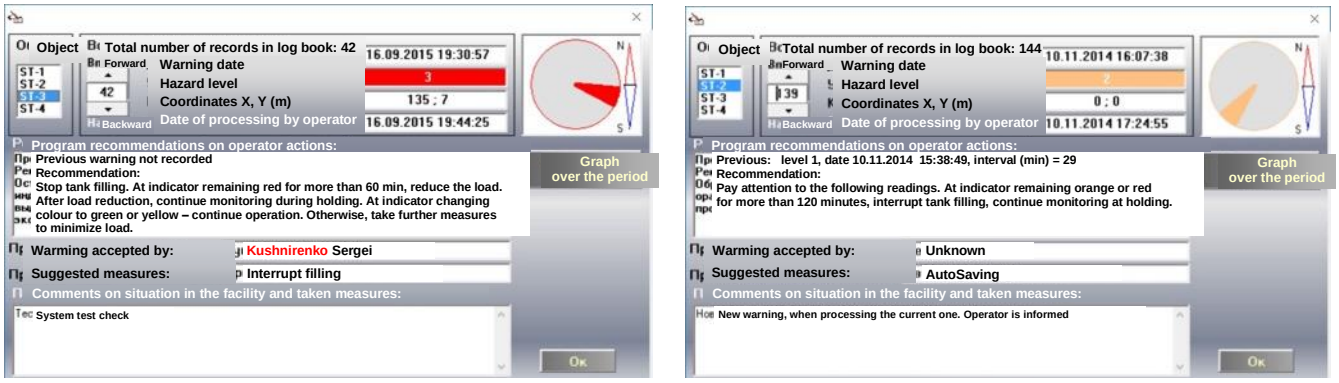

a *b*

Figure 19. Window of accepted warning log: a – after filling by the operator, b – in the case of autosaving of current warning, when receiving the next

When the log is opened, the window automatically displays the latest entry. To go through the other entries, scrolling through them using "Up" and "Down" arrows is recommended.

The other window elements are designed for displaying data on the warning and its processing. They show the time of the program receiving the warning and finishing its processing by the operator, data on the danger level and coordinates of acoustic activity centre, program recommendations for the situation and measures taken by the operator.

The dangerous sector is displayed in the right-hand upper part of the window with indication of the tank's location, with the button of starting the warning statistics graph for this tank located below it.

Considering that continuous monitoring systems operate for long periods of time, periodically generating warnings about the danger, studying the tendencies of dangerous situations arising is urgent. It enables comparison of generation of a certain warning or their group with technological processes, load parameters, climatic conditions, etc. Earlier it was not possible to perform this analysis automatically. Now acquisition of monitoring statistics is fully automated. Control elements allow selection of the time period during which warning statistics are required and plotting a graph in which the bar colour designates warning level.

Graph plotting is based on data, stored in special files (log-books). Information is processed and displayed in a window shown in Fig. 20. Users can change the period over which the statistics is required by selecting it from a list. The start date is selected by arrows, as well as when pressing a button, which allows automatic calculation of the reported period from the current calendar date. Graph data can be copied using a special button, into a clipboard for the purpose of its further use in, for instance, reporting documentation.

Data for several AE antennas can be stored in statistics files, so that the user can choose whether to display in one graph the data for all the antennas simultaneously or just for one.

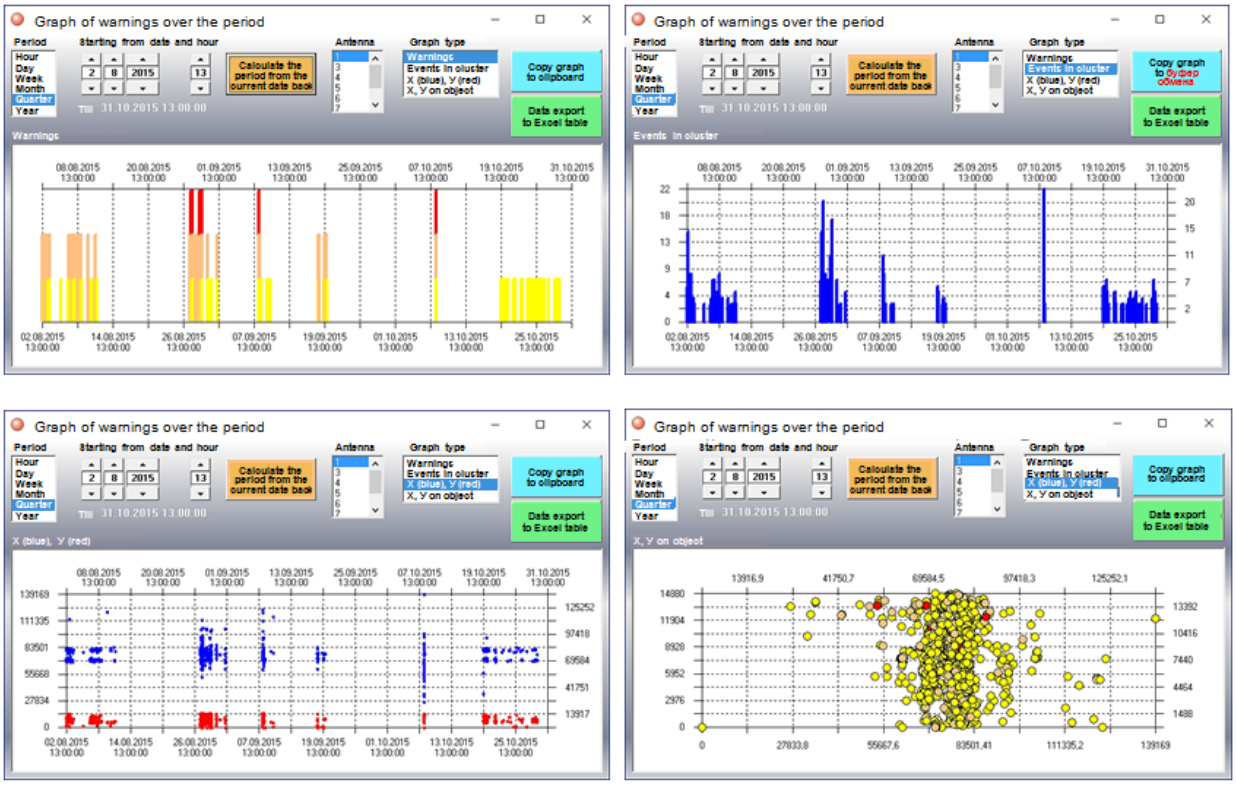

Figure 20. Window of warnings statistics of EMA-3.91 program with different graph types

Data can be presented in 4 different types of graphs.

The "Warning" graph indicates by colours and bar height the warning level at a given moment:

- 1st warning – yellow, bar height of 1/3 of the graph;
- 2nd warning – orange, bar height of 2/3 of the graph;
- 3rd warning – red, bar height takes up the full height of graph;
- 4th warning with greater danger – black, bar height takes up the full height of graph

The graph has no axis of ordinates.

The "Events in cluster" graph indicates by bar height the number of events in the cluster, when receiving the warning at a given moment.

The "X (blue), Y (red)" graph indicates cluster coordinates by points, when receiving the warning at a given moment. The scale along the ordinate axis corresponds to both the X and Y coordinates. For linear antennas just the X coordinates are shown in blue.

The "X, Y on object" graph shows cluster coordinates by circles, when receiving the warning at a given moment the X coordinate being traditionally shown along the abscissa axis and the Y along the ordinate axis. For linear antenna types this graph is shown by bars with the height of each bar representing the number of events in the cluster at the moment when the warning is received.

The warning statistics window is scalable and allows changing the graph proportions and dimensions.

Thus, an up-to-date information technology which allows for performing analysis of the state of structures over a prolonged period with its prediction for the future, determining with pre-set probability the load at which failure will occur, proceeding from accumulated warning statistics, assessing the potentially dangerous sections in the objects of control on the basis of AE monitoring data has now been developed and put into production.

Automation of monitoring and processing of incoming data leads to gradual elimination of the human factor, both from the process of adjustment and monitoring, and, recently, from the process of making decisions on the structure state and measures required to provide its safety. This, in its turn, will be the basis for introducing, in the near future, systems of fully automated safety management, in which the diagnostic data will be used not only for analysis of the state of the object of control, but also for controlling its operation.

In the case of potential danger of failure arising in such an "intelligent" structure, the software will select the optimum loading mode, issue commands to control mechanisms to ensure it, and will monitor its execution. Application of such a technology will allow an essential improvement of operational safety and, in most cases, prevention of failure and possible catastrophic consequences.

In conclusion, it should be noted that:

- prompt development of means of controlling structure material state, particularly with application of AE technology, and the attention given to this issue in many countries of the world, justify expectations of further extensive application of AE technology for development of intelligent structures and constructions that with specified accuracy and probability will themselves provide information about their state and suggest measures to overcome emergency situations;
- continuous monitoring systems, using integrated control methods and, in particular, the AE method, will be ever more widely used in monitoring first hazardous operating structures, and then also in ordinary industrial structures;
- widening of the network of specialized centres for monitoring of operating structures should be anticipated. Such centres will be staffed by highly qualified specialists, and up-to-date digital technologies and communication means will enable them to perform remote monitoring and assessing the structure state, being at any distance from the object of control. Control, from labour-consuming and inconvenient, is gradually transforming into more convenient, office technique;
- global tendencies in information technologies allow anticipating further automation of all the available processes of structure state control, including AE monitoring. Priority will be given to technological solutions with application of the most advanced trends in IT development: distributed and cloud computing, use of inexpensive high-speed connection, miniaturization and unification of developed equipment, standardization of data description on the base of HTML and XML standards.

References

1. *Aleshin N. P. New information systems of non-destructive testing and diagnostics of welded structures [Text] / N. P. Aleshin // Avtomat. Svarka. – 2003. – October-November. – P. 64-69.*
2. *Andreikiv A. E. AE method in investigation of fracture processes [Text] / A. E. Andreikiv, R. V. Lysak. – Kiev: Nauk. Dumka, 1989. – 176 p.*
3. *Bigus G. A. Studying acoustic-emission signals at deformation and fracture of samples from steel 22K [Text] / G. A. Bigus, P. B. Strelkov / Tekhn. diagnostika i nerazrush. kontrol. – 2005. – #1. – P. 10-15.*
4. *Gilmor R. Applied theory of catastrophes [Text]: in 2 books. / R.Gilmor. – M.: Mir, 1984. – Book 1. – 350 p.; Book 2. – 285 p.*
5. *Grenader, U. Lectures on the theory of images [Text]: in three vol. Vol. 1. Image synthesis / U. Grenader. M.: Mir, 1979. – 397 p.*
6. *Grenader, U. Lectures on the theory of images [Text]: in three vol. Vol. 2. Image analysis / U. Grenader. M.: Mir, 1981. – 445 p.*
7. *Grenader, U. Lectures on the theory of images [Text]: in three vol. Vol. 3. Image synthesis / U. Grenader. M.: Mir, 1983. – 430 p.*
8. *Analysis of the risk of accidents in the main ammonia pipeline "Toliatti-Odessa" of OJSC "Transammiak" [Text] / D. V. Degtyarev, Yu. A. Dadonov, I. A. Kruchinina, et al. // Trans. of 7th All-Rus. Scient. Conf. "Modern methods of mathematical simulation of natural and anthropogenic disasters" and 3rd All-Russ. Scient.-Pract. Conf. "Problems of protection of population and territories from emergencies of natural and technogenic nature", Krasnoyarsk, 13 – 17 October 2003. – Inst. of comp. model. SB RAS. – V.2. – P. 102-103.*
9. *Kovchik S. E. Characteristics of short-term crack resistance of materials and methods of their determination [Text]: Ref. book, in 4 vol. / S. E. Kovchik, E. M. Morosov; Ed. by V. V. Panasyuk, acad. of the NAS of Ukraine. – Kiev: Nauk. Dumka, 1988. – V. 1. – 436 p.*
10. *Kollakot R. Damage diagnostics [Text] / R. Kollakot. – M.: Mir, 1989. – 516 p.*
11. *Integrated expert-analytical system of evaluation, analysis and prediction of technical state of linear part of main gas pipelines (AES MG) as a component of regional and global systems of ecological monitoring [Text] / V. E. Kostyukov, A. P. Kudaev, I. A. Pavlikov, et al. // Trans. of Conf. "Information technologies and automated control systems". – Trans. of Intern. Specializ. Exhibition-Conf. of defense and dual-purpose technologies – "New technologies in radioelectronics and control systems", Nizhnii Novgorod, April 35, 2002. – V. 1. – Sect. 1 – M.: TsNII "Elektronik". – 2002. – P. 22-25.*
12. *Evaluation of the state of pipe metal after long-term operation in the system of main gas pipelines [Text] / A. A. Lebedev, S. A. Nedoseka, N. R. Muzika, N. L. Volchek // Tekhn. diagnosika i nerazrush. kontrol. – 2003. – # 2. – P. 38.*
13. *Lebedev, A. A. Method of rapid assessment of crack resistance of ductile materials [Text] / A. A. Lebedev, N. G. Chausov – Kiev: Preprint of IPS of NASU, 1998. – 43 p.*
14. *Makhnenko V. I. Improvement of methods of assessment of residual life of welded joints of structures in long-term operation [Text] / V. I. Makhnenko // Avtomat. Svarka. – 2003. – October-November. – S. 112-121.*
15. *Nedoseka A. Ya. On quantization of the process of crack initiation and propagation [Text] / A. Ya. Nedoseka // Tekhn. diagnostika i nerazrush. kontrol. – 1989. – # 1. – P. 11-15.*
16. *Nedoseka A. Ya. Fundamentals of calculation and diagnostics of welded structures [Text] / A. Ya. Nedoseka ; Ed. by B.E.Paton. 4th ed., rev. and compl. – Kiev: Indprom, 2008. – 814 p.*
17. *Nedoseka A. Ya. On evaluation of reliability of operating structures (state of the problem and prospects for development) [Text] / A. Ya. Nedoseka, S. A. Nedoseka // Tekhn. diagnostika i nerazrush. kontrol. – 2010. – # 2. – P. 7-17; 12th Intern. Business Meeting "Diagnostics-2002". – Belek, April 2326, 2002. – Vol. 2. Diagnostics of electromechanical equipment, reliability of CS and ecological monitoring. – Vol. 2. – M.: IRTs Gasprom, 2002. – 142 p.*
18. *Nedoseka A. Ya. Some features of application of acoustic emission method at control of material fracture [Text] / A. Ya. Nedoseka, S. A. Nedoseka // Tekhn. diagnostika i nerazrush. kontrol. – 2014. – # 2. – P. 311.*
19. *Nedoseka S. A. Fracture prediction by acoustic emission data [Text] / S. A. Nedoseka // Tekhn. diagnostika i nerazrush. kontrol. – 2007. – # 2. – P. 39.*
20. *Nedoseka S. A. Diagnostic systems of EMA family. Main principles and architectural features (Review) [Text] / S. A. Nedoseka, A. Ya. Nedoseka // Tekhn. diagnostika i nerazrush. kontrol. – 2005. – # 3. – P. 20-26.*

21. *On control of safe operation of equipment carrying the workload. Continuous acoustic-emission monitoring [Text] / A. Ya. Nedoseka, S. A. Nedoseka, M. A. Yaremenko, et al. // Khim. promisl. Ukraini. – 2014. – # 1. – P. 10-21.*
22. *Optimization of transducer arrangement and improvement of accuracy of acoustic emission source location [Text] / S. A. Nedoseka, M. A. Ovsienko, L. F. Kharchenko, M. A. Yaremenko / Tekhn. diagnostika i nerazrush. kontrol. – 2015. – # 3. – P. 18-25.*
23. *On application of AE technology at continuous monitoring of piping of power complexes operating at high temperature [Text] / B. E. Paton, L. M. Lobanov, A. Ya. Nedoseka, et al. // Tekh. diagnostika i nerazrush. kontrol. – 2014. – # 3. – P. 7-14.*
24. *Panasyuk V. V. Fundamentals of material fracture mechanics [Text]: Ref. book in 4 vol. / V. V. Panasyuk, A. E. Andreikiv, V. Z. Parton; Ed. by V. V. Panasyuk, acad. of NASU. – Kiev: Nauk. Dumka, 1988. – V. 1. – 487 p.*
25. *Pat. 2226272. Russian Federation, MPK[7]G 01 N. Method of acoustic emission control and diagnostics of tanks for liquefied gas storage [Text] / V. I. Tarasenko,.B. G. Kim, V. N. Rumyantsev, A. V. Grishin ; publ. 27.03.2004.*
26. *Paton B. E. Modern directions of investigations and developments in the field of welding and strength of structures [Text] / B. E. Paton // Avtomat. Svarka. – October-November. – 2003. – P. 7-13.*
27. *On some ways of construction of automatic information-measuring systems for diagnostics of welded structure reliability [Text] / B. E. Paton, I. V. Kudriavtsev, A. Ya. Nedoseka, A. E. Korotynskii // Avtomat. Svarka. – # 9. – 1974. – P. 1-5.*
28. *Paton B. E. Technical diagnostics: yesterday, today and tomorrow [Text] / B. E. Paton, L. M. Lobanov, A. Ya. Nedoseka // Tekhn. diagnostika i nerazrush. Control. – 2003. – # 4. – P. 6-10.*
29. *Paton B. E. Acoustic emission and structure life [Text] / B. E. Paton, L. M. Lobanov, A. Ya. Nedoseka, et al. – Kiev: Indprom, 2012. – 312 p.*
30. *Paton B. E. On the status of work on technical diagnostics of industrial equipment, structures and constructions in Ukraine [Text] / B. E. Paton, A. Ya. Nedoseka // Avtomat. Svarka. – 1998. – # 11. – P. 39.*
31. *Koumanin V.i. Kovalev, I.a., S.v. Alekseev Durability of metal in terms of creep. -M.: metallurgy, 1988. -202 s.Pustovoj V. N. Metal structures of hoisting machines (Fracture and residual life prediction) [Text] / V. N. Pustovoj – M.: Transport, 1992. – 256 p.*
32. *AE diagnostic system software EMA-3.9 [Text] / A. Ya. Nedoseka, S. A. Nedoseka, M. A. Yaremenko, et al. // Tekhn. diagnostika i nerazrush. kontrol. – 2013. – # 3. – P. 16-22.*
33. *Skalskii V. R. Assessment of accumulation of bulk damage of solids by acoustic emission signals [Text] / V. R. Skalskii // Tekhn. diagnostica i nerazrush. kontrol. – 2003. – # 4. – P.29-36.*
34. *Tu, J. Principles of image recognition [Text] / J. Tu, R. Gonsales – M.: Mir, 1978. – 411 p.*
35. *Feller V. Introduction into the probability theory and its applications [Text] / V. Feller. – M.: Mir, 1984. – V. 1. – 528 p.; V. 2. – 738 p.*
36. *Frolov K. V. Determination of strength, residual life and viability of structures [Text] / K. V. Frolov, N. A. Makhutov, M. M. Gadenin // Avtomat. Svarka. – 2003. – October-November. – P. 89-96.*
37. *Application of acoustic emission method for rapid control of fracture of concretes with plasticizer additives [Text] / N. G. Chausov, S. A. Nedoseka, O. I. Boginich, et al. // Tekhn. diagnostika i nerazrush. kontrol. – 1998. – # 3. – P. 12-16.*
38. *Cherepanov G. P. Quantum fracture mechanics [Text] / G. P. Cherepanov // Probl. Prochnosti. – 1990. – # 2. – P. 39.*
39. *Obodovsky, B. Application of a Permanent Acoustic Emission Monitoring System on Four Ammonia Storage Tanks [Text] / B. Obodovsky, A. Fedchun, A. Nedoseka // Ammonia Plant Safety. – AIChE Technical Manual. – 2006. – Vol. 39. – P. 24-34.*
40. *Balderston, H. L. The broad range detection of incipient failure using the acoustic emission phenomena [Text] / H. L. Balderston // A symposium presented at the December Committee Week American Society for Testing and Materials. – Bal Harbour, 7-8 December 1971. – P. 297-317.*
41. *Chausov, N. G. Accelerated strength check by the acoustic emission method for concrete with additives [Text] / N. G. Chausov, S. A. Nedoseka, N. D. Gakh // International Conference "Acoustic Emission 99". – Brno, 15-17 June 1999. – P. 51-56.*
42. *Stone, D. E. Acoustic Emission parameters and their interpretation [Text] / D. E. Stone, P. F. Dingwall // NDT international. – 1977. – 10. – P. 51-56.*
43. *Forli, O. NDT offshore: a review of current practice [Text] / O. Forli, G. A. Raine // INSIGHT. – June 1996. – Vol. 38. – № 6.*

44. *Gillis, P. P. Dislocation motions and acoustic emission [Text] / P. P. Gillis // A symposium presented at the December Committee Week American Society for Testing and Materials. – Bal Harbour, 7-8 December 1971. – P. 20-29.*
45. *Tsuda, H. Development of Fiber Bragg Grating Sensors for Structural Health Monitoring [Text] / H. Tsuda // JSNDI. – 54-2 (2005), P. 71-75. (in Japanese).*
46. *Use of acoustic emission for the detection of weld and stress corrosion cracking [Text] / C. E. Hartbower, W. G. Reuter, C. F. Morais, P. P. Crimmins // A symposium presented at the December Committee Week American Society for Testing and Materials. – Bal Harbour. – 7-8 December. – 1971. – P. 187-221.*
47. *Nakamura, Yosio. Amplitude distribution of acoustic emission signals [Text] / Yosio Nakamura, C. L. Veach, B. O. McCauley // A symposium presented at the December Committee Week American Society for Testing and Materials. – Bal Harbour, 7-8 December 1971. – P. 164-186.*
48. *Paton, B. E. Diagnostic of designs and safety of an environment [Text] / B. E. Paton, A. J. Nedoseka // the Report on international conference "the Human factor and environment". – International Institute of Welding. – July 19-20 1999. – Lisbon, Portugal.*
49. *About experience of Ukraine in the solution of problems of safety control exploitation of welded structures and preservation of an environment [Text] / B. E. Paton, A. J. Nedoseka, L. M. Lobanov, S. A. Nedoseka // the Report № IIW DOC XI -735 – 00 on commission XI "International Institute of Welding". – July 9-14 2000. – Florence, Italy.*
50. *Nishinoiri, S. Evaluation of Microfracture Mode in Ceramic Coating during Thermal Cycle Test using Laser AE Technique [Text] / S. Nishinoiri, M. Enoki, K. Tomita // Materials Transactions. – 45-1 (2002). – P. 92-101.*
51. *Reid, Stanley. Experience Of Using A Non-Intrusive Approach To The Inspection Of A 23 Year Ammonia Storage Tank [Text] / Stanley Reid // 49th AIChE Safety in Ammonia Plants and Related Facilities Symposium. Denver, Colorado. – Ammonia technical manual. – 2004. – P. 219-230.*
52. *Kishi, T. Acoustic Emission – Beyond the Millennium [Text] / T. Kishi, M. Jhtsu, S. Yuyama. – Elsevier Science Ltd. – 2000. – 239 p.*
53. *Sogabe, T. Monitoring and Source Location of Acoustic Emissions from Atmospheric Corrosion of Water-Stage Cylindrical Tank Bottom Plate Exposed to Outdoor Weathering [Text] / T. Sogabe, K. Matsuuri, M. Takemoto // JSNDI. – 531 (2004). – P. 35-39 (in Japanese).*
54. *Tetelman, A. S. Acoustic emission testing and micro cracking processes [Text] / A. S. Tetelman, R. Chow // A symposium presented at the December Committee Week American Society for Testing and Materials. – Bal Harbour, 7-8 December 1971. – P. 30-40.*
55. *Investigation on AE Signal/Noise Processing in Corrosion Camage Evaluation of Tank Bottom, in Progress in Acoustic Emission [Text] / Z. Li, S. Yuyama, M. Yamada et al. // J. of Acoustic Emission. – 2005. – Vol. 23. – P. 171–178.*

3.2.2 PZT sensors for SHM applications – contributor: TECPAR / ITWL (PL)

Brief overview of SHM technologies

Studies to use measurements of characteristic features of objects, or to monitor critical areas to prevent catastrophic events have been carried out worldwide for many years now [1,2]. There is no 'one and only' effective method that enables detection or description of each and every damage to the structure. In accordance with the assumptions made by Ch. Farrar [3] there exist the following axioms for the SHM implementation:

1. *"All materials have inherent flaws or defects at some level;*
2. *The assessment of damage requires a comparison between two different system states;*
3. *Identifying the existence and location of damage can be done in an unsupervised learning mode, but identifying the type of damage present and the damage severity can only be done in a supervised learning mode;*
4. *A. Sensors cannot measure damage. Feature extraction though signal analysis and statistical classification are necessary to convert sensor data into damage information;*

and:

B. Without intelligent feature extraction, the more sensitive a measurement is to damage, the more sensitive it is to changing operational and environmental conditions.

5. *The length and time scales associated with damage initiation and evolution dictate the required properties of the SHM sensing system;*
6. *There is a trade-off between the sensitivity to damage of an algorithm and its noise rejection capability;*
7. *The size of damage that can be detected from changes in system dynamics is inversely proportional to the frequency range of excitation."*

Structural Health Monitoring is then simply the use of NDI principles associated with in-situ NDI testing of the structure oriented applications. The main goal of the SHM is thus real time damage detection and from the cost point of view, a decrease of the time required for the inspection [4]. There also exist a few challenges associated with the implementation of the SHM technologies for the aerospace community.

These challenges are connected with:

- Costs of the sensor for potential technology;
- Ease of use and local vs global application;
- Need for validation (similar to NDI);
- Certification (reliability analysis, environmental impact etc.);
- Implementation to the maintenance.

If we move to the use of the SHM in the aerospace application few questions have to be addressed to the potential application of the SHM technologies [5]:

"Validation of the ISHM reliability/capability as a function of time/usage:

- *What damage type, size, and location will be reliably sensed?*
- *What is the expected rate of false-positive indications?*
- *What is the service life of the sensors?" e.g. Durability: 40% of strain gages failing within 15 years (Ware, et. al.) "*

There are exist several SHM technologies which are used for damage detection, loads monitoring, deviant analysis (e.g. vibration), corrosion monitoring. Application for that potential SHM technologies differ one to another from the following point of view:

- Technology readiness level (TRL);
- Maturity of the technology for the real case use (than laboratory application);
- Global vs local application;
- Signal analysis
- Reason for sensing.

One of the interesting issues from the point of view of SHM use in 'real aerospace applications' is to answer the key question – what the main goal for the application of such technologies in aerospace components is. This answer is provided by the work done at SANDIA [6]. The Internet survey was addressed to key NDE/SHM personnel including: OEM, manufacturers, airlines, R&D centres, academia etc. Part of the results of the survey are presented in Fig. 21. One of the major applications of SHM is dedicated to fatigue crack detection in the aircraft structure. The consecutives are connected with the composites application what shows potential interest of the diagnostics community in the development of in situ diagnostic capabilities for composites.

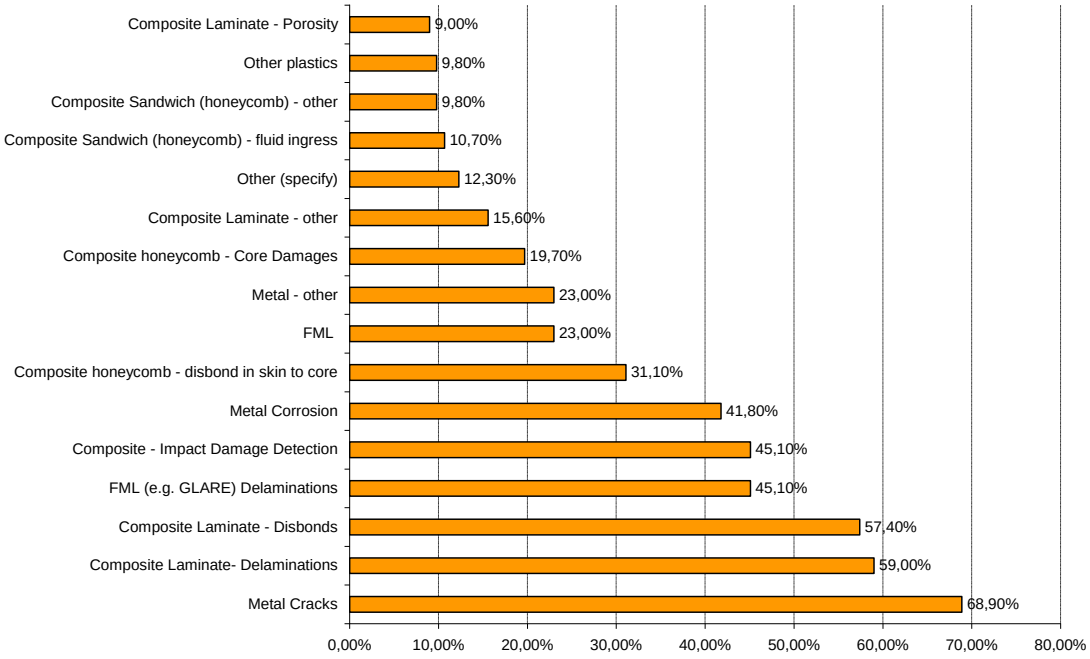

Figure 21. Potential use of the SHM technology

The list of the potential SHM technologies for the aerospace application is presented below [7,8].

A. Electrical strain gauges

Sensors used for load monitoring. Well known and established technology for local stress distribution. An established and reliable technique where strain gauges are bonded into the structure of the aircraft.

They are relatively inexpensive, can achieve total accuracy of better than ± 0.10%, are available in a short gauge length, have high primary sensitivity, and have only moderate thermal sensitivity. Recently the new technologies of the printing sensors have emerged. That technology definitely has the best reputation and is the most commonly used in the aerospace community. Because of the large experience the use of that technology on the major problems identified is connected with low durability of the sensor.

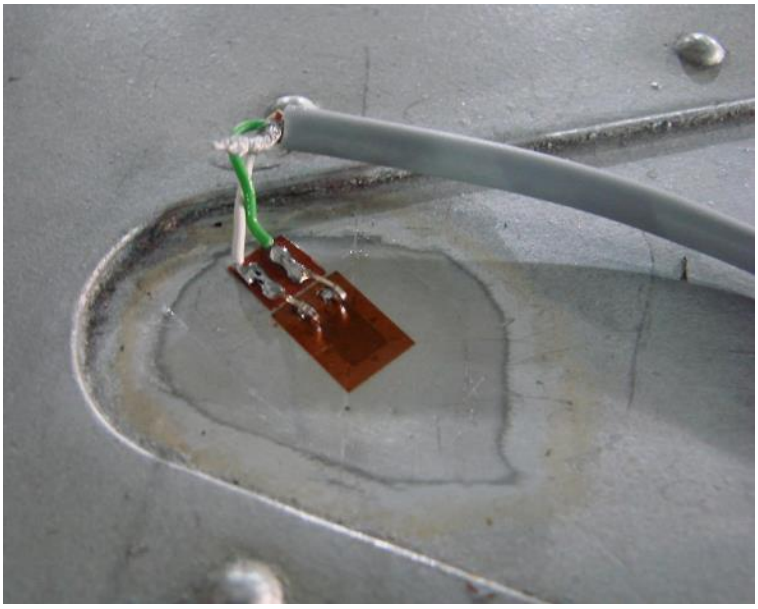

Figure 22. Strain gauge in the structure for load monitoring

Pros: validated and simple technology, low cost of the sensor;
Cons: need for cabling installation and soldering, low durability of the sensors;
Type of monitoring: local area monitoring.

B. Electrical ladder sensors

Simple, reliable and low cost technique that allows cracks of different size to be detected. Similarly to the strain gauges, this technology involves the use of foil sensors bonded to the surface of the monitored location.

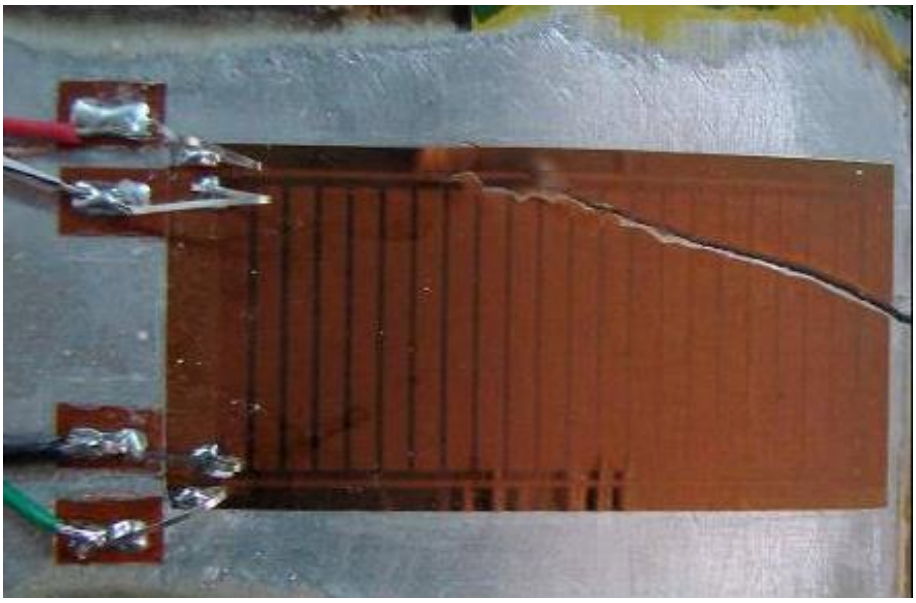

Figure 23. Resistive ladder sensor

The sensor needs to be permanently bonded to the structure in a hot-spot area. When a propagating crack appears under the sensor, it causes a local deformation and gradually tears the foil of the sensor. Concurrently with the foil, permanent open out of conductive path occurs. Electrical resistance is measured between the sensor's two terminals, and any changes affect the output signal.

Pros: simple technology, low cost of the sensor, good detectability if the crack is under the sensor;
Cons: need for cabling installation and soldering, low durability of the sensor;
Type of monitoring: local area monitoring.

C. Optical fibre Bragg grating (FBG)

Although foil resistive gauges currently dominate on the market, a high growth of commercially available fibre-optic solutions for strain measurement has occurred over the last few years. That is rather sensor than any type of monitoring technique18. FBG is to be applied to an optical fibre of 100 μm in diameter or less that can be integrated into a structure.

FBG's are structures made in core of the single mode optical fibre characterized by periodic changes in the value of the refraction index occurring along the axis of the optical fibre. As a result of these changes part of the optical wave transmitted by the optical fibre is reflected by the Bragg grating's structure, and the remainder is propagated along the optical fibre's core without any loss.

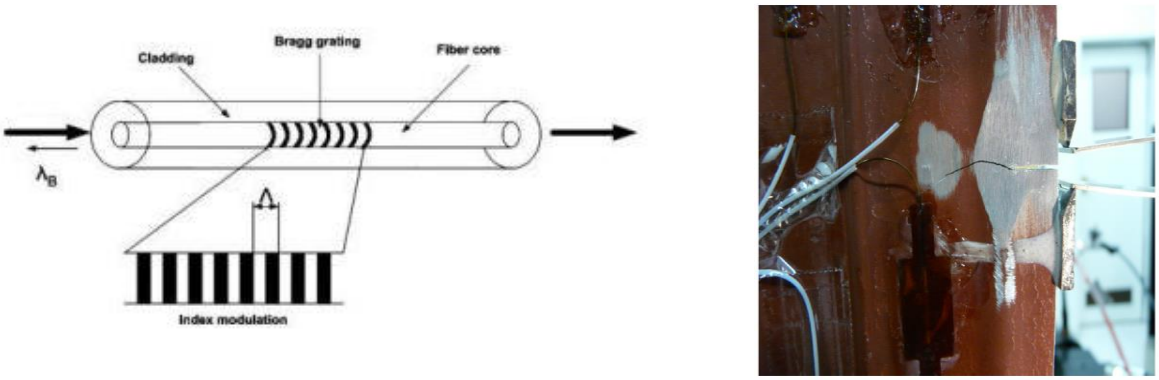

Figure 24. Fibre Bragg Grating Sensor

The sensor is able to monitor any kind of strain resulting from mechanical loads, pressure, temperature, acoustic vibrations or others. A major advantage of the sensor is that a large number of sensors (depending on sampling frequency) can be placed along a single fibre, which significantly reduces wiring complexity. Because it works on an optical basis the system is immune to any electromagnetic interference and makes it easy to compensate for the temperature effect. It has shown robustness with regard to in service application.

Pros: multiple sensors in one wire, electrical free connections, resistant to electromagnetic disturbances;

Cons: costs of the sensor and interrogation unit;

Type of monitoring: local area monitoring (global with the meaning of multiple sensors use).

D. Acoustic emission

Acoustic emission is a recognized NDT technique which enables 'listening' to damage (i.e. crack, delamination) progression developed during operation. AE testing uses changes in signal strength associated with the sudden release of energy emitted because of a changing stress field. That change of the stress field may be connected with the potential growth of the damage in the structure.

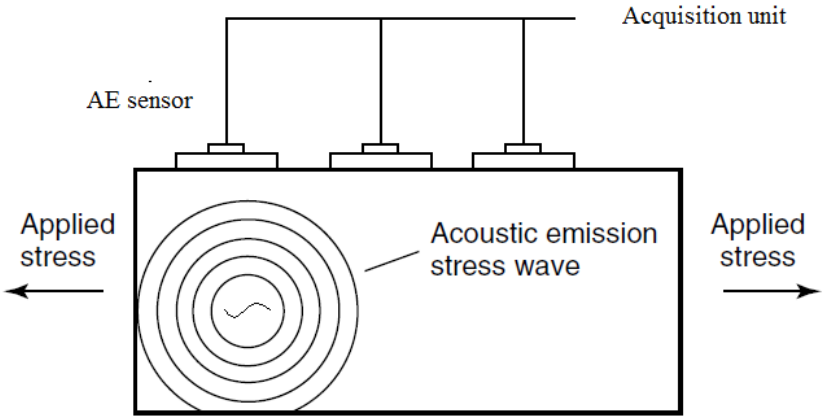

Figure 25. Acoustic emission method

This technique is potentially suitable for global monitoring, however it can only operate when the structure to be monitored is in operation. In that case signals are collected which may be affected by background noise which can complicate the situation for specific applications. The technique is passive, which means that external forces have to be applied to introduce the stresses in the object under investigation. There are several types of acoustic emission methods such as continuous emission and burst emission.

Pros: global monitoring, approved for some NDT applications, no requirements to hold sensor close to the damage;

Cons: does not give direct information about damage severity, complex signal analysis, cabling installation necessity;

Type of monitoring: global monitoring.

E. Nonlinear acoustics:

Traditional active acoustic/ultrasonic methods utilize the linear effects of the wave phenomena such as: reflection, scattering, transmission and attenuation of the elastic waves by structural inhomogeneities to detect structural damages.

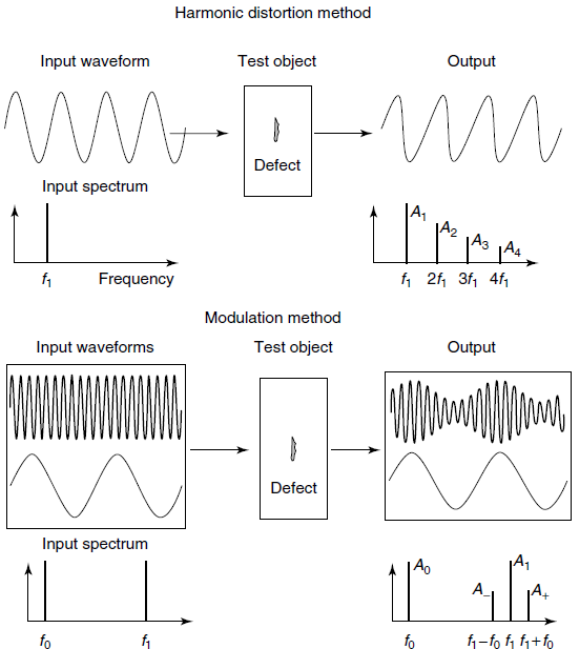

Figure 26. Concept for damage detection with the use of nonlinear acoustics

The use of nonlinear approach for damage sensing deals with the model of the elastic waves introducing stress between the edges of the damage and leading it to a bilinear (nonlinear) stress-strain relationship. Another type of material degradation associated with increased nonlinearity is micro- and mesoscopic fatigue damage accumulation. Here the stronger nonlinearity is due to dislocations, hysteresis, formation of slip planes, and microcrack development and clustering. Scheme for the method is presented in Fig. 20. A signal with a specific frequency is introduced to the tested article. Nonlinearity in the object (as the damage itself) introduce nonlinearities for the waveform so that the spectrum include additional harmonics. Analysing such spectrum components (especially in most cases of the second harmonics) leads to inference about damage presence. There are two primary methods of testing with the use of Non Linear Acoustic Methods: harmonic distortion and modulation. The first correlates the amplitude of the second harmonic (sometimes higher-order harmonics and even intermodulation and sub harmonics) with the presence and severity of the damage. The second one employ the nonlinear interaction of two signals: typically lower frequency modulating vibration and higher frequency probing ultrasound.

Pros: better damage resolution than in linear ultrasonic, use in more complex geometries than ultrasonic;

Cons: laboratory level for the application, requirement for the good baseline signal of the structure;,

Type of monitoring: global monitoring.

F. Acoustic waves propagation:

Acoustic waves are elastic waves that propagate in the structure of the material being inspected. There are many techniques used for the assessment of the material with the use of that technology and such as: ultrasonics, guided waves including acusto - ultrasonics. For the purpose of the SHM the physics of the guided waves is used due to its robustness and possibility of long range propagation (e.g. LRUT – Long Range Ultrasonic).

In the guided waves approach, their energy is guided by the boundaries of the structure. In guided-wave terminology, the structure is referred to as the waveguide, and guided waves include waves on free surfaces (Rayleigh waves), waves in plates (Lamb waves), waves in rods, waves in solid and multi-layered media, isotropic and anisotropic structures.

Guided wave phenomena exist over a wide frequency range from <1 Hz seismic waves generated by earthquakes to >100 MHz surface waves used in acoustic microscopes. Sensing capabilities are based on the linear acoustics principles and waves phenomena such as: reflection, absorption, refraction and mode conversion. There is wide range of approaches for the sensing capabilities including:

- single actuator – sensor ;
- arrays (compact, linear, sparse);
- nodes (multiple sensors, single actuator).

There are also diverse solutions for the actuators (mostly PZT used). In most cases PZT used are generating waves from the point of generation spherically (like source point of radiation). For many applications such approach is inconvenient due to the multiple reflection existence. To avoid that phenomena, unidirectional MFC piezo-composite transducers were elaborated to create one directional field of wave propagation [9]. This approach enables creation of specially designed arrays of transducers inspection of elements with a complicated shape (e.g. ribs, omega shape stiffeners etc.).

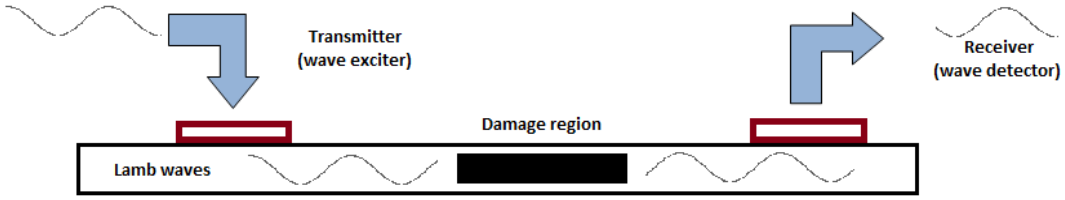

Figure 27. Use of guided waves approach principles

Figure 27 presents the principles of the use of guided waves for damage detection in plate-like structures. A variety of techniques is used in many applications for damage detection based on the Rayleigh-Lamb wave as well as the so-called acousto-ultrasonic technique. In that approach an actuator (usually a piezoelectric transducer) sends an acoustic signal into the structure to be monitored which is then recorded either by the same transducer (pulse-echo) or a different sensor (pitch-catch technique). Usually the network of the transducers is permanently bonded to the structure with the use of special adhesive. A reference signal (the so-called baseline) is taken for the undamaged condition and is compared to all readings from the measurements where the difference in signal is considered to be correlated to damage. In that method the most comprehensive techniques for signal analysis as well for inference about the damage are used.

Pros: high potential for the commercial application (highest assed TRL), ability for global monitoring, signal analysis enables damage recognition and damage size estimation, use of classifiers allows for automated inference about the damage presence;

Cons: need for cabling, the use of baseline is required, need for consideration of the use special algorithms for stress and temperature compensation

Type of monitoring: global monitoring.

G. Laser vibrometry:

The principle of this technique is very similar to acousto-ultrasonics where the laser now takes over the sensor role by being able to scan a larger area. The advantage is the wide scanning area.

A disadvantage is however the access to the component to be monitored which the laser requires.

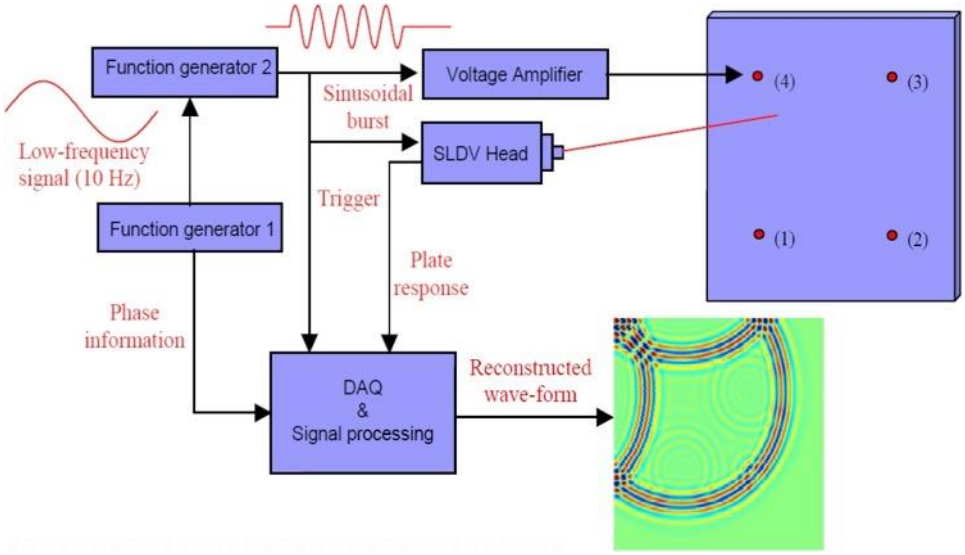

Figure 28. Scheme of the laser vibrometry unit

The way the laser vibrometer operates is similar to the laser interferometer. The main task of that unit is to measure the difference in the frequency (or phase) between the main beam which is the reference beam and the measurement beam reflected from the test article. As the beam source laser as well as laser diodes are used. Measurement beam is guided to the surface of the test article where the beam is reflected and compared with reference beam. Modulation of the measurement signal due to the displacements of the surface because of the wave propagation (the Doppler phenomenon is applied) is then used for the heterodyne process. The output signal which is the sum of the different frequencies from the heterodyne process is acquired and further processed in the system. The final output of the unit is a Frequency Modulated (FM) signal where the carrier frequency is modulated due to the Doppler frequency connected with vibration of the test article.

Pros: wide area of monitoring, fast and very reliable results directly visible in the acquired images;

Cons: direct access to monitored element (not efficient for the substructure), reflection problems, temperature affected;

Type of monitoring: global monitoring.

H. Electromechanical Impedance:

Electromechanical impedance is closely related to the mechanical impedance of a monitored structure. The electrical admittance of the PZT Y, which is the inverse of the electrical impedance Z, can be defined by the following equation [10]:

$$\underline{Y} = j\omega a\left[\underline{\varepsilon_{33}^{T}} - \frac{\underline{Z}_s}{\underline{Z}_s + \underline{Z}_a} d_{31}^2 \underline{Y}_{11}^{E}\right]. \quad (1)$$

where: Z_s is the mechanical impedance of the monitored structure, Z_a is the mechanical impedance of the piezoelectric transducer, a is the geometrical constant of the piezoelectric transducer, d_{31} is the piezoelectric strain coefficient, $\underline{Y}_{11}^{E}$ is the complex Young's modulus, and $\underline{\varepsilon}_{33}^{T}$ is the complex dielectric constant of the PZT material evaluated at zero stress.

a) b)

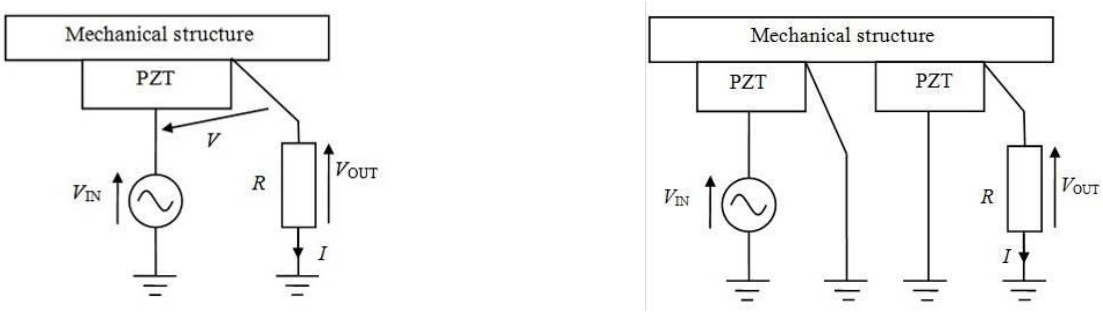

Figure 29. Methods for the measurement of the electromechanical impedance: point frequency response function (a), transfer frequency response function (b)

The two methods used to evaluate the electromechanical impedance are shown in Fig.29. The circuit presented in Fig.29(a) assumes the usage of only one PZT acting as both an actuator and a sensor. The diagram represents the method with a self-sensing actuation and allows to measure a point frequency response function (FRF) of the impedance. The circuit shown in Fig.29(b) corresponds to the second method which is used to evaluate a transfer FRF. The diagram includes two PZTs, an actuator and a sensor, which are mounted in different locations in a structure. In both cases the monitored structure is exposed to high frequency vibrations by applying alternating voltage Vin to one PZT.

The measured voltage V_{out} depends on the voltage V, which is generated in the PZT according to the direct piezoelectric effect. Eventually, the determined complex electrical impedance Z directly corresponds to the variation of the mechanical impedance resulting from any change of the mechanical properties of monitored structure when a damage appears. To qualitatively asses the changes of registered impedance plots, the necessary damage metrics such as Root Mead Square Deviation and Cross Correlation can be applied.

Pros: sensitive to gradual changes of the structural integrity (such as crack propagation), less than wave propagation dependent from the geometry;

Cons: necessity of bonding sensor close to the damage location, necessity to proper selection of damage index functions, more laboratory dedicated;

Type of monitoring: local monitoring.

I. Comparative vacuum monitoring (CVM):

This technique is provided by Structural Monitoring Systems (SMS) is based on a two chamber system of very thin channels introduced into a silicon based sensor. The sensor is placed onto the location prone to cracking. One of the chambers is evacuated with vacuum to be held. Once a crack emerges under the evacuated chamber the pressure increases, which defines the presence of a crack. Detailed visual description of the way the system is operating is presented in the Fig. 30.

The method works well for local monitoring where the location of cracking is well known. However for global monitoring the approach becomes rather complicated. The technique is currently widely explored and validated in various trials with aircraft manufacturers and operators.

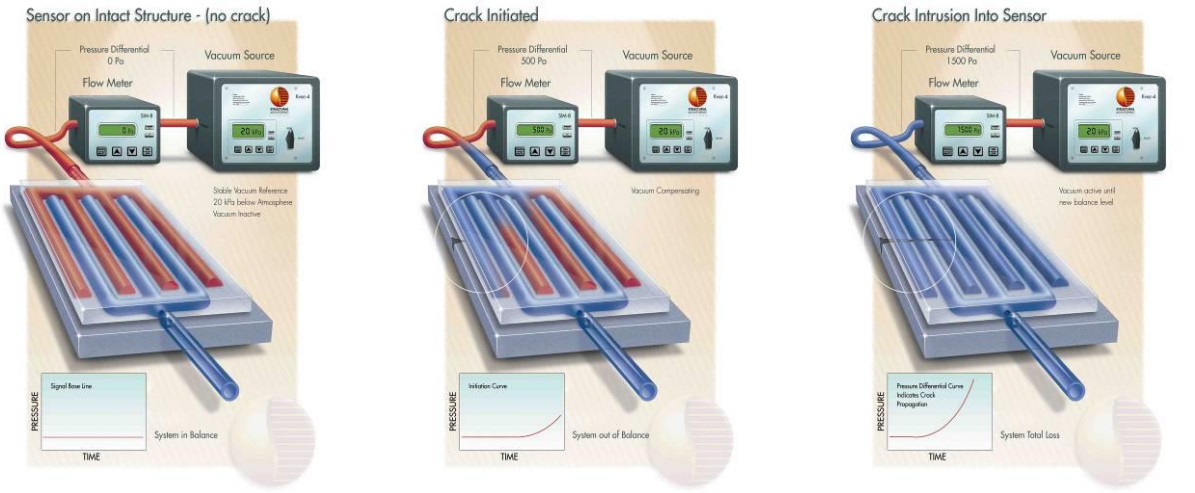

Figure 30. Principles of the system operation for the crack detection

Pros: sensitive to crack detection, possible to design any required shape of the sensor, electrical free, system was used on commercial aircrafts;

Cons: monitoring only for damage located under the sensor;

Type of monitoring: local monitoring.

J. Eddy current sensors (magnetic sensors):

Eddy-current testing (ET) is a non-destructive testing (NDT) technique that uses time-varying magnetic fields to induce eddy currents in a conducting material. ET is used to assess the material under test conditions or to detect flaws. The principle is the generation of electromagnetic fields in the way that is known from high frequency eddy current testing.

The presence of a flaw (e.g. crack) or a variation in a material condition (e.g. residual stress effects on magnetic permeability) is detected by the ET sensor in the region immediately under the sensor.

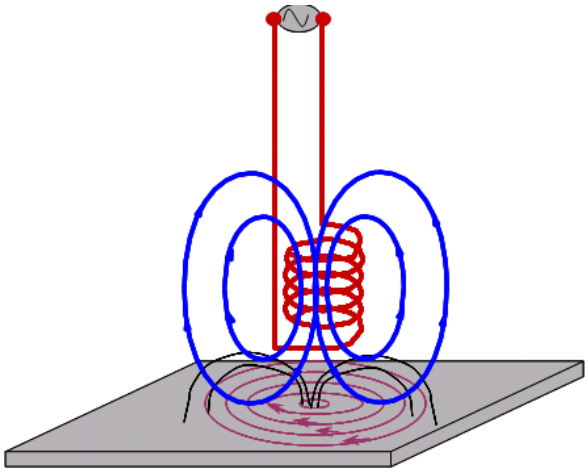

Figure 31. Eddy Current generation in the test article

Thus, ET is a local measurement. Eddy-current in situ sensors exists but the focus is on surface-mounted and embedded sensors for SHM, using onboard instrumentation or portable data-acquisition units. Using a portable data-acquisition system with onboard ET sensors is a direct replacement for conventional ET (NDT), but offers the advantage of allowing for the inspection of difficult-to-access locations without disassembly to gain access.

Pros: sensitive to crack detection, possible to design required shape of the sensor, possible to determine approximate depth of the defect, diverse application possible;

Cons: local monitoring, limitations to ferromagnetic elements as well as low conductivity articles;

Type of monitoring: local monitoring.

K. LPR sensors:

A Linear Polarization Resistor (LPR) corrosion sensor it is a device that corrodes at the same rate as the structure on which it is placed. The sensor is made up of two micromachined electrodes that are interdigitated at 150mm apart. The corrosion reaction – both oxidation and reduction – produces a corrosion current that can be pre-determined empirically for each sensor type, this I/V (Current/Voltage) form is called a Tafel plot [11].

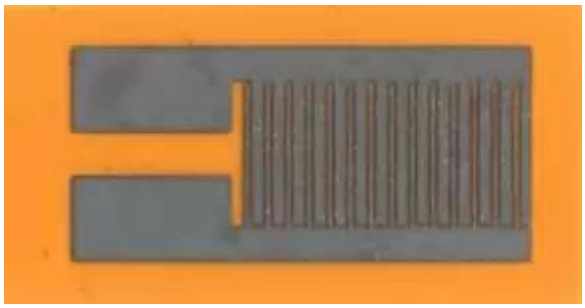

Figure 32. LPR sensor

The sensor itself is made from shim stock of the same material as the structure that is being monitored. The shim is usually 25mm thick (0.001") and is attached to a Kapton backing sheet of similar thickness. This gives the sensor a total thickness of ca 50mm, although a thickness of up to 200mm is possible if required. The shim is machined (pattered) using a photolithography technique, this allows for a varied design layout so that sensors can be fitted deep into tight structures such as bridge cables and lap joints. The sensor can be placed directly on the metal surface of the structure to be monitored. Painting and other surface preparations can be performed on top of the sensor with no damage to the sensor or coating. The sensors are unobtrusive in operation and require no maintenance or inspection.

Pros: sensitive to corrosion growth, corrosion growth rate determination possibility;

Cons: local monitoring, relatively clean aqueous electrolytic environments necessary for use;

Type of monitoring: local monitoring.

L. Other solutions:

There are many other solutions which are being developed for the use potentially in the aerospace environment. There are: MEMS, wireless strain sensors, optical based sensors (DMI SR2), RFID sensors, Fibre Optic Sensors (FOS), techniques based on brittle coatings, magnetic sensors which utilize magnetostriction phenomena, chemical sensors which are also used in several lab trials in scientific test. Most of them still are at a low TRL level. The work presented only mentions potential technologies which are found in some aerospace applications (mainly laboratory). To identify clearly what the TRL is the following classification were used:

Mimics TRLs used by NASA & military - this classification system clearly defines benchmarks, direction and maturity of emerging Technologies:

- ***TRL 1*** *- Physical principles are postulated with reasoning;*
- ***TRL 2*** *- Application for physical principles identified but no results;*
- ***TRL 3*** *- Initial laboratory tests on general hardware configuration tocsupport physical principles;*
- ***TRL 4*** *- Integration level showing systems function in lab tests;*
- ***TRL 5*** *- System testing to evaluate function in realistic environment;*

- ***TRL 6*** *- Evaluation of prototype system;*
- ***TRL 7*** *- Demonstration of complete system prototype in operating environment;*
- ***TRL 8*** *- Certification testing on final system in lab and/or field;*
- ***TRL 9*** *- Final adjustment of system through mission operations.*

So far the highest ranked TRL in the aerospace for the SHM application of 8-9 is for electrical strain gauges and crack propagation sensors, FBG sensors as well as CVM. PZT applications have reached the level of 5-6. Therefore, to increase TRL and determine both diagnostic capabilities and limitations to be used then throughout the operational phase, it seems quite reasonable and of significance to carry out research on PZT applications and other abovementioned techniques.

PZT sensors

The most common way to actuate elastic waves is to use special electromechanical properties of piezoelectric ceramics. Piezoelectric ceramics have the property of developing an electric charge when mechanical stress is exerted on them. In these materials, an applied electric field produces a proportional strain. The electrical response to mechanical stimulation is called the direct piezoelectric effect, and the mechanical response to electrical stimulation is called the converse piezoelectric effect. Ceramics are inorganic non-metallic materials. Piezoelectric ceramics differ from piezoelectric crystals in that they must undergo a poling procedure for the piezoelectric phenomenon to occur.

For each material there is a characteristic Curie temperature. Above the Curie temperature electric dipoles inside the material exist in random orientations. When a strong electric field is applied they become aligned in the direction of the field and remain partially aligned after the field is removed, provided the material is first cooled well below its Curie temperature. In this state the ceramic is said to be poled. When the poled ceramic is subjected to a small electric field the dipoles respond collectively to produce a macroscopic expansion along the poling axis and contraction perpendicular to it [12-18].

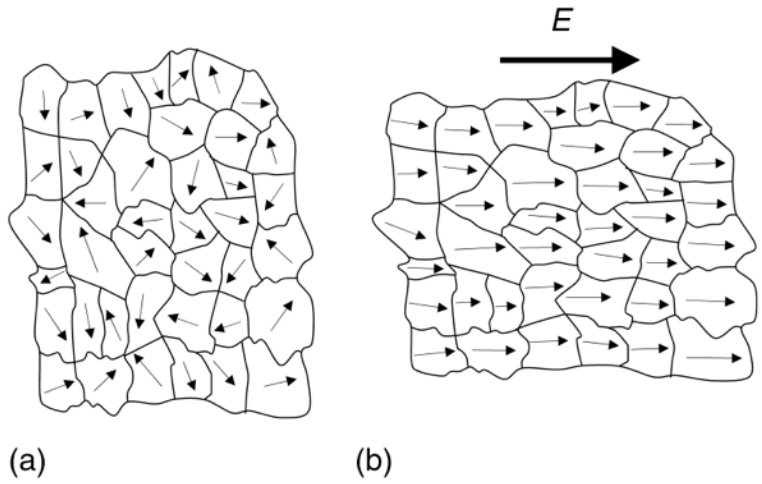

Figure 33. Polycrystalline perovskite ceramics: (a) not pooled and (b) after pooling [13]

The advantages of PZT ceramics are: simple technology and low manufacturing costs, easy machining which allows to obtain transducers of different shapes. Beside single layer transducers also multi-layered ones can be manufactured, by joining many layers of PZT ceramics with electrodes. This allows for obtaining a higher range of attainable displacements. In SHM systems also Interdigital Transducers – IDT are used [15], which allows for directional actuation of elastic waves. Their additional advantage is possibility to adjust the length of the wave, which is appropriate for detection of damage of given type. PZT ceramics are also mixed with epoxy resins, for production of the so-called Macro Fibre Composite MFC – transducers [15], characterized by their high elasticity. In this way also highly integrated sensor patches are manufactured, e,g. SMART Layer® [15], which are ready to be integrated directly with the structure.

Yet another way to obtain elastic piezoelectric transducers is to use polymer transducers, e.g. polyvinylidene PVDF [12,15], which additionally has very small thickness. The inertia of piezoelectric transducers is low, thus in SHM systems they are used as actuators and sensors of elastic waves of high frequencies, sensors of vibrations, strain gauges in fast processes, as well as accelerometers [12,13].

Structural damage, irrespectively of their type, cause local changes of material properties affecting elastic waves propagating through damaged area [13]. Therefore PZT transducers can be widely applied for SHM. Applications of piezoelectrics in SHM systems include the so-called passive monitoring techniques, when they are used only as receivers of elastic waves actuated by an event leading to damage (e.g. impacts) or the waves emerge by releasing energy by developing damage – Acoustic Emission (AE). PZT networks can be used also as active elements – actuating in a monitored elements elastic waves.

Multilayer piezoelectric transducers are electromechanical devices for generating movements in the micrometre range. The conversion of electrical energy into mechanical motion takes place without the generation of any magnetic field or the need for moving electrical contacts. Piezoelectric devices are capable of response times in the microsecond range and can develop blocking forces up to several kN and their stroke varies approximately linearly with applied voltage.

Piezoelectric actuators possess unique and interesting properties. Dimensional changes proportional to the applied voltage can be adjusted with infinite resolution. They can be operated over billions of cycles without wear or deterioration. Speed of response is very high, limited only by the inertia of the object being moved and the output capability of the electronic driver. Virtually no power is consumed or heat generated to maintain a piezoelectric actuator in an energized state. Multilayer actuators may be fabricated from thin sheets of tape-cast ceramic [19].

During dynamic operation of a piezoelectric actuator, the PZT material will undergo a certain degree of aging, which will be observed as a small loss of displacement and blocking force, when comparing a virgin actuator with an actuator that has undergone a certain amount of actuations. The blocking force is defined as the force required for pushing back a fully energized actuator to zero displacement. The loss of performance is primarily encountered for the initial cycles, after which the aging becomes almost negligible. Aging is thus a logarithmic function of time [19]:

$$d(t) = d(t_0) + A\log\left(\frac{t}{t_0}\right),$$

where:

- A is the “aging rate” constant, specific to the composition, microstructure and the processing history of an element
- d is a constant representing the piezoelectric sensitivity by relating mechanical strain with the applied electric field, i.e. the ratio of strain to the electric field applied.

The below voltage-stroke diagram shows an example of a stacked actuator that has been measured for performance at four steps during an accelerated lifetime test [19]:

- in the virgin state
- after having undergone 10^7 cycles
- after having undergone $3x10^7$ cycles
- after having undergone 10^8 cycles.

The free stroke refers to the displacement achieved by the actuator at a given voltage level without the actuator working against any external load. The loss of performance is in the order of 10% after the first 10^7 cycles.

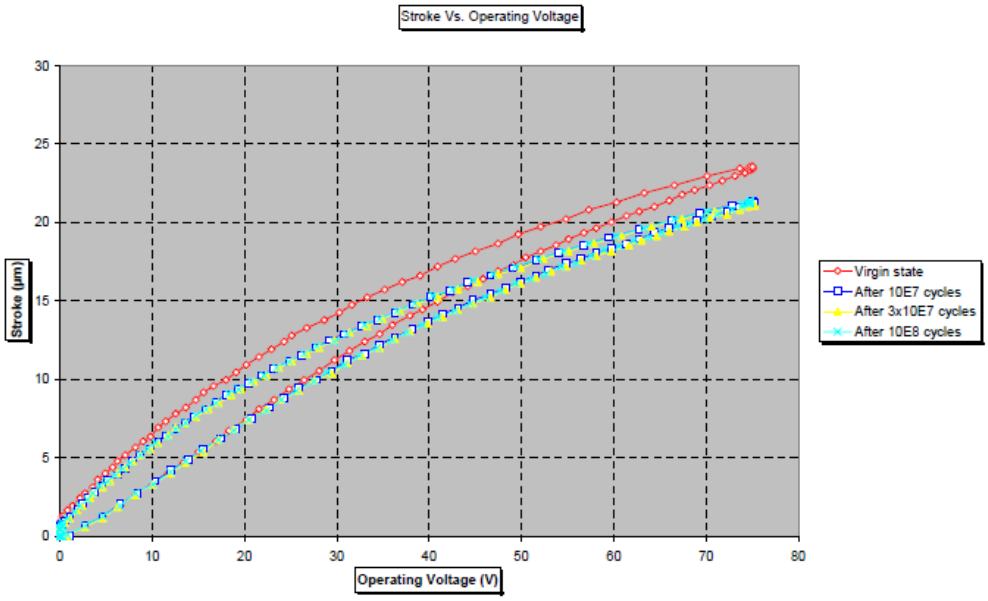

Figure 34. The voltage – stroke diagram showing aging performance loss of a PZT actuator [19].

Signal processing and damage detection algorithms I: damage indices

One of the major obstacle in direct application of Lamb waves in structure evaluation is the complexity of signals excited in real structures. Two examples of baseline signals obtained for structures of simple geometry and containing riveted joints and other wave reflectors are presented on the following figure (Fig. 35).

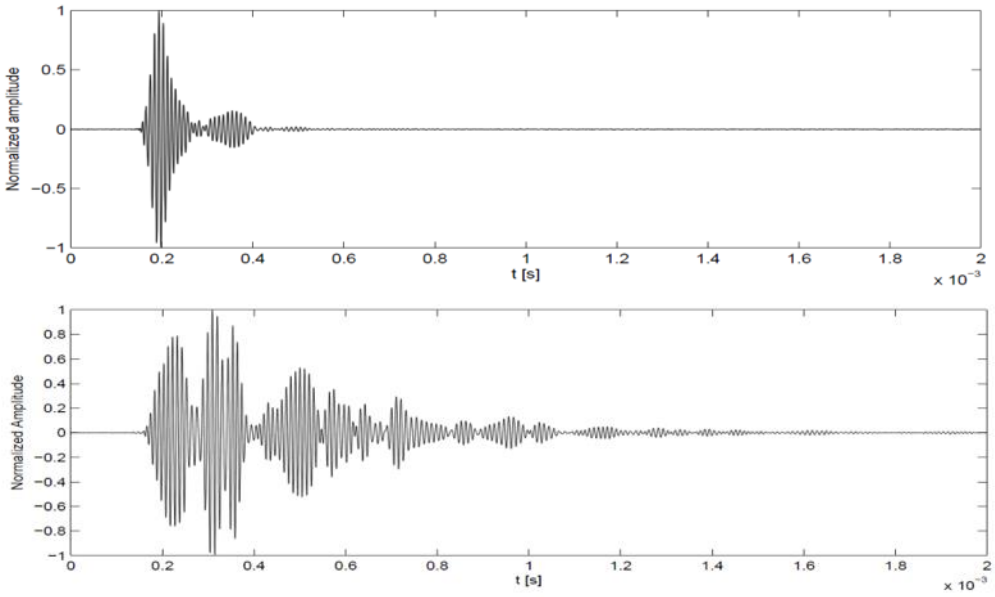

Figure 35. Examples of reference signals for structures of different type.

Reliable SHM systems should therefore provide different type of damage assessment which would allow for cross-validated evaluation of the structure:

- qualitative data - damage presence in a given network cell, its kind and the degree of criticality;
- quantitative data - exact location and size of a damage.

Basic information concerning the health of the structure can be provided by the so-called Damage Indices (DI's). Denoting as f_{gs} the signal generated in transducer g and received in sensor s and as $f_{gs,b}$ its baseline, i.e. the reference signal collected for the undamaged state of the structure, some basic DI's can be defined using the following simple signal characteristics [20]:

L^1 symmetric characteristic – $$DI_1(g,s) = \frac{\left|\int (|f_{gs}| - |f_{gs,b}|)dt\right|}{\int |f_{gs,b}|dt}, \quad (1)$$

L^2 symmetric characteristic – $$DI_2(g,s) = \frac{\left|\int (f_{gs})^2 - (f_{gs,b})^2 dt\right|}{\int (f_{gs,b})^2 dt},$$

correlation with the baseline – $$DI_3(g,s) = cor(g,s).$$

Similar DI's can be obtained using Fourier filtered signals, their envelopes or other signal transformations. These DI's are correlated with the total energy received by a given sensor therefore can capture the two main modes of guided wave interaction with a fatigue crack. Low information content carried by those DI's, makes them more persistent under varying sensor working conditions. This should improve the false calls ratio of the system.

There are remarkable examples of applications of analogous DI's to determine localization of a damage [21-23]. In these methods two stage algorithms are used. First for each sensing path $g \to s$, i.e. a signal received in sensor s originated from generator g, the structure is quantified into a damaged or undamaged state. This quantitative assessment can be performed using certain threshold level of one or multiple DI's. Then if the structure is considered as damaged a probability density of a damage localization in a given network cell is calculated. This density depends on DI's values and properly defined distance of a given point from a sensing path $g \to s$. Finally joint probability for a damage localization is provided using probability maps obtained for all possible sensing paths in the network cell.

There are several limitations of the described SHM method. In particular in order to obtain accurate damage location probability map there is necessity to consider sensing paths for many transducers what influence on computational and system implementation costs. Furthermore improper functioning of a single sensor in the network decrease number of reliable sensing paths which can disturb this probability density. Another obstacle in this approach is system sensitivity adjustment. In complex structures, which contain many wave reflectors, e.g. edges, joints, welds, rivets, etc. resulting map for sensitive algorithms can be noised [24], whereas weakening susceptibility of sensing paths cause risk of damage missing. However the main disadvantage of that method is the difficulty in estimating damage size. Since damage indices $DI_j(g,s)$ (Eqn. (1)) used for structure quantification in these algorithms depends strongly on damage localization with respect to given sensing path $g \to s$ it is very difficult to use regression or classification models in estimating size of a damage. In order to overcome the last issue the Averaged Damage Indices (ADI's) can be defined [25]:

$$ADI_j := \frac{1}{n(n-1)} \sum_{\substack{g,s: \\ g \neq s}} DI_j(g,s), \quad (2)$$

where n is the number of transducers in a network measurement node. Averaged damage indices (ADI's) are less dependent on the damage localization which makes them better suited for damage size estimation, in particular they are invariant with respect to sensors permutation.

These indices remain structure quantification possibility also in the case of improper functioning of several transducers of the network. The procedure of averaging (Eqn. (2)) is highly sensitive to outlying observations, emphasizing the importance of the sensor self-diagnostic component of the system. Relying on the ADI's defined above (Eqn. (2)) effective fatigue crack growth predictors can be obtained by means of statistical dimensional reduction methods, e.g. Principal Component Analysis (PCA) or Fisher's Linear Discriminant (FLD) [26].

PZT sensors for SHM applications: case studies

Laboratory test of aircraft specimens. In order to illustrate the proposed damage detection algorithms the results of fatigue test of an aircraft structure specimen are presented in this section [27]. Two independent piezoelectric transducers (PZT) networks, containing 4 sensors each were deployed on the structure (Fig. 36).

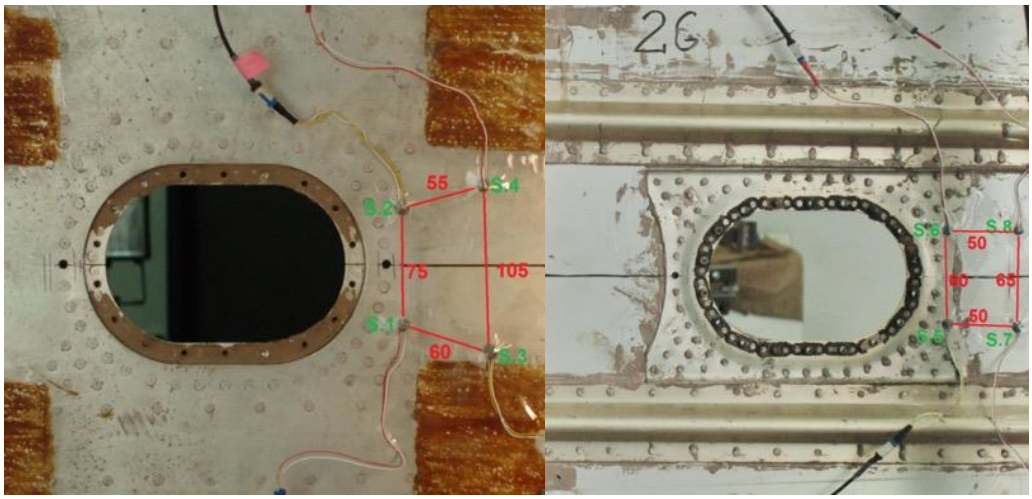

Figure 36: The specimen and the network deployed (network dimensions given in millimetres)

Signals were gathered under three different structure loads at each level of the damage development. The two chosen Principal Component Based efficient damage predictors (EDP's) with the best data separation properties as well as the first two Fishers' linear discriminant [26] EDP's are presented on the following plots (Fig. 37).

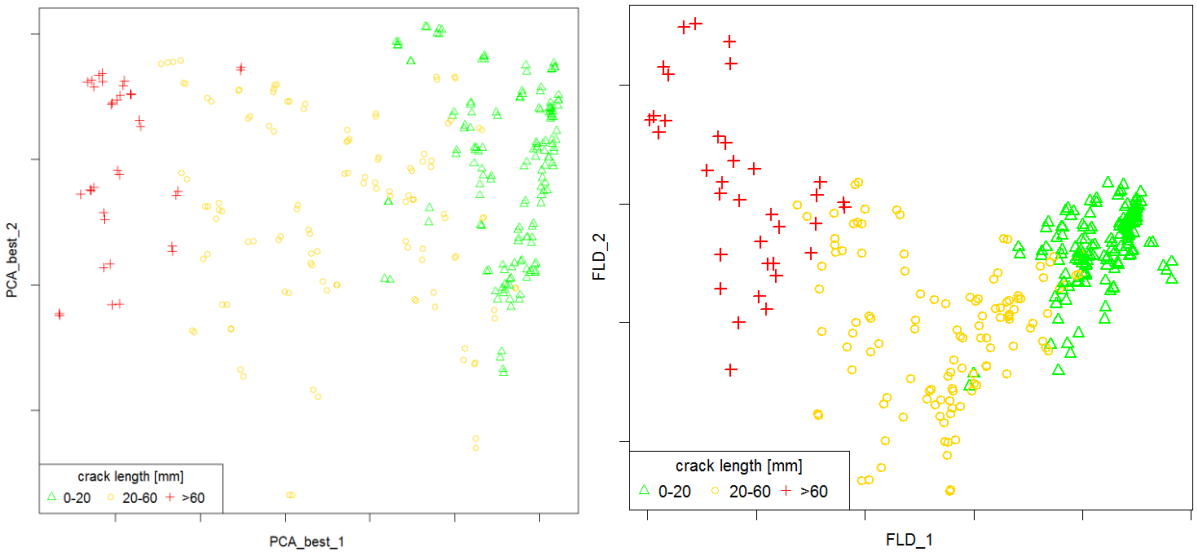

Figure 37. PCA (left) and FLD (right) based EDP's.

In the case of PCA method, only the first EDP distinguish data corresponding to different crack length, whereas in the case of Fishers' method both of the indices FLD_1, FLD_2 improve data separation. The data are well separated in both cases, with negligible overlaps, which may be caused by different stress distributions in the structure during measurements. Under high loads changes of Fisher's predictors LDA_1, LDA_2 for smaller cracks are comparable to those obtained for longer cracks under free end conditions. This yields misclassification probability between second (20-60 mm cracks) and third class (>60 mm cracks) of the damage severity.

Based on Fishers' efficient damage predictors FLD_1, FLD_2 nearest neighbour (NN) and LDA classification models were obtained. Their classification regions are presented on the following plot (Fig. 32).

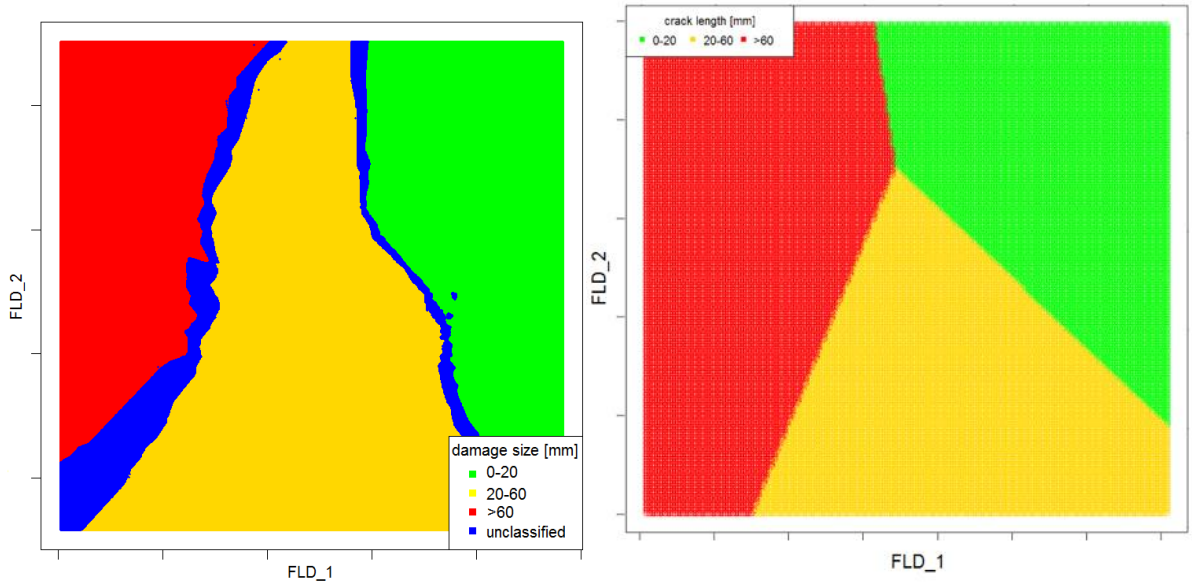

Figure 38. NN (left) and LDA (right) data classification domains.

The nearest neighbour model reproduces the gap between undamaged (0-20 mm crack length) and severely damaged (>60 mm crack length), however classification regions of LDA model due to their regularity are more stable making the model better suitable for real applications.

PZT network application for fatigue crack growth monitoring during fatigue test of a helicopter tail boom

The fatigue test of a helicopter tail boom is a part of the European Defence Agency's ASTYANAX (Aircraft fuselage crack monitoring sYstem And prognosis through on-boArd eXpert sensor network) project [28]. The platform used for the project is Mi-8/17 helicopter. The tail boom of the helicopter was equipped with FBG, PZT sensors as well as crack gauges. In Fig. 33 a PZT network and crack gauges installed near an introduced crack are presented.

Two kind of PZT transducers were used: single- and multi-layered. The following parameters of PZT excitation were used:

- excitation frequency [kHz]: 100, 150, 200, 250, 300;
- duration: 3 or 8 periods;
- window type: Hanning.

The signal from PZT network is gathered under varying loads which can contribute to the DIs drift effect [20].

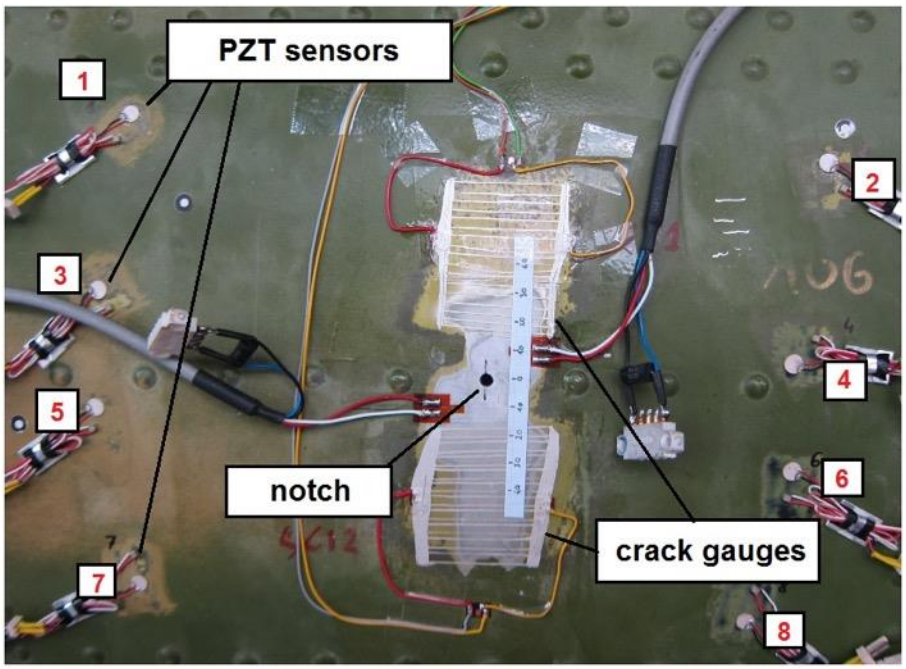

Figure 39. PZT sensors and crack gauges deployed on the helicopter structure with numeration of PZT network

In order to illustrate DIs change within a network a map:

$$I(x,y) = \max_{g,s} DI_1(g,s) R_{gs}(x,y), \qquad R_{gs}(x,y) = \left(\frac{l_{gs}}{l_{gp} + l_{gs}} \right)^{40}$$

is used, where l_{gp} , l_{gs} denoting the distance of the point *p* from the generator *g* or the sensor *s* respectively and l_{gs} is the distance between generator *g* and sensor *s*. The DI value on a given sensing path is weighted with a map R_{gs} representing the geometry of a given sensing path.

Fig. 40 shows the map before (Fig. 10(a)) and after (Fig. 10(b)) the compensation of the DI [20] for single layered transducers at the frequency 150 kHz. The change of compensated DI is the highest for sensing paths running in close proximity of the crack (Fig. 10(b)), whereas uncompensated DI can change also for paths for which signal should not be influenced by a damage (Fig. 10(a)), which can lead to a false indication of the system.

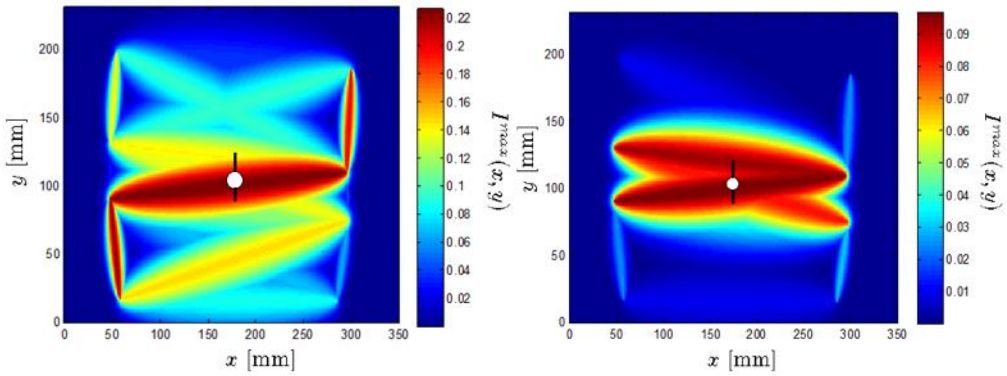

Figure 40. Visualisation of Damage Index change within the network using: (a) not compensated and (b) compensated DI.

PZT network application for fatigue crack growth monitoring during Full Scale Fatigue Test of PZL-130 ORLIK aircraft

Full Scale Fatigue Test of PZL-130 Orlik aircraft was performed due to structure modifications. That test opened an opportunity for a SHM system installation at selected aircraft hot spot locations (Fig. 35) monitoring as well as early damage detection as alternative approach which may support or in the future partially replace the scheduled NDI inspections [29].

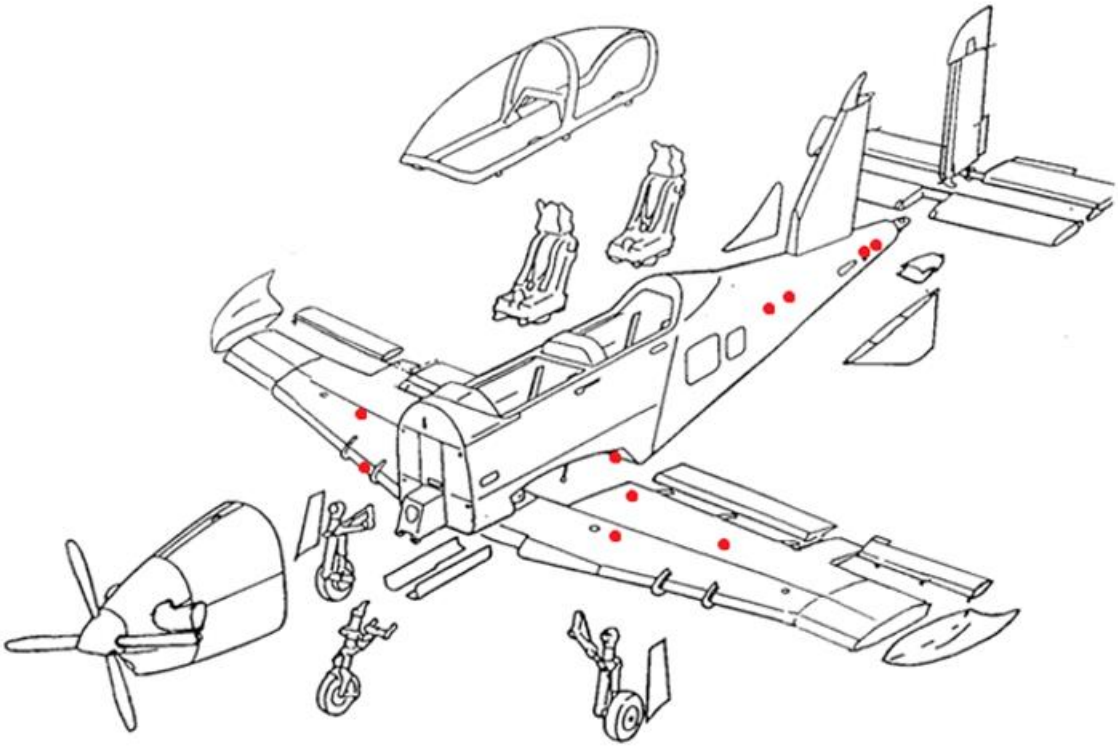

Figure 41. Selected aircraft hot-spots.

The SHM system building blocks are schematically presented on the figure (Fig. 41). These are:

- PZT network divided into several measuring nodes;
- Remote Monitoring Unit (RMU) – based on DSP architecture CPU;
- Data Storage Unit (DSU);
- Graphical User Interface (GUI).

The core of the RMU consists of four subsequent routines:

- signal collecting and its storage in DSU if indicated by sensor self-diagnostics component;
- signal processing based on several signal Damage Indices (DI's) correlated with the fatigue crack growth;
- sensor self-diagnostic component validating the PZT network, e.g. noise detection, sensors' surface coupling strength, significant sensor working conditions changes detection;
- data classification methods for damage growth assessment.

One of the key issues in applying of PZT-based monitoring systems to structures used in aerospace is to ensure sensor network durability in extremely varying environmental conditions. Thus a self-diagnostic tool network allowing for signal decoherence tracking in time is a vital component for any such application. Furthermore the most of data classification models are sensitive to outlying observations, therefore efficient sensor self-diagnostic prior to crack growth assessment is crucial for proper system operation, e.g. avoiding misclassification.

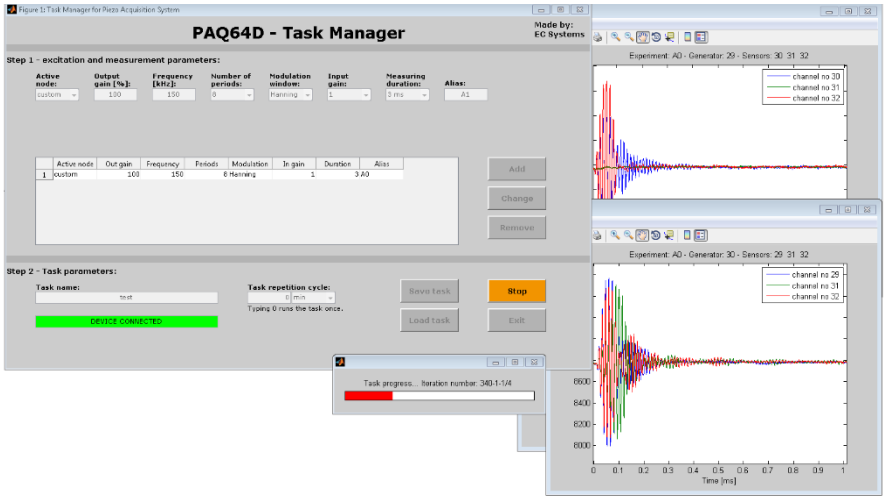

Figure 42. PZT sensor network remote monitoring unit control panel

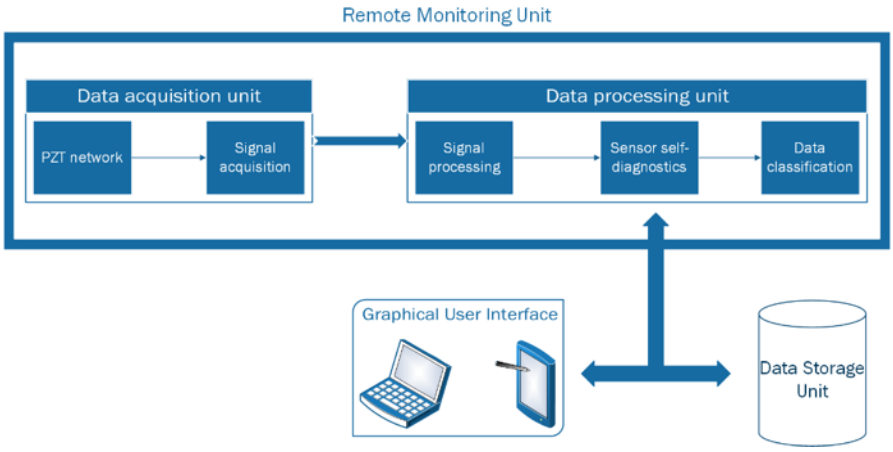

Figure 43. SHM system block diagram

In the proposed approach signals which do not pass the sensor integrity check are stored in DSU for further expert assessment as shown in Fig. 43.

Damage detection capabilities of the system are discussed based on two chosen monitored hot-spots (Fig. 44). In both of the locations Resistance Crack Gauges (RCG) adapted to the structure geometry were installed in order to verify the system indications. The crack was developing in the network shown in Fig. 44(b) and the other hot-spot (Fig. 44(a)) remained undamaged. One of the network nodes (Fig. 44(a)) was installed on a structure containing riveted joints and other wave reflectors, the other structure (Fig. 44(b)) was of relatively simple geometry. The Averaged Damage Indices for both of the nodes are presented in Fig. 45. It was noticed that the number of well separated groups of data, corresponding to different extent of the crack, agrees with the number of sensing paths crossed by the crack. The data corresponding to subsequent periods of the monitoring of the undamaged structure are not separated (Fig. 45).

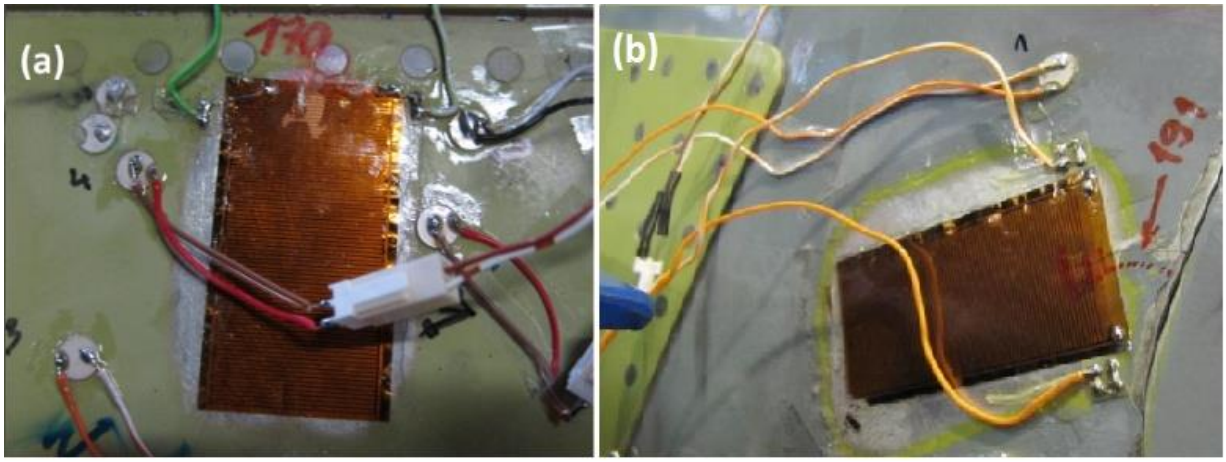

Figure 44. Example of monitored hot-spots

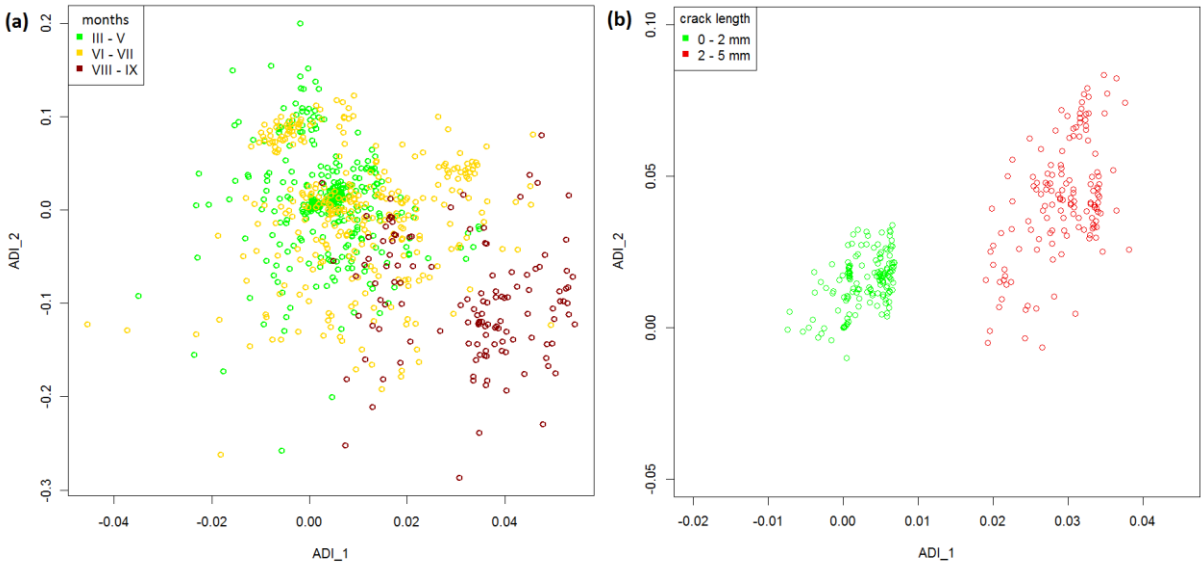

Figure 45. Averaged Damage Indices for the monitored hot spots

References

1. *M. Abe, „Monitoring of a Long Span Suspension Bridge by Ambient Vibration Measurement," Structural Health Monitoring 2000, Stanford University, Palo Alto, California, pp. 400–407.*
2. *S.W. Doebling, S „A Summary Review of Vibration-Based Damage Identification Methods," The Shock and Vibration Digest, 1998, Vol. 30, No. 2, pp. 91-105.*
3. *K. Worden, C. R. Farrar, G. Manson and G. Park "The Fundamental Axioms of Structural Health Monitoring," Proceedings of the Royal Society A: Mathematical, Physical and Engineering Sciences Issue 463 (2082) June, 2007.*
4. *D. Roach, S. Neidigk, „Does the Maturity of Structural Health MonitoringTechnology Match User Readiness", 9th International Workshop On Structural Health Monitoring, September 10-12, 2013, Stanford.*
5. *C.A. Babish "Requirements Associated With Transition of ISHM into USAF Aircraft," ISHM Conference, 2009.*
6. *S. Neidigk, B. Smith, D. Roach, "Use of Technology Assessment Databases to Identify the Issues Associated with Adoption of Structural Health Monitoring Practices", ATA NDT Forum 2010, 20-23 Sep, Albuquerque, New Mexico USA.*
7. *Ch. Boller, n. Meyendorf, „State-of-the-Art in Structural Health Monitoring for Aeronautics", Proc. of Internat. Symposium on NDT in Aerospace, Fürth/Bavaria, Germany, December 35, 2008.*
8. *Ch. Boller, F.K. Chang, Y. Fuijno, Encyclopedia of Structural Health Monitoring, Volume 4, Willey, ISBN: 978-0-470-05822-0, January 2009.*

9. *Wilkie, W.K. Bryant, G.R., High, J.W. et al., „Low piezocomposite actuator for structural control applications" Proceedings SPIE 7th Annual International Symposium on Smart Structures and Materials, Newport Beach, CA, March 5-9, 2000.*
10. *G. Park, H. Sohn, C.R. Farrar, Overview of piezoelectric impedance-based health monitoring and path forward, Shock Vib. 35(6) (2003) 451-463.*
11. *www.analatom.com*
12. *Stepinski, T., Uhl, T., Staszewski, W. Advanced Structural Damage Detection: From Theory to Engineering Applications. John Wiley & Sons, 2013.*
13. *Giurgiutiu, V. Structural health monitoring: with piezoelectric wafer active sensors - 2nd ed. Academic Press, 2014.*
14. *Ostachowicz, W., Kudela, P., Krawczuk, M., & Zak, A. Guided waves in structures for SHM: the time-domain spectral element method. John Wiley & Sons, 2011.*
15. *Su, Z., Ye, L. Identification of damage using Lamb waves: from fundamentals to applications. Springer, 2009.*
16. *Qin, Q.-H. Advanced mechanics of piezoelectricity. Springer, 2013.*
17. *Heywang, W., Lubitz, K., Wersing, W. Piezoelectricity: evolution and future of a technology, vol. 114. Springer, 2008.*
18. *Helke, G., Lubitz, K. Piezoelectric PZT ceramics. In Piezoelectricity. Springer, 2008, pp. 89–130.*
19. *http://www.noliac.com/*
20. *K. Dragan and M. Dziendzikowski. A method to compensate non-damage related inuences on damage indices used for pitch-catch scheme of piezoelectric transducer based Structural Health Monitoring. Structural Health Monitoring, 15(4):423437, (2016).*
21. *Q.W. Wang and B.X. Sun 'Structural damage localization and quantification using static test data', Struct. Health Monit. Vol. 10(4) (2010), p. 381.*
22. *T.R. Hay, R.L. Royer, H. Gao, X. Zhao and J.L. Rose 'A comparison of embedded sensor Lamb wave ultrasonic tomography approaches for material loss detection', Smart Mater. Struct. Vol. 15(4) (2006), p. 946.*
23. *D. Wang, L. Ye, Y. Lu and Z. Su 'Probability of the presence of damage estimated from an active sensor network in a composite panel of multiple stiffeners', Compos. Sci. Technol. Vol. 69(13) (2009), p. 2054.*
24. *T. Clarke and P. Cawley 'Enhancing the defect localization capability of a guided wave SHM system applied to a complex structure', Struct. Health Monit. Vol. 10(3) (2010), p. 247.*
25. *M. Dziendzikowski, A. Kurnyta, K. Dragan, S. Klysz, and A. Leski. In situ Barely Visible Impact Damage detection and localization for composite structures using surface mounted and embedded PZT transducers: A comparative study. Mechanical Systems and Signal Processing, 78:91-106, (2016).*
26. *T. Hastie, R. Tibshirani, J. Friedman: The Elements of Staistical Learning: Data Mining, Inference, and Prediction, second ed., Springer Science+Business Media, New York, 2009.*
27. *K. Dragan, M. Dziendzikowski, S. Klimaszewski, S. Klysz, A. Kurnyta. Energy correlated damage indices in fatigue crack extent quantification. Key Engineering Materials, 569-570:118-1193, (2013).*
28. *M. Dziendzikowski, K. Dragan, A. Kurnyta, S. Klimaszewski, A. Leski, and G. Vallone. Fatigue cracks detection and their growth monitoring during fatigue test of a helicopter tail boom. In F.-K. Chang and F. Kopsaftopoulos, editors, Structural Health Monitoring 2015. DEStech Publications, Inc, (2015).*
29. *K. Dragan, M. Dziendzikowski, A. Kurnyta, A. Latoszek, A. Leski, and S. Kªysz. An on-line multiway approach to in-situ ndi looking at the PZL-130TCII. Fatigue of Aircraft Structures, 1:5-11, (2013).*

3.2.3 Problems of the installation of FBG sensors in composite structures – contributor: KhAI (UA)

The installation of FBG sensors in composite structures for structural health monitoring requires measures and techniques to guarantee their reliability and durability. Embedding the FOBG sensors during manufacturing is a tedious task because it involves many difficulties such as the selection of ingress and egress points of the sensor data lines, the possible effect of the embedded sensors and ancillaries on the mechanical properties of the composite and the risk of sensor breakage during fabrication. Usually the sensors are surface-mounted or integrated into the composite structure.

Surface mounting is less challenging than embedding but also less suitable, due to the high fragility of the optical fibre. The literature contains extensive research regarding the strain transfer between surface-mounted FBG sensor and substrate. Due to the intense temperature/pressure conditions occurring during curing, the primary coating of the optical fibre was polyimide with a polyimide recoating on the grating location after inscription of the FOBGs to improve the mechanical performance. In this case, the adhesive layer thickness and mechanical properties play an important role in the transfer of strain to the fibre core.

The low resistance of fibre optic sensors to damage and the difficulties with fibre handling are important application problems. On the other hand, FOBG sensors embedded into the structure provide limited information on the buckling mode changes. Only the onset of buckling can be indicated. The subsequent development of the buckling waves and their changes are not generally indicated. This lack of sensitivity to these responses can be caused by the fact that the embedded FOBG sensors are placed into the structure very close to the neutral axis. Due to buckling, an additional bending originates in the structure. Both of these situations can result in the embedded sensors' lack of sensitivity to the local buckling.

Regarding final failure, the FOBG measurements do not provide a clear warning, possibly because final failure occurs suddenly. However, the ultimate tensile strength of the composites decreases to an extent due to the embedded FBG and optical fibres. Nevertheless the wider acceptance of the use of these sensing systems is still hindered by issues regarding sensor performance, especially when embedded, detection capability, maintainability, size and weight of the available interrogation equipment, and the lack of a standardisation and certification framework.

Due to their small size and flexibility, optical fibres can be embedded in composite structures during the manufacturing process. The advantages are the enhanced protection of the fragile fibre sensor and the possibility of strain monitoring and damage detection in different locations inside the material. However, sensor integration in composites presents a number of issues and shortcomings that need to be addressed properly. Some of the most relevant among them will be discussed briefly in the following sections.

Mechanical Coupling

This embedment can give rise to additional issues, as standard sensors are usually too large in comparison with the thickness of the (resin-enriched) regions between the laminate where they can be deployed during the manufacturing stage. The local distortion of the microstructure has been shown to result into a shorter lifetime of these structures, due to the inception of small defects that can eventually coalesce to provide a failure mode on their own. It is necessary to avoid the SHM system being the source of damage, since it is something that the system is supposed to feel and prevent as much as possible.

Despite being very small, a standard telecom fibre has a size (125 μm) which is much larger than commonly used composite fibres (e.g. 5–10 μm for carbon fibres). As a result, resin-rich regions are created around the fibre, especially in the woven fabric. Figure 1 clearly shows the comparison between the sizes of the sensor and the host material for different types of fabrics. Even with the small-diameter (50 μm) fibres that have been developed for sensing purposes in aerospace structures, the difference is still an order of magnitude. However, it has been demonstrated that small-diameter fibres do not produce any significant modification of the mechanical properties in the host structure. Standard telecom fibres exhibit a similar minimally intrusive behaviour when embedded parallel to the reinforcing fibres.

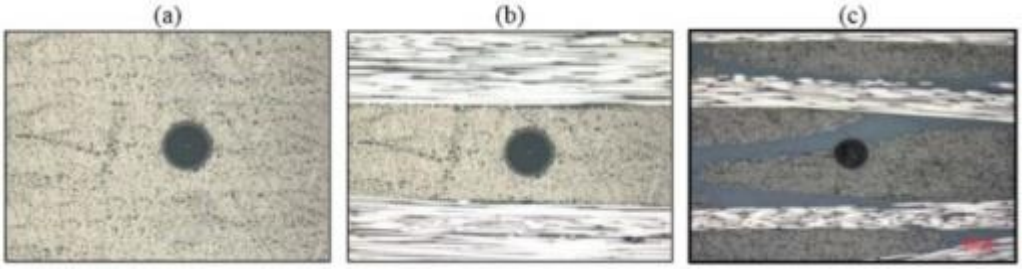

Figure 46. Optical fibre section in (a) unidirectional; (b) cross-ply and (c) woven fabric [5]

Fibre Protection at Ingress-Egress Points

Ingress and egress points of the fibre in the material are critical locations due to the sharp pressure gradient and therefore the severe bending experienced by the fibre. The concentrated stress acting during some manufacturing processes, such as the vacuum bag technique, and later under operating conditions, cause severe optical loss and may lead to fibre breakage. Different approaches have been reported in the literature to mitigate this problem. The simplest method consists in the use of small plastic tubes protecting the fibre along short sections inside and outside the material. The tubes are usually made of polytetrafluoroethylene material (PTFE, also-called Teflon) or polyvinylidene fluoride (PVDF), and may be reinforced by using a metal coil. Moreover, their openings must be sealed to avoid the ingress of the resin. In order to allow cutting and polishing of the surface after manufacturing, the fibre ingress and egress points should be located before the end section of the composite structure. In this case, care must be taken to avoid sharp curvature of the fibre and thus prevent high optical loss. However, when the fibre is embedded below several plies this method is not applicable.

Partially embedded (also-called “surface-mounted”) or embedded connectors offer another possible solution. In the first case, the connector can be positioned on one of the surfaces of the composite structure. When the fibre is embedded between internal plies, this solution is also difficult to implement. Embedded connectors are devices specially designed to overcome this problem; only the female part of the connector is embedded so that proper machining of the composite element surface is still possible. These connectors are often miniaturised to be less invasive. However one potential source of decreased reliability is the deformation that the embedded connector might experience during the manufacturing process which may affect the alignment. In addition, the use of embedded or partially embedded connectors requires a careful assessment of the potential reduction in the strength of the composite.

Most of these problems can be avoided by using the so-called free-space coupling, which enables coupling of free-space light into and out of an embedded FBG sensor without the use of a physical connector. This result is obtained by splicing a multimode fibre to a single mode fibre Bragg grating, and using hand polishing to integrate 45° mirrors into the ingress and egress point of the fibre and the grating respectively. Although the estimated total loss is quite high (23 dB), this technique makes it possible to accurately measure strain values up to 2000 μm and increase system robustness and simplicity.

Finally, during composite part manufacturing it is important to protect the outer section of the fibre from excess resin that may escape from the layers pile.

Spectral Response in Embedding Process

The spectral sensitivity of an embedded fibre optic sensor can deviate from that of the non-embedded sensor for a number of reasons. During the heating phase of the manufacturing process, the fibre is subjected to the stress created at the boundary between the coating and the composite ply; however, during the cooling phase, this stress is only partially released. This results in residual strains acting inside the material and on the fibre. Consequently, the sensor spectral response is affected by the existence of transverse and often non-uniform strain fields.

In the literature, it was observed that the spectrum of two embedded FBG sensors was severely distorted after the manufacturing process. The Bragg wavelength peak split into two spectral components, due to the existence of transverse strain. This effect is attributed to birefringence of the optical fibre and the difference between the peak wavelengths may be used as a measure of the transverse strain. However, such a distortion of the FBG spectrum prevents measurement of the longitudinal strain based for example on the commonly available algorithms for Bragg wavelength detection, such as the Full Width Half Maximum (FWHM) method. Even if the algorithm used to track both peaks and FBG sensors was added for multi-axial measurements, it would be necessary to distinguish the two spectral components of regular shape. That is not always the case, as transverse strain or local strain gradients can cause severe distortion of the spectrum. The fibre coating plays, however, an important role in minimising the effect of transverse strain due to the manufacturing process. When an acrylate or polyimide coating are used, the Bragg wavelength is simply shifted due to longitudinal transverse strain, but the spectrum is not distorted. Even in this case though, the accurate measurement of pure longitudinal strain with a uniaxial FBG sensor may be undermined depending on the load amount, type and point of application. For all these reasons, and considering also that the strain is transferred across the coating to the fibre core, accurate calibration of the embedded sensors after the manufacturing process and critical evaluation of the actual operating conditions are mandatory to ensure the reliability of the measured data.

When it comes to damage detection rather than simple strain monitoring, the information given by the distorted spectrum of bare embedded FBG can be quite useful. By relating the distortion to the specific defect and damaging mechanism, it is possible to detect cracks, delamination or debonding in various types of composite laminates. A similar method to detect impact damage can be used with distributed sensors. In those cases, the use of optoelectronic demodulators with full spectrum detection capability is needed. In addition, the fibre optic sensor must be in close proximity to the damage location, requiring an a-priori estimation or knowledge of the defect position.

Increasing of SHM reliability

The reliability of the Fibre Optic Ribbon Tape (FORT) concept is studied to measure and monitor the real-time strain induced in the composite materials under prolonged cyclic loading and also for accuracy and repeatability of real-time measurement. The FORTs are nothing but pre-assembled composite ribbon tapes, where the optical fibre is embedded in between the two composite lamina. The main advantage of the FORT assembly is easy mounting and handling of optical fibre and also protection from atmospheric degradation.

Multi agent systems seem very reliable and efficient for the larger composite laminates where different types of sensing elements are used for various types of damage. The most important advantage of multi agent systems is wide coverage for various modes of failure and damage, because it consists of different types of sensors for various damage types. Also the uniformly distributed sensor and its network can deal and fuse various kind of information about the failure and damage induced in the composite's structure.

The recently developed Micro Electro-Mechanical Sensors (MEMS) have been hailed as the SHM for composite materials because of their easy handling, tiny size and negligible weight. In the Micro Electro Mechanical Systems (MEMS), the mechanical and electrical sensing element is combined together in a single silicon chip at micro scales. After the invention of MEMS, considerable efforts have been made toward development and integration of MEMS into composite structures for health monitoring purposes. A local transmissibility vibration-based diagnostic algorithm based Structural Health Monitoring system for aircraft structures using smart wired piezoelectric arrays of accelerometers (MEMS) as sensor is proposed.

However, limited attention was devoted to the damage severity, location, and the residual strength of the damaged composites. To be a better Structural Health Monitoring system, it should provide not only real-time strain, but also degree of damage and residual strength of the damaged composites.

Also, the SHM should provide information about the various modes of failure occurring in composites such as delamination, fibre pull-out, matrix failure, etc. Hence, the future research should focus more on the damage assessment, failure mode prediction and residual strength evaluation of the damaged composites, in order to fulfil the purpose of the SHM System for the polymer composites.

Conclusions

The problems of introducing sensors into a composite panel:

- damage to the sensors during of the panel manufacturing: fracture, connection to the connector - flowing of the binder, glue, machining of the panel - pruning is difficult
- determine the critical sensor location: there are zones where deformations or stresses change little (for example, setting in the middle, close to the neutral axis), then it is difficult to separate the real changes in the readings from the noise. Because of the heterogeneous structure, the readings of the sensors on the surface and on the layers differ
- sensors affect the mechanical properties of the panel: the introduction of foreign bodies, the formation of areas with excessive binder content - reduces the strength of the panel, can cause stratification due to low adhesion to the main material or the discrepancy between the ultimate deformations of the panel and the sensor.
- width of composite fracture forms
- the sensor dimensions are larger than the fracture zone and may further contribute to structural failure
- low maintainability of sensors embedded in the composite
- lack of regulatory issues of standardization and certification of such equipment
- aging, relaxation, creep of the composite in the process of exploitation - how to recognize this defect or the processes associated with changing the properties of the composite
- operation - providing approaches to sensor connectors to read information. The difficulty of providing an aerodynamic surface due to the large size of the connectors. To ensure the smoothness of the vertex, the connectors are removed to the back of the panels to which access is difficult to operate. If the exit to the aerodynamic surface, then it is necessary to ensure the protection of the connector in the process of exploitation
- preference is given to sensors with smaller dimensions, but the probability of their damage increases
- apply polyimide to the sensor surface, increase the operating temperature of the sensor to 20 °C, improve adhesion to the composite, and compensate for residual technological stresses. The initial sensor noise is stable, but the sensitivity of the sensor decreases.
- increase reliability - Use tape sensors that duplicate the measurement. In case of damage to one, others work. Duplication of different types of sensors, piezo, opto, strain gauges.
- the formation of channels in the composite, and after the manufacture of the panel, the insertion of sensors into the channel
- apply a special tool for gluing the optical fibre and connector
- solve the problem of choosing the location of optical fibre sensors: directly, sinusoidally, with what amplitude of the sinusoid, inside - on the surface of the composite, how close to damage is the sensitivity evaluation of the sensor, depending on the current load, experimental evaluation methods or KEM.

  How to solve the problem: It is necessary to answer 4 questions

  ⇒ Where to put? Based on the model, conditions of loading and work, taking into account the manufacturing and installation technology, the map of setting the sensors is optimized

  ⇒ What sensors to deliver? In the course of optimization, the limiting deformations occurring in the structure will be obtained, the sensors will be selected from the condition of the sensor panel, with the required measuring range and sensitivity

⇒ How to deliver? Development of TP, equipment for the implementation of the entrance and exit of fibre, where the fibres are most often broken, the equipment for connecting to the connector which ensures that the binder does not leak. TP must provide reliability and stability.

⇒ How to exploit? The design of the connector and panel design, taking into account their overlapping and at the same time providing a free approach during operation and external requirements, for example, smoothness of the contour. Improve the maintainability of such panels.

References

1. *R. P. BEUKEMA, Embedding Technologies of FBG Sensors in Composites: Technologies, Applications and Practical Use, 6th European Workshop on Structural Health Monitoring - Tu.4.C.4-8*
2. *Roman Ruzek, Martin Kadlec, Konstantinos Tserpes, Evanggelos Karachalios, Strain Monitoring in Stiffened Composite Panels Using Embedded Fibre Optical and Strain Gauge Sensors, 7th European Workshop on Structural Health Monitoring July 8-11, 2014. La Cité, Nantes, France*
3. *R. Balaji and M. Sasikumar //Structural Health Monitoring (SHM) System for Polymer Composites: A Review\\ Indian Journal of Science and Technology, Vol 9(41), DOI: 10.17485/ijst/2016/v9i41/85832, November 2016*
4. *Raffaella Di Sante , Fibre Optic Sensors for Structural Health Monitoring of Aircraft Composite Structures: Recent Advances and Applications, Sensors (Basel). 2015 Aug; 15(8): 18666–18713.*
5. *Geert Luyckx, Eli Voet, Nicolas Lammens, and Joris Degrieck, Strain Measurements of Composite Laminates with Embedded Fibre Bragg Gratings: Criticism and Opportunities for Research, Sensors (Basel). 2011; 11(1): 384–408.*

3.3 Training provided

The participants of the AERO-UA Pilot Projects 3.2a, 3.2b, and 3.3b working meeting on July 3-4 2017 at the University of Manchester on in Warsaw were:

No.	*Name*	*Organisation*
1	Prof Mojtaba Moatamedi	Aerospace Research Institute (UoM)
2	Dr Adam Joesbury	Aerospace Research Institute (UoM)
3	Dr Matthieu Gresil	i-Composites Lab (UoM)
4	Prof Prasad Potluri	Northwest Composites Centre (UoM)
5	Prof Constantinos Soutis	Aerospace Research Institute (UoM)
6	Dr Lina Smovziuk	National Aerospace University (KhAI)
7	Dr Fedir Gagauz	National Aerospace University (KhAI)
8	Dr Valeriy Fadeyev	Public Joint Stock Company (FED)
9	Dr Krzysztof Dragan	Technology Partners Foundation (TECPAR) / Air Force Institute of Technology (ITWL)
10	Dr Michal Dziendzikowski	Technology Partners Foundation (TECPAR) / Air Force Institute of Technology (ITWL)
11	Dr Iryna Bilan *(via Skype)*	Frantsevich Institute for Problems of Material Science (NASU)

3.4 Scientific results

Transfer Impedance Approach to composite structures monitoring – contributor: TECPAR / ITWL (PL)

In the first half of the project a new method for composite structures monitoring by use of PZT sensors was investigated. In the so-called electromechanical impedance (EMI) approach, sinusoidal steady state voltage is applied to PZT actuator in a given frequency range. Then, for a single transducer, its impedance is measured in a given range [1], while for actuator-receiver PZT sensor pairs, the receiver voltage, i.e. the output voltage, can be measured for the structure state assessment [2].

Figure 47 presents an example of a voltage obtained for three different PZT transducers, sensing distribution of elastic waves excited by a generator sourced with sinusoidal voltage. If one of the transducers of a PZT network integrated with a structure transmitting elastic waves, i.e. the generator - g - is powered with sinusoidal voltage U_{in} at frequency ω, then the voltage U_{out} obtained at any given receiver - s is also sinusoidal and has the same frequency, in accordance with Linear Time Invariant (LTI) systems theory. Therefore the ratio, called the transmission function:

$$TF_{gs} = \frac{U_{out}}{U_{in}} \tag{1}$$

does not depend on time and can be written as a complex function:

$$TF_{gs}(\omega) = \frac{U_{out}}{U_{in}} = \frac{|U_{out}|\, e^{i\omega t + \varphi_{gs}(\omega)}}{|U_{in}|\, e^{i\omega t}} = |TF_{gs}(\omega)|\, e^{i\varphi_{gs}(\omega)}, \tag{2}$$

representing relative amplitude ratio $|TF_{gs}(\omega)|$ and phase difference $\varphi_{gs}(\omega)$ between output and input signals. Both parts of the transfer function depend on many factors, e.g. the geometry of the network, the technology of PZT transducers integration with the structure, but can be also influenced by a presence of damage near the sensing path *g*–*s*, i.e. the line which joins the generator *g* with the sensor *s*.

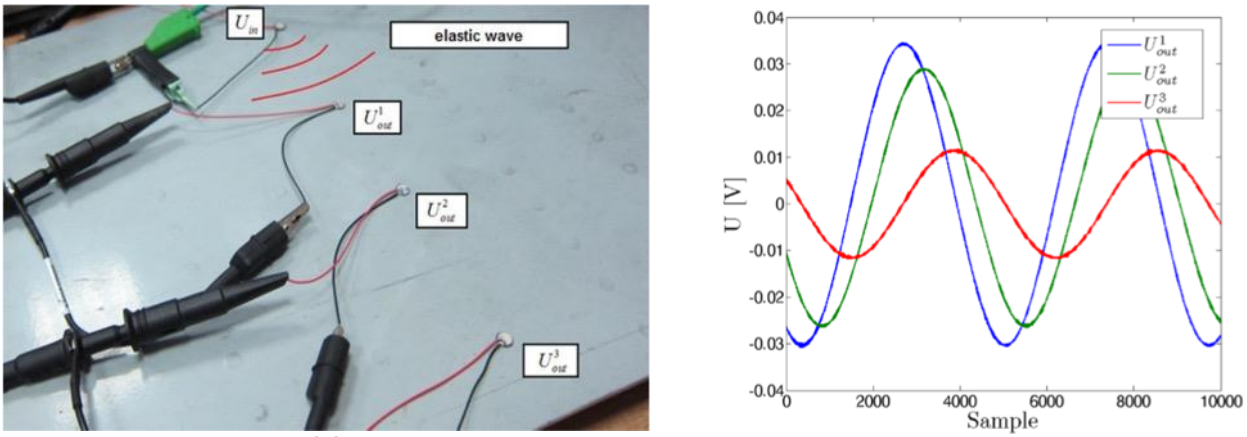

(**a**) (**b**)

Figure 47. Example of a sinusoidal steady state excitation of PZT sensors (a) PZT network; (b) Output voltages acquired on PZT sensors.

The dependence of the transmission function on the signal frequency can be quite complex, therefore its direct application is of limited usefulness. For structure assessment, some comparison of the baseline transmission function TF^0_{gs}, obtained for the initial state of the structure, with the actual transmission function TF_{gs} is needed.

This can be done by Damage Indices of the form:

$$DI_{gs}(\omega) = \frac{TF_{gs}(\omega)}{TF_{gs}^{0}(\omega)} = \frac{|TF_{gs}(\omega)|}{|TF_{gs}^{0}(\omega)|} e^{i(\varphi_{gs}(\omega)-\varphi_{gs}^{0}(\omega))}. \quad (3)$$

Assuming that the voltage on the generator U_{in} is maintained the same, the modulus of DIs

$$|DI_{gs}(\omega)| = \frac{|U_{out}(\omega)|}{|U_{out}^{0}(\omega)|} \quad (4)$$

describes the ratio between output voltage amplitudes on the sensor *s* at a given frequency for the actual and baseline measurements. Therefore, the DIs captures the information about output voltage amplitude as well as phase changes in a given frequency range. For undamaged structure, the DIs should be concentrated in the vicinity of the point *1+i0* in the complex plane (Fig. 48). If damage is present in the structure, its influence on the output voltage amplitude or the phase is expected, at least for some range frequencies, therefore DIs should exhibit some divergence from the origin, i.e. the point *1+i0* (Fig. 48).

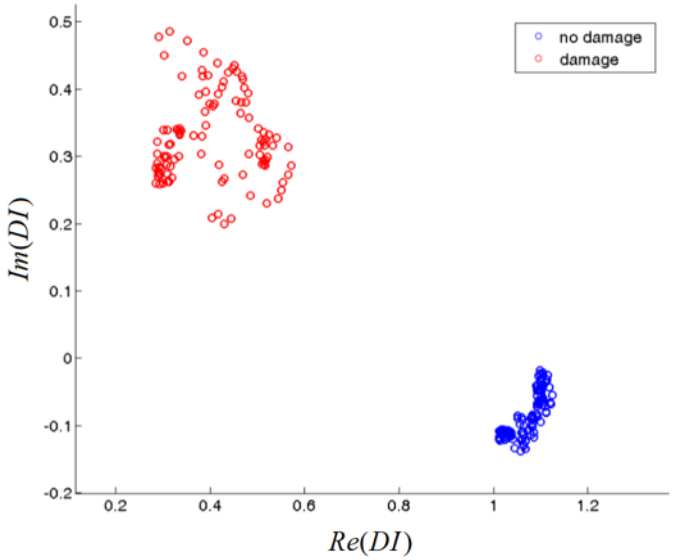

Figure 48. Example of DIs obtained for the pristine state of the structure and when a damage is present

It is worth noting that almost all of the information of the signal is carried by the DIs. Assuming the baseline transmission function TF_{gs}^{0} and input voltage U_{in} are known, $U_{out}(\omega)$ can be reconstructed from the DIs. The proposed method should therefore detect all damage types with an impact on the acquired signals in terms of the amplitude and the phase.

Design and Preparation of the Experiment

An experiment designed to verify basic properties of the Damage Indices proposed for structure monitoring was designed. The specimen under study was a GFRP panel made of 16 plies of HCS2401-015 – HEXCEL Fiberglass Prepreg. The stacking sequence of the layers was [0/45/0/45/0/45/0/45]s. In the symmetry plane of the specimen, a network of PZT discs SMD05T04R111 made by STEMINC Inc. was deployed. The diameter of PZT transducers is 5 mm and the thickness is 0.4 mm. After deployment of PZT transducers, the specimen was cured in the autoclave in accordance with the technical specification of the material being used.

Four PZT discs of the same type were deployed on the surface of the specimen, precisely above four selected transducers embedded in the specimen structure. Also, the orientation of the attached sensors was maintained the same as for the sensors underneath them. Fig. 49 presents the geometry of PZT networks. For both networks, for the network attached to the specimen surface as well as for the embedded network, one of PZT transducers was selected as the guided waves actuator whereas the remaining three sensors were used as sensors. Therefore three sensing paths for each of the networks were considered in the study (Fig. 49):

- G-S1 of the length 167 mm;
- G-S2 of the length 213 mm;
- G-S3 of the length 90 mm.

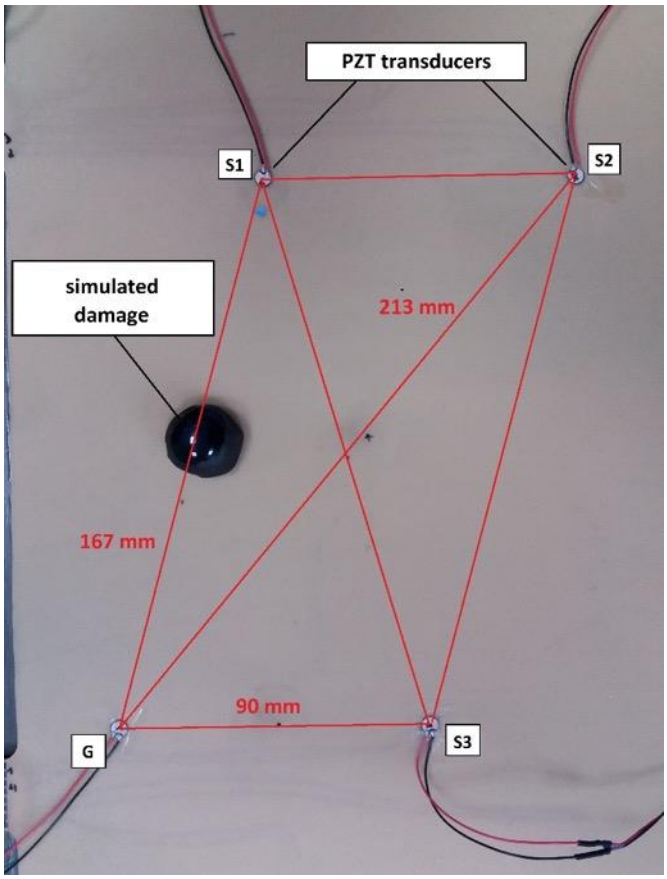

Figure 49. The geometry of the PZT network.

It is worth noting that not only the lengths of the networks sensing paths were different, but also their orientation with specimens' plies and respective orientation between actuator and sensor for a given sensing path.

For both PZT networks, the measurements were conducted according to the following scheme:

1. Measurement for the pristine state of the structure.
2. Measurement for simulated damage on sensing path G-S1.
3. Measurement for simulated damage on sensing path G-S2.
4. Measurement for simulated damage on sensing path G-S3.

The measurement scheme was repeated six times for each network. The damage was simulated by a mass element attached to the specimen by bitumen in the middle of a given sensing path. The bituminous mass used for the attachment was additionally attenuating elastic waves propagating between the sensors. The actuator G was powered by sinusoidal steady state voltage source in the frequency range of 240 – 350 kHz. The frequency increment step was 1 kHz, peak-to-peak amplitude was set to 88 V.

The figure below presents a comparison of DIs distribution for different sensing paths in the presence of simulated damage and for the pristine state of the structure. The data from all repetitions of measurements are merged for the purpose of comparison.

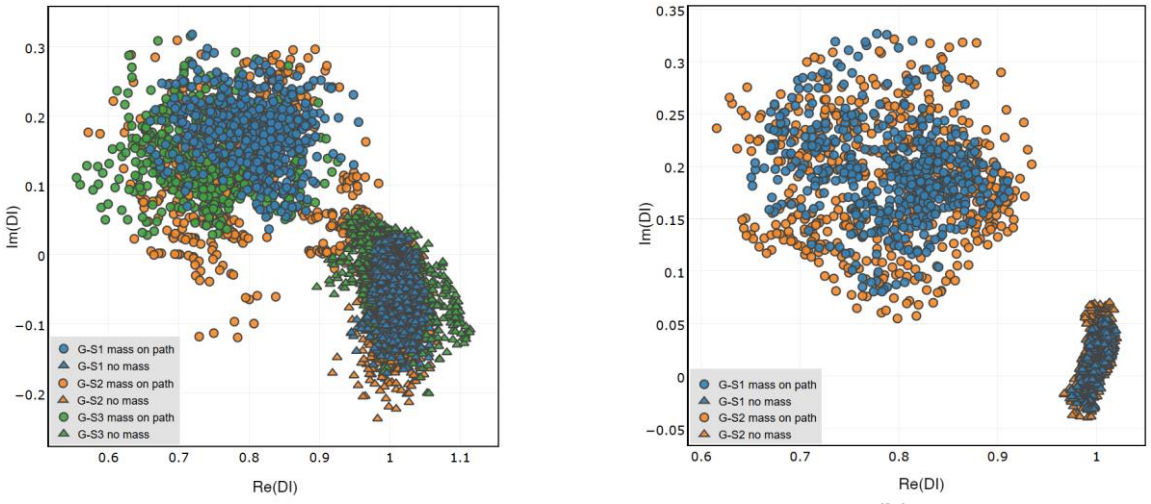

Figure 50. Comparison of DIs obtained for the pristine state of the structure and for simulated damage presence: (a) Attached network; (b) Embedded network

Remarkably, for both networks the DIs obtained at certain conditions are confined in similar domain, irrespective of the sensing path being considered. It is worth noting that the material being studied exhibits mechanical anisotropies, as well as piezoelectric discs used for the study [1], i.e. the power of emitted or gained elastic waves usually depends on the direction of their incidence on a sensor. However the results do not depend significantly either on the direction of the sensing paths or on respective orientation of generator and sensor. Also, the distance between sensors constituting a sensing path is not relevant for the domain where the data is concentrated. These properties are of particular importance for damage classification possibility. Stability of indications under similar conditions, e.g. presence of a given type of damage on a sensing path, allows for definition of domains in the DIs complex plane corresponding to different damage scenarios.

Further perspectives

Based on the provided experience of Aero-UA project partners, a joint study on the efficiency of different approaches to SHM of composite structures was delivered. The method presented will be further developed by TECPAR / ITWL (PL). In cooperation with KhAI (UA) and E. O. Paton Electric Welding Institute at NASU (UA) composite specimens equipped with a network of PZT sensors will be delivered by KhAI. The efficiency of the method proposed by TECPAR / ITWL will be tested towards detection of damage of composite structures, caused by low energy impacts. Further, fatigue or destructive (Compression After Impact) tests will be performed, in order to test Acoustic Emission system capabilities for continuous composite structure monitoring by E. O. Paton Electric Welding Institute at NASU.

References

1. *Giurgiutiu V. Structural Health Monitoring with Piezoelectric Wafer Active Sensors, 2nd ed., Academic Press: Tokyo, Japan, 2014.*
2. *Song H.; Lim H. J.; Sohn H. Electromechanical impedance measurement from large structures using a dual piezoelectric transducer. J Sound Vib. 2013, 332(25), 6580-6595, DOI: doi.org/10.1016/j.jsv.2013.07.023.*

3.5 Feasibility study

3.5.1 EU-UA SHM technology development opportunities

Structural Health Monitoring (SHM) is an emerging technology which can play an important role in aircraft maintenance and safety management. EU and UA Partners involved in the project have complementary experience in SHM application and development, which created a great opportunity to bridge gaps of SHM technology in its introduction into aerospace industry. In summary, key identified fields of cooperation between the project Partners in the SHM area are as follows:

- design, modelling, manufacturing and testing of composite structures: KhAI – UA, UoM – EU;
- application of guided wave approach to aerospace structure monitoring (both metallic alloys and composites): TECPAR/ITWL – EU, UoM – EU;
- application of the acoustic emission method to industry infrastructure monitoring (metallic alloys): NASU – PEWI (UA).

In order to identify areas of common effort of EU and UA Partners involved in Pilot Project 3.1b towards bridging the gaps with respect to state of the art, a joint investigation of the SHM field has been performed. The following areas were considered in the analysis:

- Strengths of the technology in characterizing the state of the structure with respect to traditional Non-Destructive Testing methods and opportunities for the aerospace industry resulting from SHM application.
- Weaknesses which are immanent for SHM technology and cannot be easily resolved;
- Gaps of the current state of technology development which can be resolved in order to increase SHM performance and current or emerging demands of the aerospace industry.

Identified strengths, weaknesses and the gaps of SHM are listed in the table below.

Table 1. Strengths, weaknesses and the gaps of SHM technology

Strengths and opportunities	Weaknesses	Gaps, demands
SHM allows for continuous *in-situ* structure monitoring providing end-users with current information about its state.	Sensor technologies provide very local structure monitoring (eddy current sensors, resistance crack gauges) with high resolution of damage characterization (e.g. crack growth) or broader areas can be monitored (PZT transducers, FBG sensors) with limited accuracy of damage characterization.	Durability of SHM sensors needs to be comparable with aircraft service life or aircraft overhaul periods in order to provide continuous structure monitoring, at least for areas that are hard to access.
SHM sensors can be installed and operated in areas that are hard to access by traditional NDT methods.	Introduction of additional sensors increases manufacturing costs of the aircraft.	There exist strong end-user expectations of SHM technology for composite structure monitoring (Fig. 21).
Introduction of SHM can lower operational costs by increasing the time between subsequent NDT inspections in accordance with *damage-tolerance* design.		There exist expectations of improving damage detection capabilities of SHM technology (increased resolution, probability of detection, etc.).

Strengths and opportunities	Weaknesses	Gaps, demands
Introduction of SHM will increase safety of aircraft operation.		SHM technology should be resistant to interference of external factors in order to keep an acceptable false calls ratio.
Individual tracking of the state of the structure can improve management of overhauls and aircraft structure inspections which can lower maintenance costs and increase fleet availability.		
The current approach to aircraft inspections may become inefficient in the case of massive use of unmanned aerial systems (especially of long endurance) due to a lack of a highly skilled workforce (operational costs of low cost UAV inspections may become unacceptable). Introduction of SHM technology could resolve this issue (by indicating which UAVs need to be inspected).		

3.5.2 Assumptions of the study

Based on identified gaps of SHM technology and demands of the aerospace industry, the topic of the feasibility study was established, corresponding to Partners' areas of expertise and experience. Due to the growing use of composites in aerospace and the requirements of industry relating to development of composite structure monitoring technologies the EU and UA Partners' investigations within Pilot Project 3.1.b were focused on composite structures. Two directions of investigations were pursued:

1. Application of the acoustic emission system developed by NASU-PEWI for CFRP structures monitoring. The system has been successfully applied to industry infrastructure monitoring, within the Pilot Project its capabilities for composite structure monitoring were investigated.
2. Development of "smart" CFRP structures with embedded PZT transducers. Composites, besides attachment of sensors to the surface of the element, also allow for immersion of sensors into the internal structure of the composite. This technology of sensor integration can be beneficial for:
   - improvement of damage detection capabilities of the embedded sensors compared to surface-mounted sensors (due to better acoustic coupling of sensors with the structure);
   - increased durability of sensors and resistance to external factors (existence of the protection layer over the sensor).

   However, the introduction of a foreign object into the internal structure of a composite may adversely affect the mechanical properties of the structure, i.e. decrease strength. Within the study both the beneficial and adverse effects of sensor integration with the structure were investigated.

The topic of the pilot project corresponds to identified needs relating to SHM technology development and is adjusted to common EU and UA capabilities to bridge the gaps with respect to the state-of-the-art.

3.5.3 Results of the study

Application of Acoustic Emission method to composite structure monitoring

Acoustic emission testing of composite material – Part I

E.O. Paton Electric Welding Institute. NAS of Ukraine carried out the AE (acoustic emission) series of testing samples from the Udo UD CST 150/300 composite material based on the ARALDITE 564 binder, manufactured by the N.E. Zhukovsky National Aerospace University "Kharkiv Aviation Institute".

Table 2. Mechanical properties of carbon fibre Udo UD CST 150/300 (based on ARALDITE 564 binder)

Parameter	Value	Variation coefficient, %
The modulus of tensile elasticity in the direction of the texture base E_1, GPa	161.48	8.59
Strength limit of tensile in the direction of the texture base F_{1P}, MPa	1811.3	7.14
The modulus of elasticity in compression in the direction of the texture base E_1, GPa	121,84	6,88
Strength limit of compression in the direction of the texture base F_{1P}, MPa	458,3	21,14
μ12 Poisson coefficient of tension	0.26	13.96
μ12 Poisson coefficient of compression	0.3	8,22
The modulus of elasticity in the weft texture direction E_2, GPa	9.9	9.87
Strength limit in the direction of weft texture F_{2P}, MPa	11.6	28.64
μ21 Poisson coefficient	0.064	35.6
Destructive stress $\sigma_в$, for (+45), MPa	162,0	12,93
Shear modulus G_{12}, GPa	4,317	4,93
Stress F_{12}, MPa	35,5	7,67
Destructive stress $\sigma_в$, of specimen compression (+45), MPa	143,0	8,04
The modulus of elasticity of specimen compression (+45), GPa	17,88	27,62

The initial purpose of the study was to determine the principal testability of this composite material using sensors, equipment, and AE technologies implemented using EMA-4 instruments (Fig. 51). An assessment was made of the possibility of using EMA instruments for detecting damage and monitoring the state of composite structures based on carbon fibre reinforced plastic. The CFRP sample provided was a thin plate measuring 310x260x2.1 mm.

Studies on the acoustic conductivity of the material and the accuracy of the sources of AE signal coordinates' location on the plane were carried out using four DAE-01sensors, each of which was alternately used as a generator of acoustic waves. The sensors were placed at a small distance from the edge of the sample, so that they formed a location antenna with a size of 230x200 mm. After checking the acoustic conductivity, the original plate was cut into 310x30 mm bands which were used as samples for tensile tests. Some of the samples were weakened by circular concentrators (Fig. 52) with the aim of establishing the possibility of their location by the AE method in the loading process.

Figure 51. EMA-4 (Evaluation of Materials Ability) devices in 4 and 16 channel versions

The first experiments showed that the material under study has a high acoustic sensitivity comparable to that of many metals. The passage of AE waves through the material was normal. The ability to determine the coordinates of the signals was provided with enough accuracy. In addition, manual tapping of the sample with a thin metal rod in different directions was performed, and the coordinates were also determined well.

When determining the location of AE sources using sensors as a generator of waves, the velocities of AE waves in the material were selected so that the calculated coordinates of the AE signals emitted by the sensors and then received by the AE device, as accurately as possible coincided with the coordinates of the sensor-emitter.

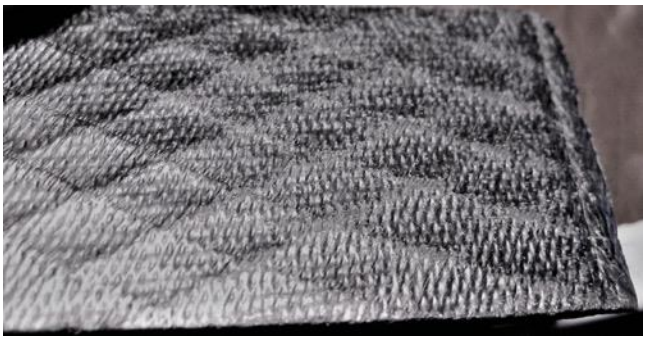

a

b

Figure 52. a) the reinforced structure of the material is clearly visible, b) the sample with circular concentrators after rupture

If, during metal sounding, the velocities in the longitudinal and transverse directions usually practically do not differ and, depending on the material, constitute from 3 to 5 mm / μs, then for the material Udo UD CST these speeds differ almost twice. Achieving the picture shown in Fig. 53 was possible by setting a speed of 8 mm / μs in the X direction corresponding to the short side of the plate, and 4 mm / μs in the Y direction corresponding to the long side.

Note that in the EMA-3.9 program which was used during testing the centres of acoustic activity combined into clusters are shown with flags whose colour indicates the amplitude of the last AE event that has entered the cluster, and the number next to the flag shows how many AE events complete the cluster.

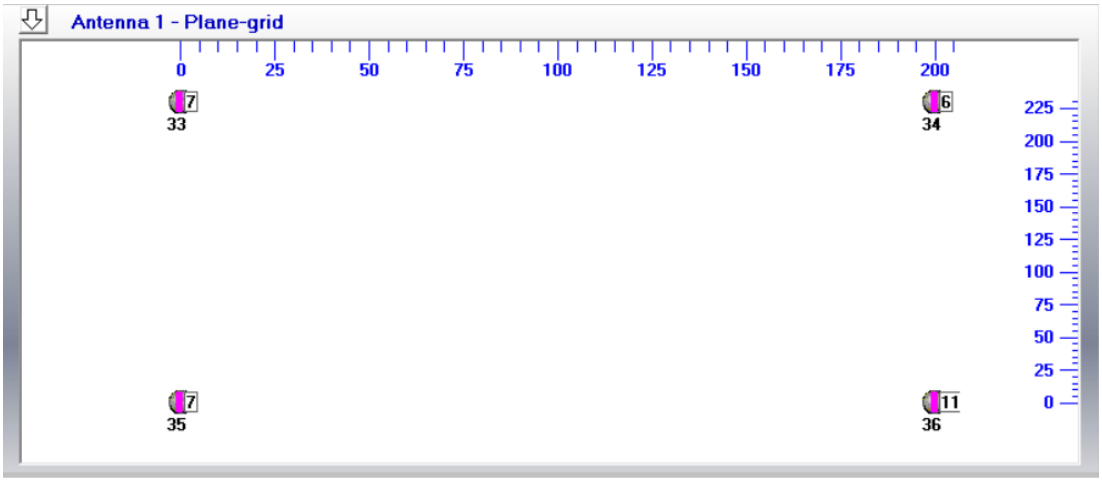

Figure 53. Results of the plate sounding by the generator of acoustic signals built into the sensors. The high accuracy of determining the coordinates is visible in the figure (the centers of acoustic activity are shown by flags and coincide with the locations of the AE sensors)

The results of determining the velocities of the AE waves are confirmed by manual knocking of the plate at individual points located diagonally from each other (Fig. 54). It can be seen that the coordinates of the strikes on the plate fit well on the conditional diagonal. The presented experiments were repeated several times, and the results of their processing showed that, firstly, this material is testable from the point of view of AE, and, secondly, that it provides the necessary accuracy in determining the coordinates of AE sources.

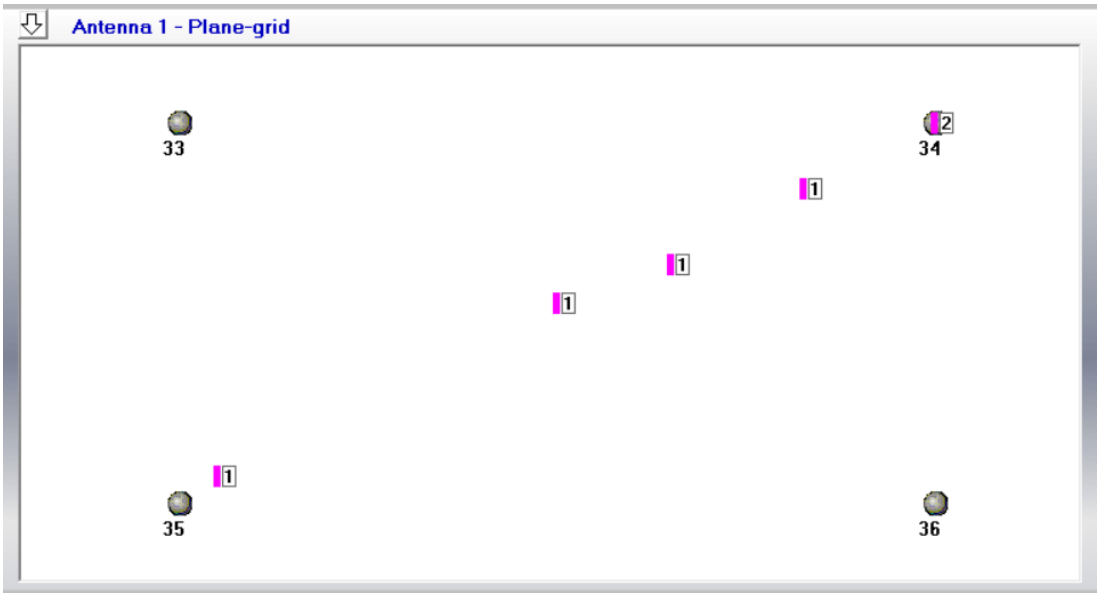

Figure 54. The results of the sounding of the plate by manually tapping the metal rod. The centers of acoustic activity are shown by flags and coincide with the sites of strikes on the plate

The determination of the velocities of AE waves in a material is a necessary step before its mechanical tests, since they make it possible to determine the coordinates of the sources of AE waves that have arisen and to determine their nature and degree of influence on the overall state of the material. Further testing of the material was carried out by stretching samples of a size of 310x30 mm in a tensile testing machine with tough loading conditions. EMA-3 equipment was used. Two sensors were used to locate the coordinates of the AE sources, with the distance between the sensors varied in different experiments.

The first tests were carried out on samples without concentrators and showed that in the process of loading, acoustic emission occurs at various points along the length of the sample and is distributed fairly uniformly (Fig. 55a). At the same time, the occurrence of AE events is not uniform in time, and we can clearly distinguish two groups of such events - one at the beginning of loading, the second just before destruction. Note also that before destruction a sharp rise in the level of continuous AE by a factor of 2 occurs (Fig. 55b).

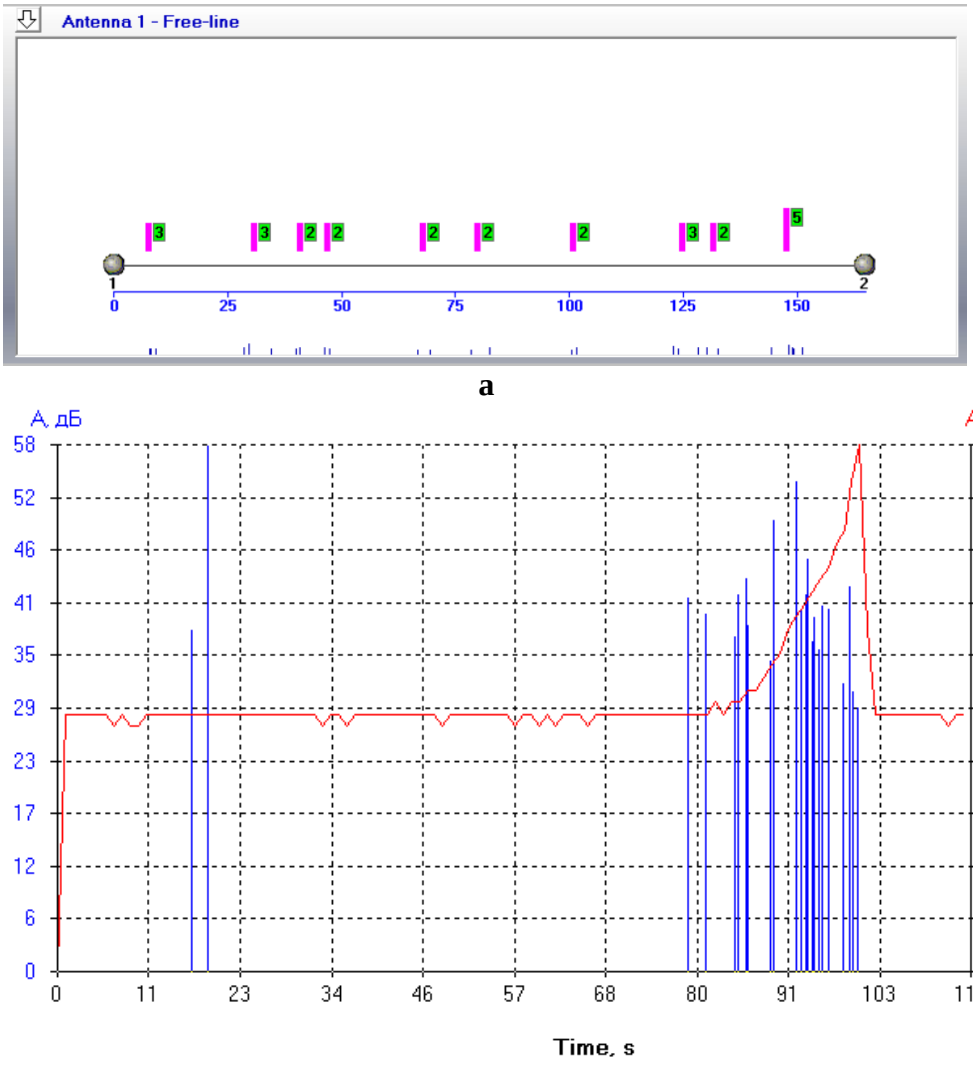

Figure 55. The results of the specimen without concentrators test. a) AE distribution along the sample length; b) AE amplitude (A, bar graph) and continuous AE (Av, linear graph) depending from time

Tests of a specimens with concentrators are of considerable interest since their fixation by the AE method on a specimen can serve as a basis for determining the location of concentrators in real structures. The sample layout with circular concentrators with diameters of 5, 3 and 2 mm, respectively, is shown in Fig. 56.

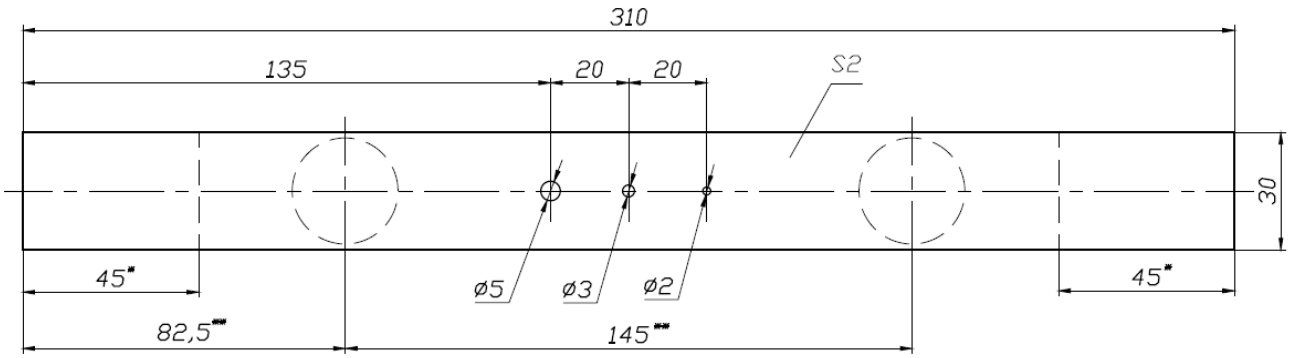

*Figure 56. Scheme of the specimen with concentrators. *) distances to sensors and between sensors, **) distances from the grips of a testing machine*

In the case of loading a specimen with a concentrator, the picture is somewhat different from that shown in Fig. 55. AE events form larger clusters which indicates the presence in the material of the sources of concentration in which destruction develops most intensively. Despite the small holes in the specimen obtained by drilling, the zone of development of destruction near each of them exceeds the dimensions of the holes themselves.

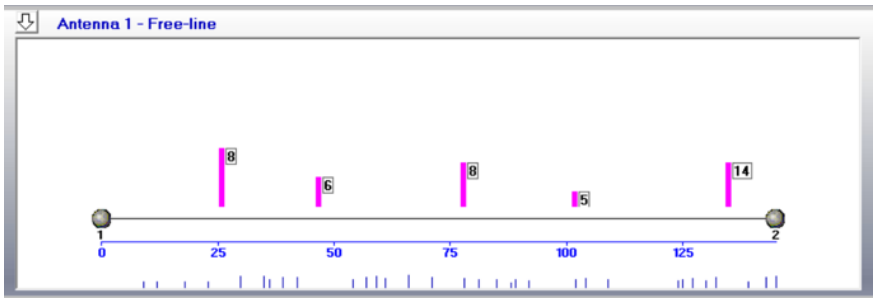

a

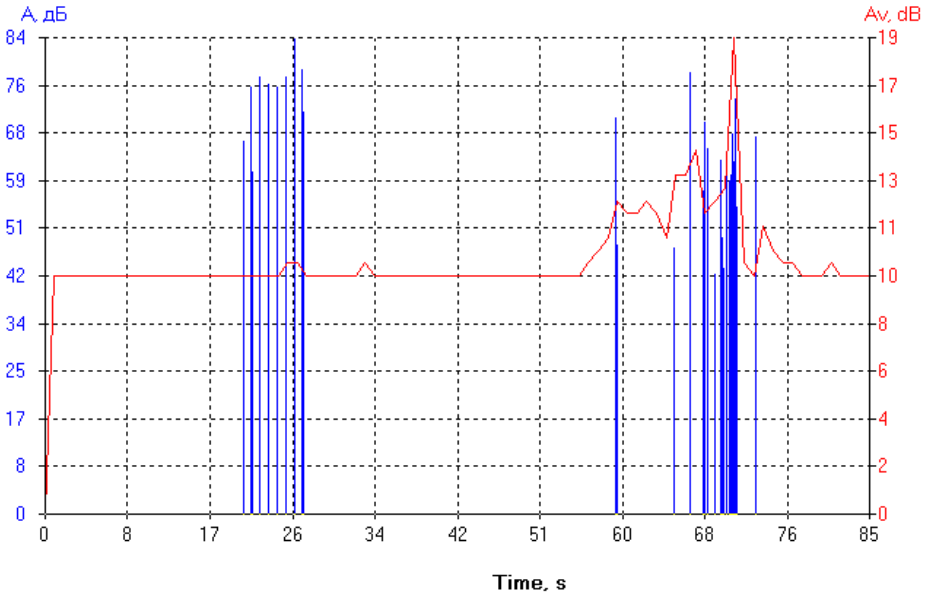

b

Figure 57. The results of the specimen with concentrators test. a) AE distribution along the sample length; b) AE amplitude (A, bar graph) and continuous AE (Av, linear graph) depending from time

Among the clusters formed by processing the AE events and presented on Fig. 57a, the three middle ones correspond to the locations of the concentrators with a fairly high accuracy.

AE shows the centre of the cluster at 47 mm, while the centre of the concentrator hole is located at 52.5 mm from the AE sensor. The second cluster has a centre of 78 mm with a centre of the corresponding concentrator hole located at 72.5 mm. The third - 102 and 92.5 mm, respectively. For the first two clusters, the difference in determining the coordinates of the AE source, i.e. the concentrator is 5.5 mm, despite the fact that the recommended measurement error should not exceed 5% of the distance between nearby AE sensors, in this case it is 7.5 mm. A slightly larger error for the third cluster is well explained by the fact that the corresponding stress concentrator has the smallest diameter, and, accordingly, the zone of destruction formation near this concentrator is smaller than the others. The destruction of the specimen occurred at the hole with the largest diameter. The reason for this, besides the wider field of influence of the stress concentrator near the hole, was also the maximum exclusion of the material during the drilling process which gave the smallest section area of the specimen for loading sensing.

This points to the additional conclusion that the most important factor is a clearer appearance of a dense group of AE events at the initial stage of loading than in the material without a concentrator. This suggests the possibility of early detection of problems with the breach of the strength and integrity of this material.

The appearance, as in the case of a specimen without a concentrator, of a double jump of continuous AE before failure also indicates the applicability of the AE method for the timely detection of the crack formation process.

The prediction of the destructive loading for composite material was also tested. The load in the process of testing was not recorded but it can be included in the experimental results, since it is known that the material strength limit is 162 MPa and that the loading curve, as it should be for a brittle material, should be linear. Conducting such a virtual experiment for a specimen with drilled circular concentrators we obtained the graph presented in Fig. 57 below.

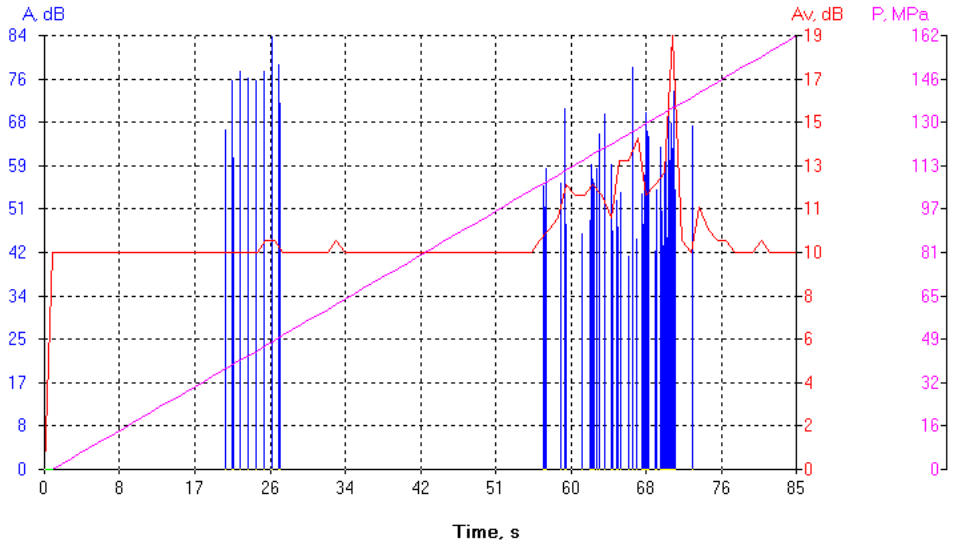

Figure 57. The results of specimen with concentrators testing, loading curve added. The parameters on the graphs are AE amplitude (A, bar graph), continuous AE (Av, line graph), loading (P, line graph) depending from time

The prediction of destruction was received at the 62nd second at the 2nd level of danger warning and amounted to 152 ... 176 MPa. Considering that the destruction occurred at a maximum loading of 162 MPa we see that in this case the error takes the required range of ± 15%.

This experiment is also interesting because the ultimate strength of the material was immediately obtained since stresses were used as the loading parameter. For those cases when the destructive loading parameter expressed in kilograms is predicted, the liquid level in millimetres or the working pressure in the

pipe in kg / cm2, it is easy to recalculate these parameters into stresses and obtain the predicted ultimate strength of the material. In the case of long-term operation, it is possible to estimate the long-term strength limit from these data.

The obtained results suggest that it is possible in principle to create a method of applying the AE technology into practice when monitoring composite materials of this type. This requires further research in this direction and obtaining a set of statistical data that would establish the necessary safety criteria for the operation of structures made of composite materials monitored by the AE method.

Acoustic emission testing of composite material – Part II

E.O. Paton Electric Welding Institute. NAS of Ukraine continue the AE (acoustic emission) series of testing specimens from the Udo UD CST 150/300 composite material based on the ARALDITE 564 binder and fiberglass made of Aeroglass 280 fiberglass and Elan-tech EC157 + Elan-tech W152XLR bonding material, manufactured by the N.E. Zhukovsky National Aerospace University "Kharkiv Aviation Institute".

Table 3. Mechanical properties of carbon fiber Udo UD CST 150/300 (based on ARALDITE 564 binder)

Parameter	*Value*
The modulus of tensile elasticity in the direction of the texture base E_1, GPa	161.48
Strength limit of tensile in the direction of the texture base F_{1P}, MPa	1811.3
The modulus of elasticity in compression in the direction of the texture base E_1, GPa	121,84
Strength limit of compression in the direction of the texture base F_{1P}, MPa	458,3
μ12 Poisson coefficient of tension	0.26
μ12 Poisson coefficient of compression	0.3
The modulus of elasticity in the weft texture direction E_2, GPa	9.9
Strength limit in the direction of weft texture F_{2P}, MPa	11.6
μ21 Poisson coefficient	0.064
Destructive stress $\sigma_в$, for (+45), MPa	162,0
Shear modulus G_{12}, GPa	4,317
Stress F_{12}, MPa	35,5
Destructive stress $\sigma_в$, of specimen compression (+45), MPa	143,0
The modulus of elasticity of specimen compression (+45), GPa	17,88

Table 4. Mechanical properties of glass fiber plastic made of Aeroglass 280 fiberglass and Elan-tech EC157 + Elan-tech W152XLR bonding material

Parameter	*Value*
The modulus of tensile elasticity in the direction of the texture base E_1, GPa	18
Strength limit of tensile in the direction of the texture base F_{1P}, MPa	317
The modulus of elasticity in the weft texture direction E_2, GPa	28,0
Strength limit in the direction of weft texture F_{2P}, MPa	530

The initial purpose of the experiments described in previous section was to determine the principal testability of one only composite material using sensors, equipment, and AE technologies implemented using EMA-4 instruments (Fig. 51), next stages are focused on two composite materials and wider spectrum of tests.

One of the next stages of researches was to obtain using the AE method whether embedded small AE sensors had influence on strength of tested materials.

And, in additional to traditional destructive AE tests of specimens, the different method was used naming “AE scanning”. This method based on sounding of specimen without its loading. In this case, one of AE sensors uses as radiant of acoustic waves, and other as receiver. If the specimen of original, not damaged material present, the comparison of acoustic properties of this material and damaged material allows obtaining the numerical value of damage.

The criterion for assessing the danger of damage accumulated in metal structures was represented as $\Delta W_{mid} = 1 - v_{dam} / v_{base}$, where a characteristic that has a sense of the rate of increase of the signal to the maximum serves as an acoustic parameter to evaluate the degree of material damage. v = A / Rt, where A is the amplitude of the output signal, Rt is the time of its increase to the maximum for the source ("base") and damaged ("dam") material. It was shown that if the speed v for the accumulated material is less than for the original material, then irreversible damage has occurred in the material. The verification of quantitative damage indicators determined by AE scanning was performed by several physical methods including direct weighing of small specimens in a liquid.

Same as in previous report studies on the acoustic conductivity of the materials tested and the accuracy of the sources of AE signals coordinates location on specimens tested were carried out using sensors DAE-01, each of which was alternately used as a generator of acoustic waves.

The specimens of fiberglass and carbon fibre, manufactured by the National Aerospace University are thin longitudinal strips, measuring 400x35x2.1 mm (Fig. 58).

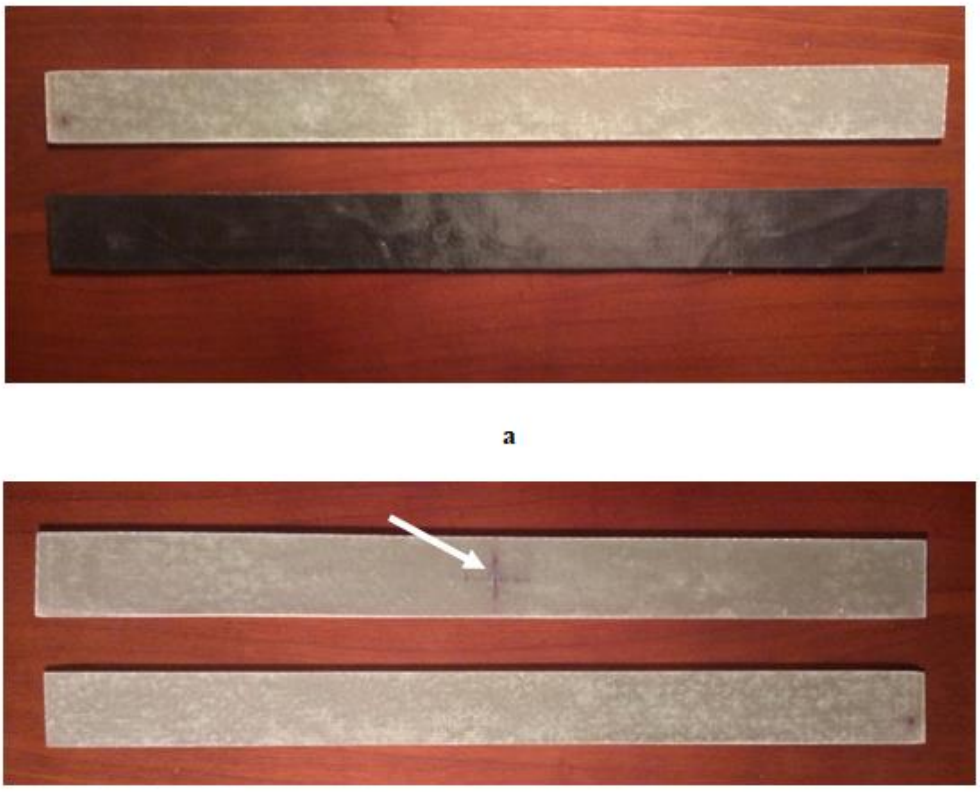

a

b

Figure 58. Specimens of fiberglass and carbon fiber are in delivery condition. At the top of (b) position, the cross maker indicated the installation location of the piezoelectric simulator — in the center of the specimen, indicated by the arrow

Specimens of fiberglass are made by the manual display of Aeroglass 280 fiberglass and Elan-tech EC157 + Elan-tech W152XLR binder (mixing ratio 100: 30). The moulding was carried out on a flat duralumin plate using a vacuum method with vacuum impregnation of a dry blank of Aeroglass 280 fiberglass fabric and pre-installed simulators of sensor sensors made of CaCO3 calcium carbonate 0.5 mm thick and 5 mm in diameter. Forming pressure 0.09 MPa. Time-temperature moulding after impregnation: 60 ° C for 6 hours. Specimens with the required dimensions were cut from the formed plate with a diamond disc. The same simulators of AE sensors were embedded into carbon fiber specimens.

The first experiments showed that the material under study has a high acoustic sensitivity comparable to that of many metals. The passage of AE waves through the material was normal. The ability to determine the coordinates of the signals was provided with enough accuracy. In addition, manual tapping of the specimen with a thin metal rod in different directions was performed, and the coordinates were also determined well.

The presented experiments were repeated several times, and the results of their processing showed that, firstly, this material is testable from the point of view of AE, and, secondly, provides the necessary accuracy in determining the coordinates of AE sources.

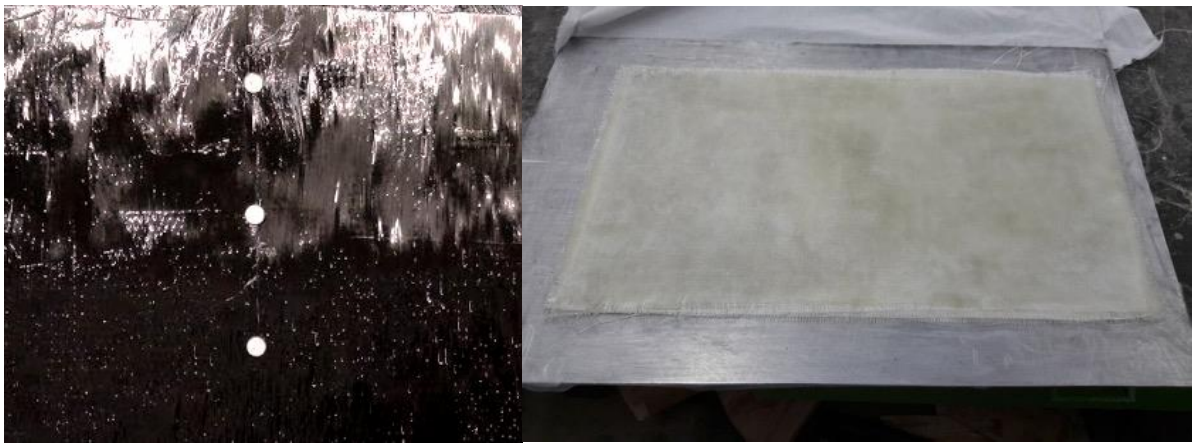

Figure 59. Installation of sensory piezoelectric sensor simulators (shown on carbon fiber, similarly done for fiberglass) and assembly of a glass cloth bag for impregnation

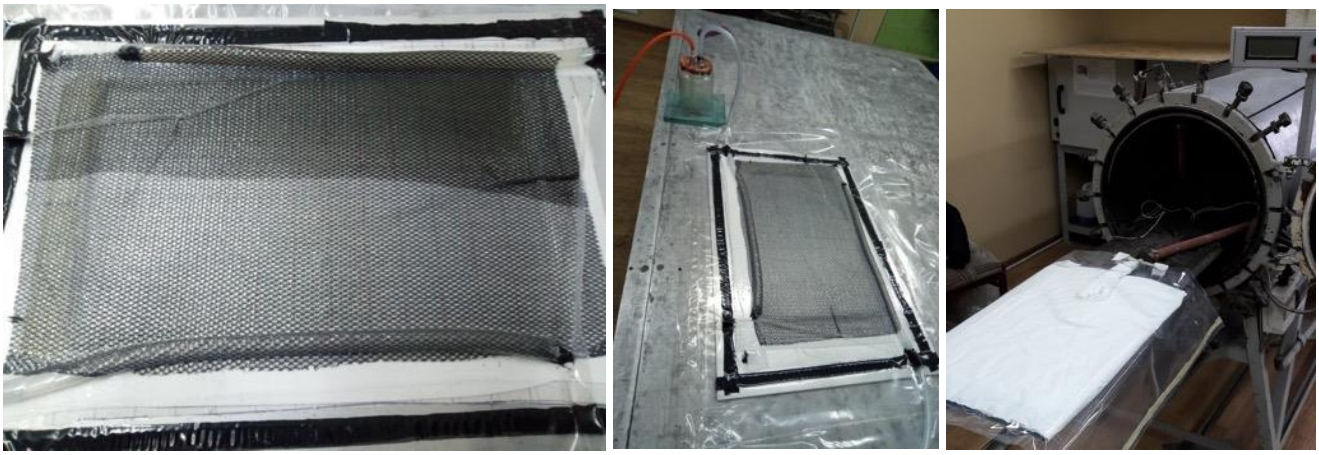

Figure 59. Binder impregnation of the bag under vacuum and specimen curing in the oven

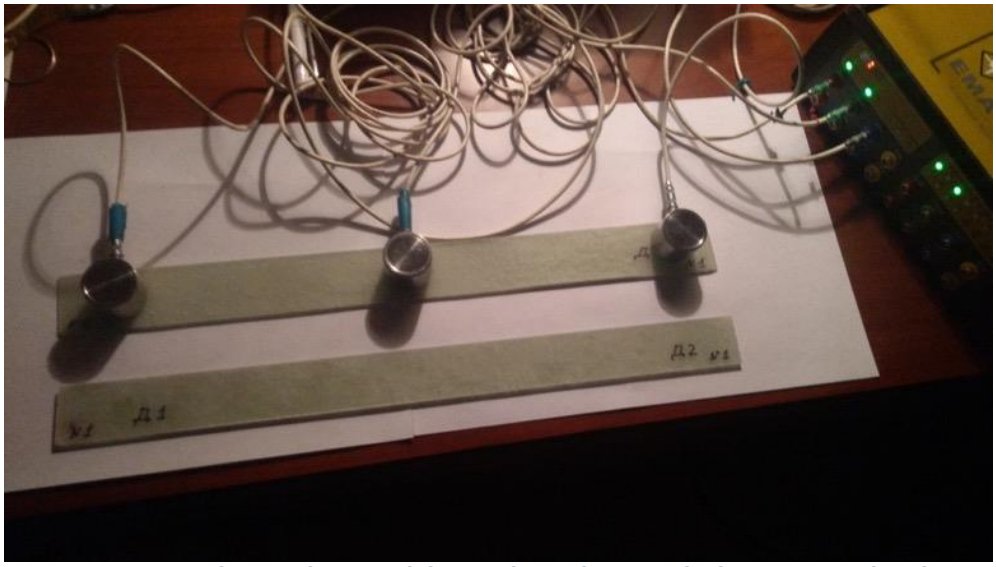

Figure 60. AE sensors on the specimen and the 16-channel EMA-4 device connected to them

The sensors were placed at a short distance from the edge of the specimen, so that they formed a linear location antenna with a total length of 330 mm (Fig. 60). When installing the third sensor, it was placed in the centre of the specimen (in the case of a piezo sensor simulator, directly above it).

Experiments have shown that the fiberglass under investigation has a high acoustic sensitivity, not worse than carbon fibre. The emitted square wave signal had the following parameters: amplitude 3V, frequency 60 KHz, duration 7 μs. When the sensor received a signal that was little distorted, it received an oscillogram similar to that shown in Fig. 61a, when changing the signal parameters, the oscillogram most often looked like the one shown in Fig. 61b.

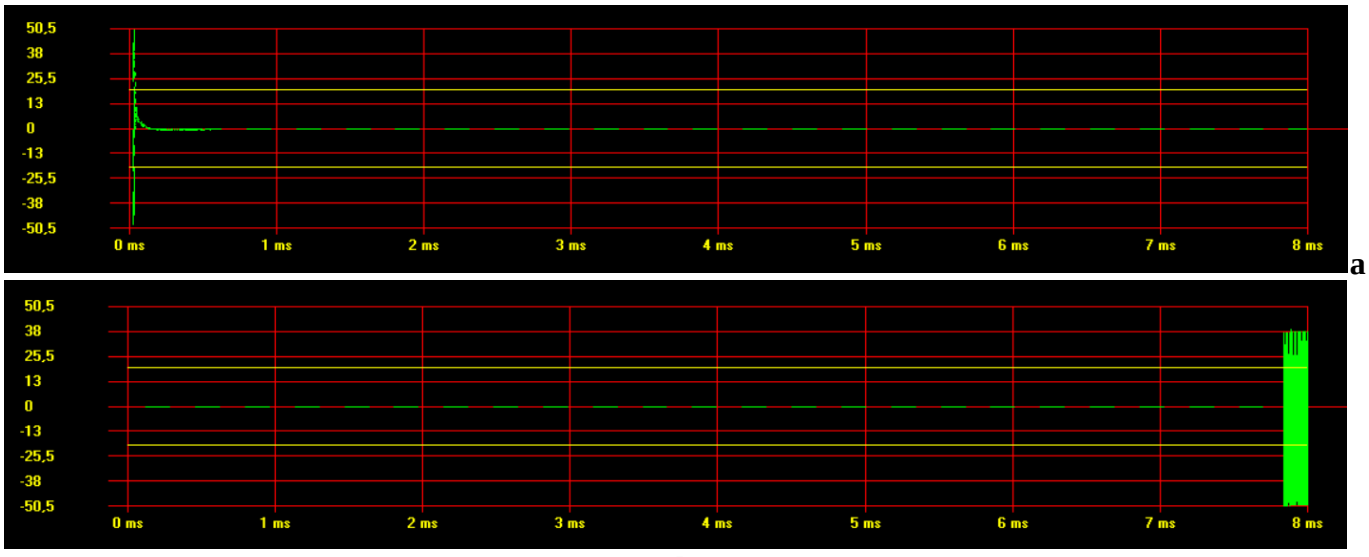

Figure 61. Typical oscillograms of AE signals received by sensors in various cases. The ordinate axis shows the amplitude of the signal, dB; on the abscissa, the time from the start of fixation of the recorded fragment of the waveform.

When determining the location of AE sources using sensors as a generator of waves, the velocities of AE waves in the material were selected so that the calculated coordinates of the AE signals emitted by the sensors and then received by the AE device, as accurately as possible coincided with the coordinates of the sensor-emitter (Fig. 62).

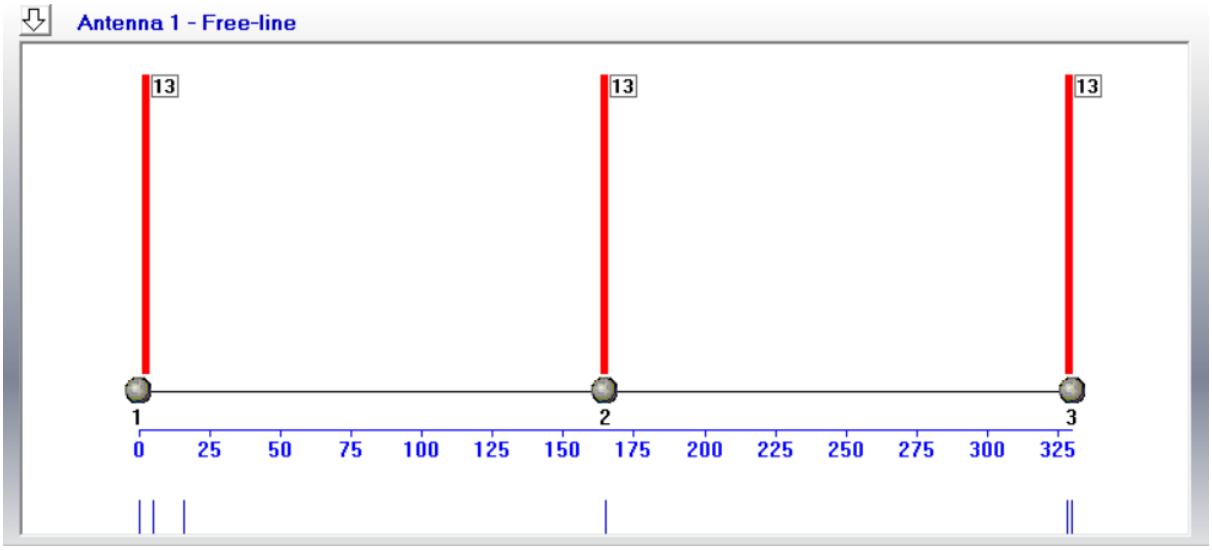

Figure 62. Results of alternate sounding of the specimen without a built-in sensors simulators. High accuracy in determining the coordinates is visible in the figure (the centers of acoustic activity are shown by flags and coincide with the locations of the AE sensors)

To ensure the correctness of the scanning results, several criteria are used. First of all, within the framework of each single test, the parameters of the signals received by the sensor should be stable, without significant scatter. Secondly, when two sensors are alternately used as receivers alternately located on opposite sides of the specimen, their data should also not have significant differences in parameters.

As part of this work, about a hundred experiments on six specimens were carried out to obtain the necessary statistics of stable results, three of which had a built-in simulator of a piezo sensor with a diameter of 5 mm in the center, which is close in some properties to the PZT19 material used in real piezoelectric sensors.

Typical graphs of the results of AE scanning of three specimens without a built-in piezo sensor simulator are shown in Fig. 63. In the left column of the graphs for the case when the emitter was sensor 1, in the right column is sensor 2. The bars show depending on the time of the AE signal receiving amplitude A, and dots show the time of their rise to the maximum Rt. When processing the measurements, software filters were used that cut out obviously incorrect data (for example, Rt = 0 μs).

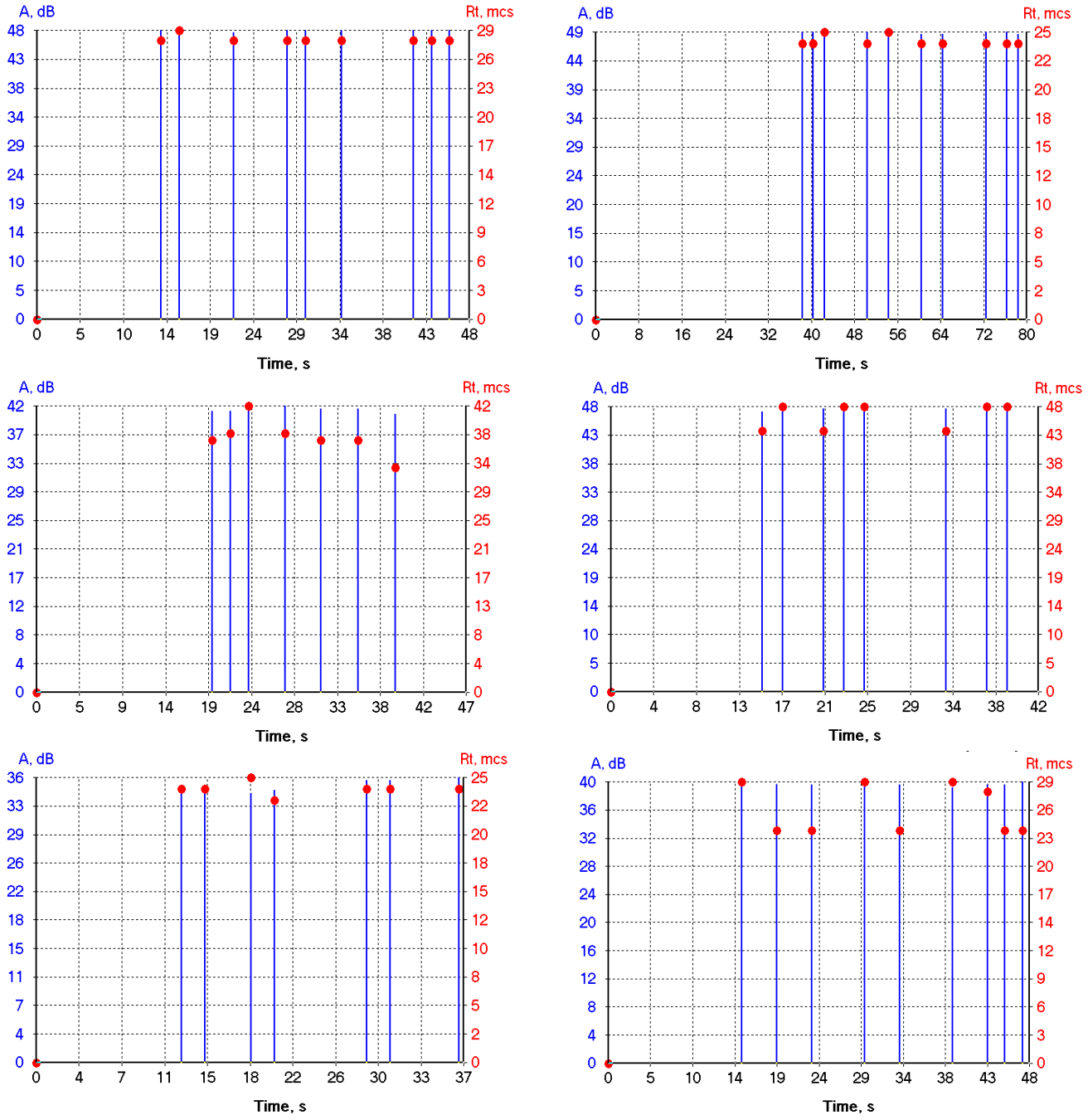

Figure 63. Results of AE scanning of specimens without a built-in piezo sensor simulator. The bars represent the amplitudes of the received signals A (dB), the points represent the time of their rise to the maximum Rt (μs)

The results are fairly stable. Although for different specimens and for different scanning directions there is some difference in the obtained values of the amplitudes A and the rise times of the signal Rt, within the framework of each specific experiment their repetition is high. Note that the minimum amplitude is 36 dB, the maximum value of Rt is 48 μs.

Further, it will be shown that these parameters for specimens with a piezo-sensor simulator are changed in the same way as previously shown for other materials — the amplitude of the received signal in the damaged material decreases, and the rise time Rt increases. Characteristic of this material is an insignificant, close to the statistical variation, a decrease in the amplitudes of the received signals in the damaged material with a significant increase in Rt.

In each specific test, it is clearly seen that the obtained amplitudes of the AE signals received from A signals had a smaller scatter than their rise time to a maximum of Rt. This phenomenon is most likely

due to the fact that the scanned material has a heterogeneous, layered structure. Even in the absence of internal defects, the features of the structure can lead to a change in the waveform, without affecting its power, as expressed by the amplitude.

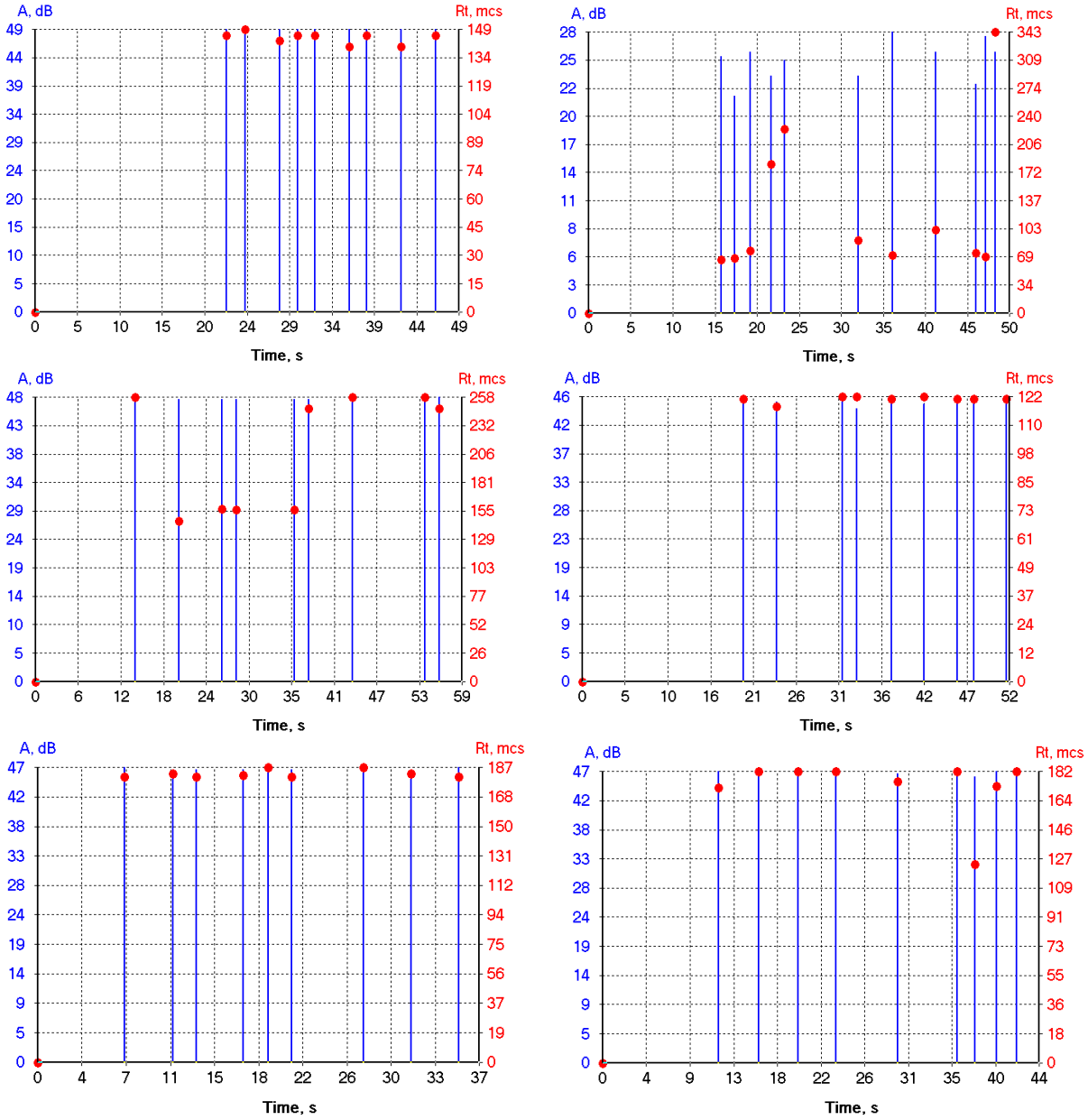

Figure 64. Results of AE scanning of specimens with built-in piezo sensor simulator. The bars represent the amplitudes of the received signals A (dB), the points represent the time of their rise to the maximum Rt (μs)

Typical graphs of the results of AE scanning of three specimens with a built-in piezo sensor simulator are shown in Fig. 64. In the left column, as in fig. 63, graphs are presented for the case when the emitter was sensor 1, in the right column - sensor 2.

To calculate the damage of specimens with a piezo-sensor simulator, the AE parameters obtained by scanning specimens without piezo plates with the same number were used as the initial data. Theoretically, they could be interchanged in any order, since they were cut from the same sheet of material, and the averaged data are not significant.

The data was processed in MS Excel. For each specimen, the values of A and Rt were obtained for each of the directions of sounding, then the amplitude growth rate of amplitudes v = A / Rt, the damage in each particular case of scanning was calculated. On fig. 10 it is shown as ΔW 1-> 2 for scanning specimen

No. 2 with signals from sensor No. 1, ΔW 2-> 1 for scanning specimen No. 1 with signals from sensor No. 2, and then by analogy. Further, the average damage value for each of the scanning directions was calculated.

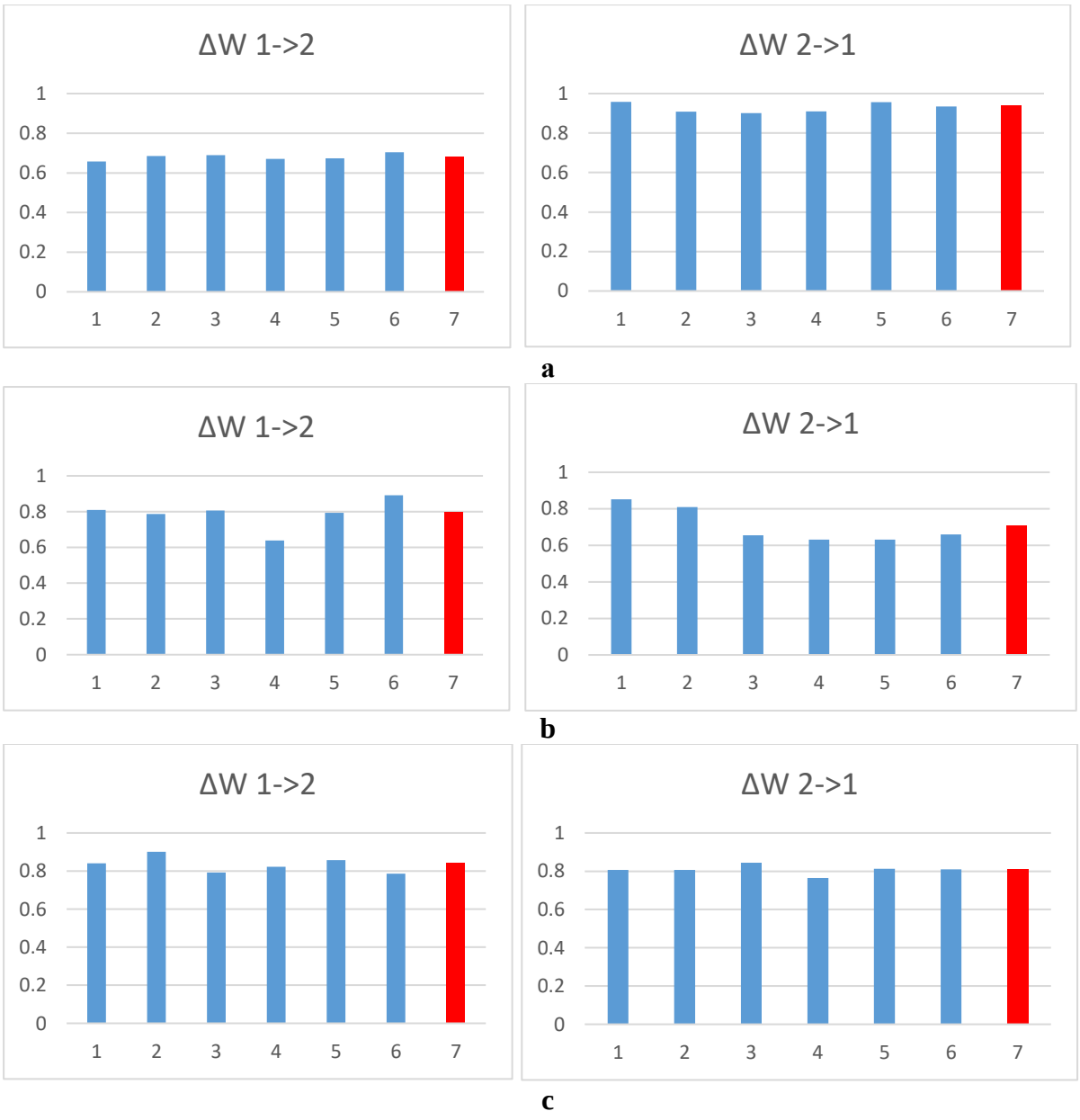

Figure 65. The results of calculating the damage to specimens with a built-in simulator of a piezo-sensor according to AE scanning data: a - specimen No. 1, b - specimen No., c - specimen No. 3

The analysis of the data presented in Fig. 64 and 65 shows, firstly, the high damage of all three specimens with built-in piezoelectric simulators, which for individual series of specimen scanning ranges from 0.65 to 0.95. Secondly, the specimen No. 1 seems to be the most damaged, for which the highest average damage is recorded when scanning from sensor No. 2, and, in addition, there is a very large scatter of measured data, which was noted for the upper right graph on fig. 64 which indicates the unevenness of the properties of the scanned material in this direction.

Theoretically, in subsequent tensile tests, down to rupture, the AE pattern should differ significantly in the direction of increasing the number of AE events for specimens with embedded simulators of piezoelectric sensors. The places of the greatest AE activity in the area of simulators should also be recorded, since they are stress concentrators.

Later, such experiments were conducted. The fiberglass specimens of both types were tested on destructive machine with hard mode of loading (fig. 66).

Figure 66. The test machine hold part with fiberglass specimen having embedded simulator of piezo sensor

The results of testing a specimen without embedded carbon plate show that more acoustic signals were radiated by the area of the testing machine holds in which the sample is fixed. The specimen has practically no serious defects. Destruction occurred in the hold part of a testing machine (Fig. 67)

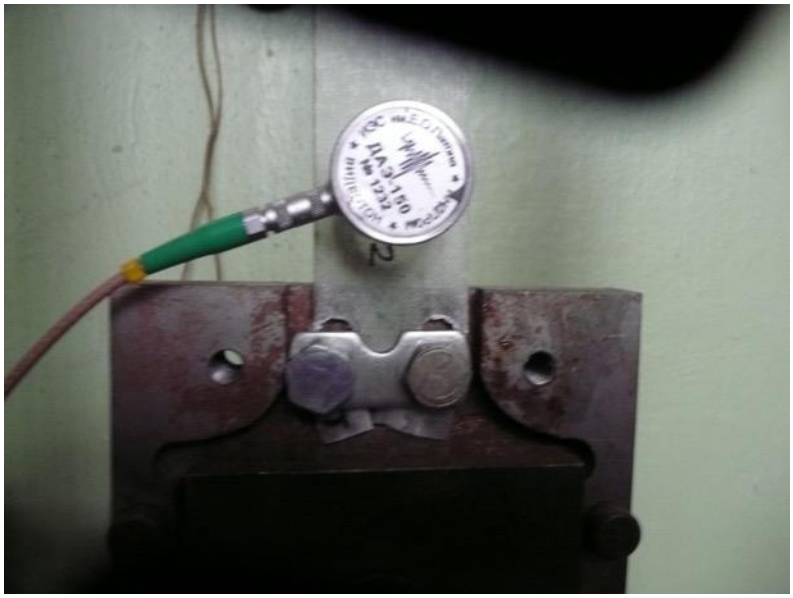

Figure 67. The area of fiberglass specimen destruction. Coordinate of destruction is near 250 mm (sensor No 2)

Lower some screens of EMA-3.9 program for this experiment is shown. Location scheme (on the bottom) combined with destruction forecast area (on the top).

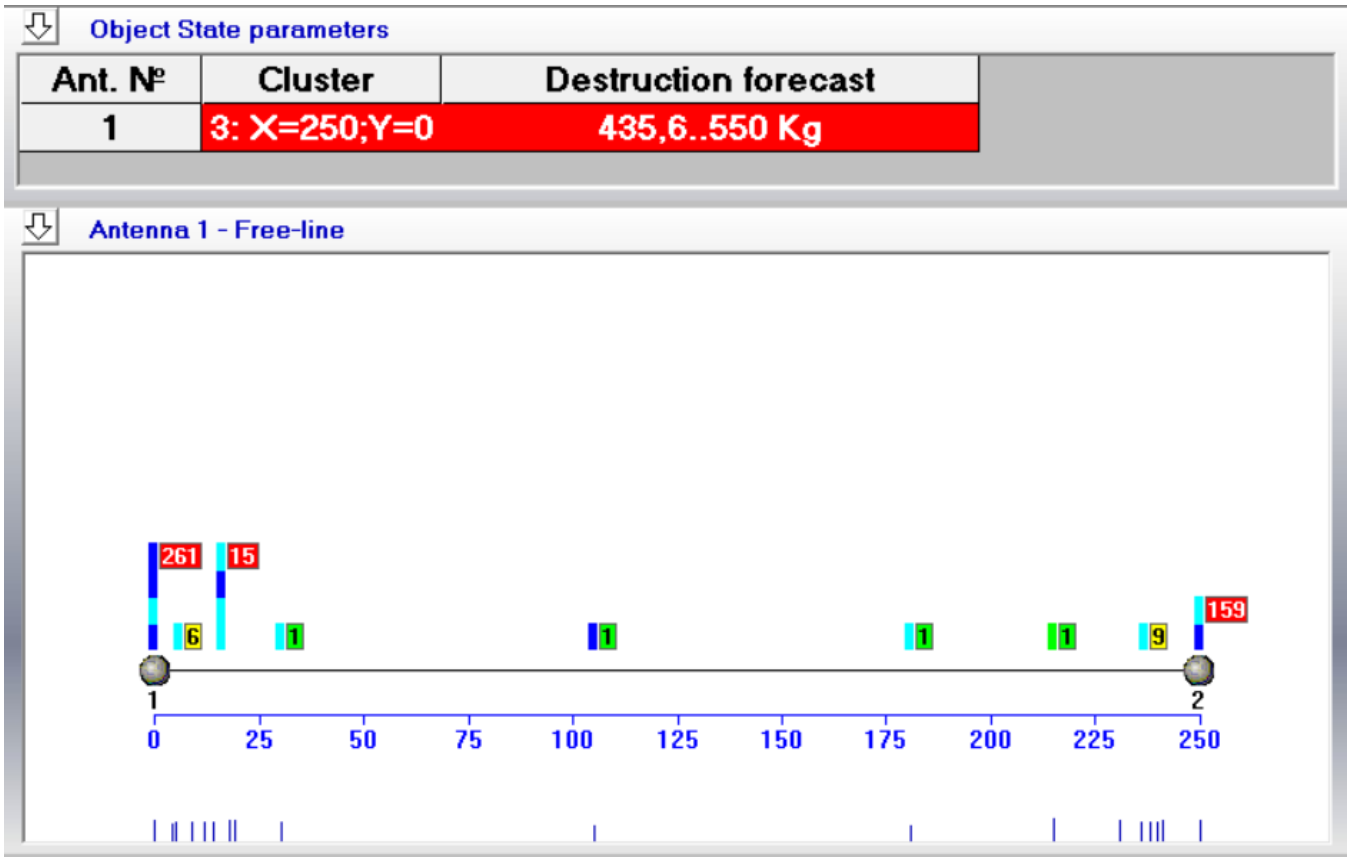

Figure 68. Results of loading the fiberglass specimen without a built-in simulator of piezo sensor. The prognostic destruction value is shown as 435.6 to 550 Kg. The prognostic place of destruction is 250 mm. The centers of acoustic activity are shown by flags

In Fig. 69 all loading process is shown. As we can see the forecast of destruction **435.6 to 550 Kg** is very close to real destructive load 470 Kg.

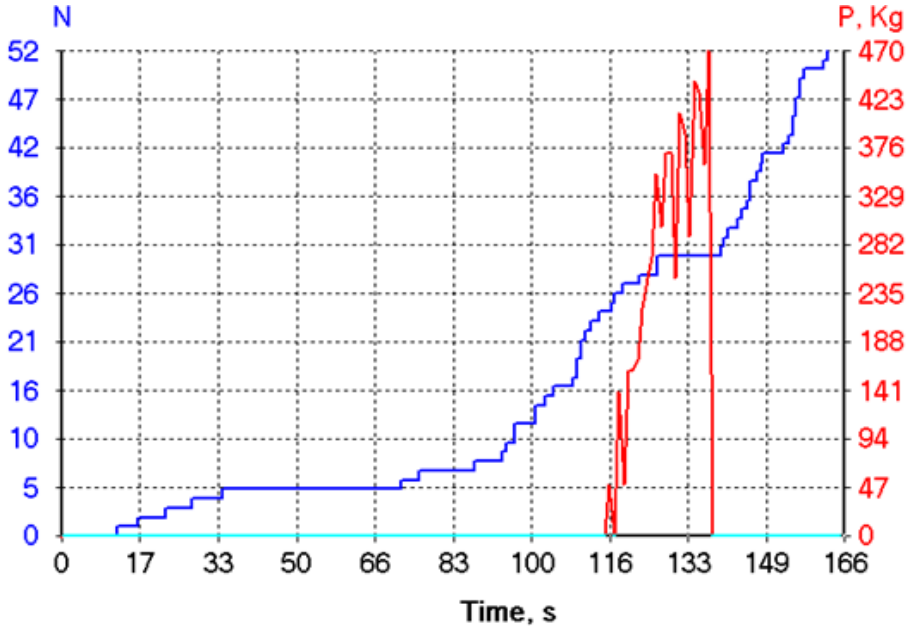

Figure 69. Results of loading of the fiberglass specimen without a built-in simulator of piezo sensor in time. N – summary curve of AE events, P – loading curve

In the results of testing of specimen already with embedded carbon plate we can see that more acoustic signals again were radiated by the area of the testing machine holds. Specimen with built-in simulator of piezo sensor shows some acoustic activity in the centre when the embedded carbon plate placed (Fig. 70). But it is not critical activity. Destruction, the same as in specimen without carbon plate, occurred in the hold part of a testing machine (Fig. 67).

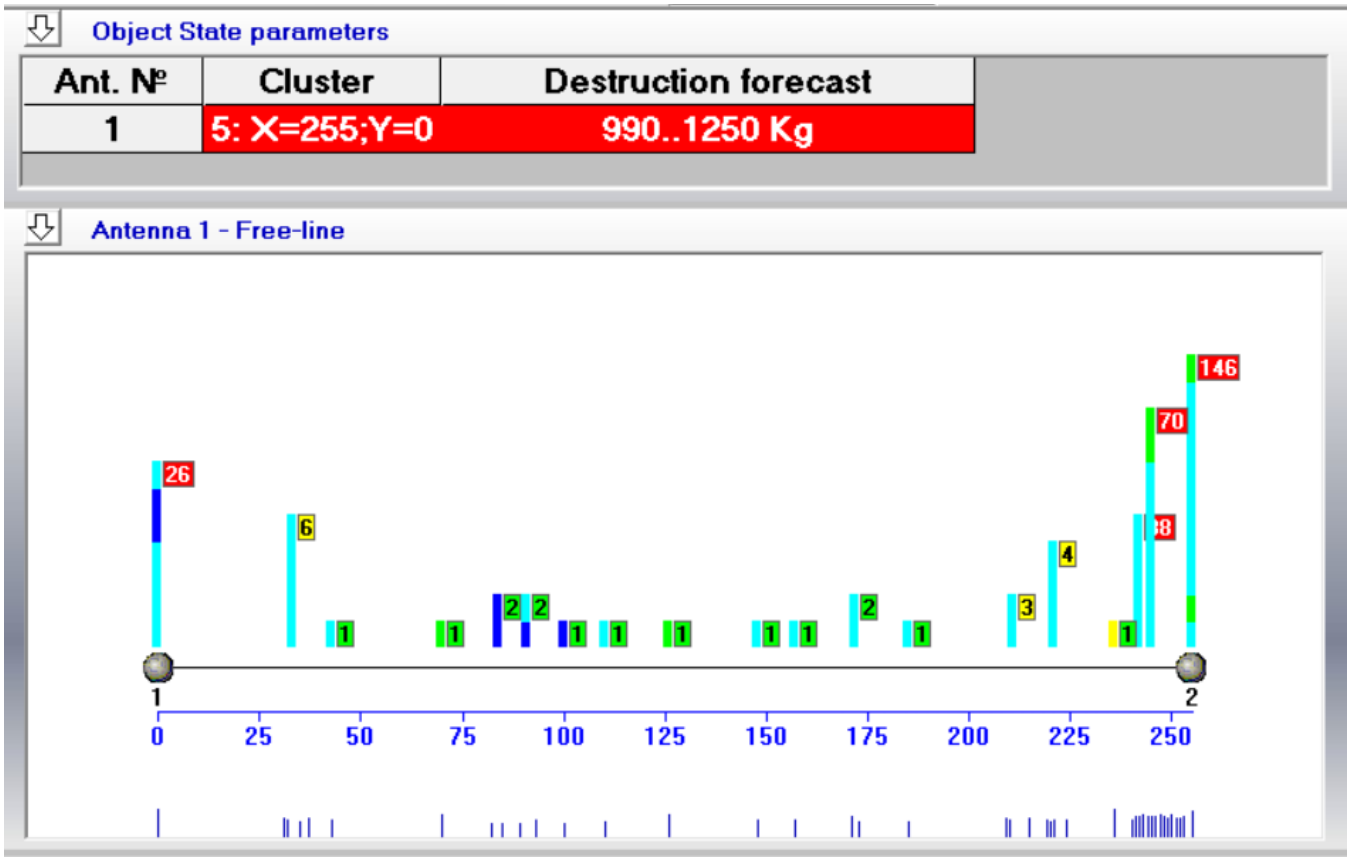

Figure 70. Results of loading the fiberglass specimen with a built-in simulator of piezo sensor. The prognostic destruction value is shown as 990 to 1250 Kg. The prognostic place of destruction is 255 mm. The centers of acoustic activity are shown by flags

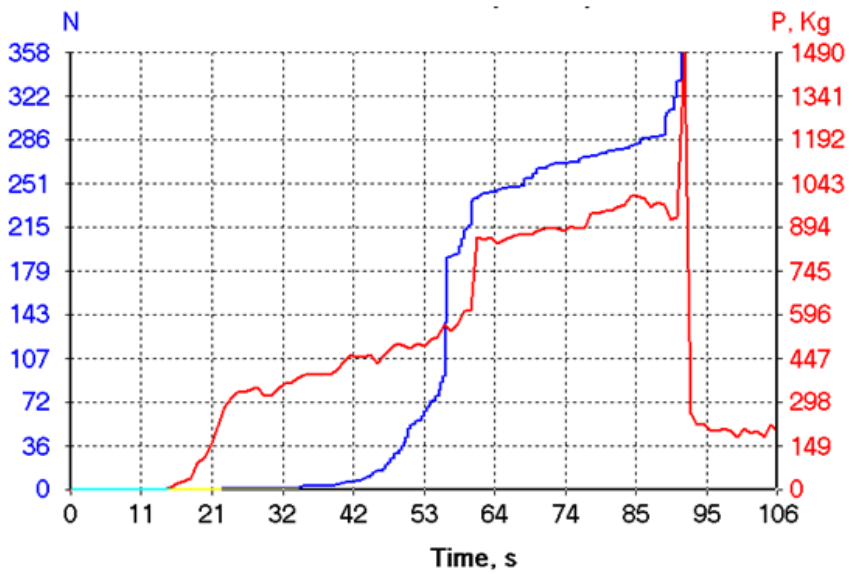

Figure 71. Results of loading of the fiberglass specimen with a built-in simulator of piezo sensor in time. N – summary curve of AE events, P – loading curve

As we can see the forecast of destruction 990 to 1250 Kg is enough close to real destructive load 1490 Kg.

In conclusion for fiberglass next main results obtained:

1. The embedded sensor simulators with chosen tested size and position has no influence on strength of main material. So, real PZT sensors of same size can be used in real structures, in particular, in aviation.
2. AE tests conducted shown that prognostic properties of EMA systems works good with fiberglass.
3. The large level of damage which AE scanning shows relates to global changes of acoustic properties in fiberglass material which have arisen during carbon plate installation and thermal treatment.

Analogous experiments were conducted with carbon fibre specimens with embedded sensor simulators. The main result of the specimens' destruction was the same as for the fiberglass, near hold part of the testing machine (Fig. 72).

Figure 72. The area of carbon fibre specimen destruction. Coordinate of destruction is near 284 mm (sensor No 2)

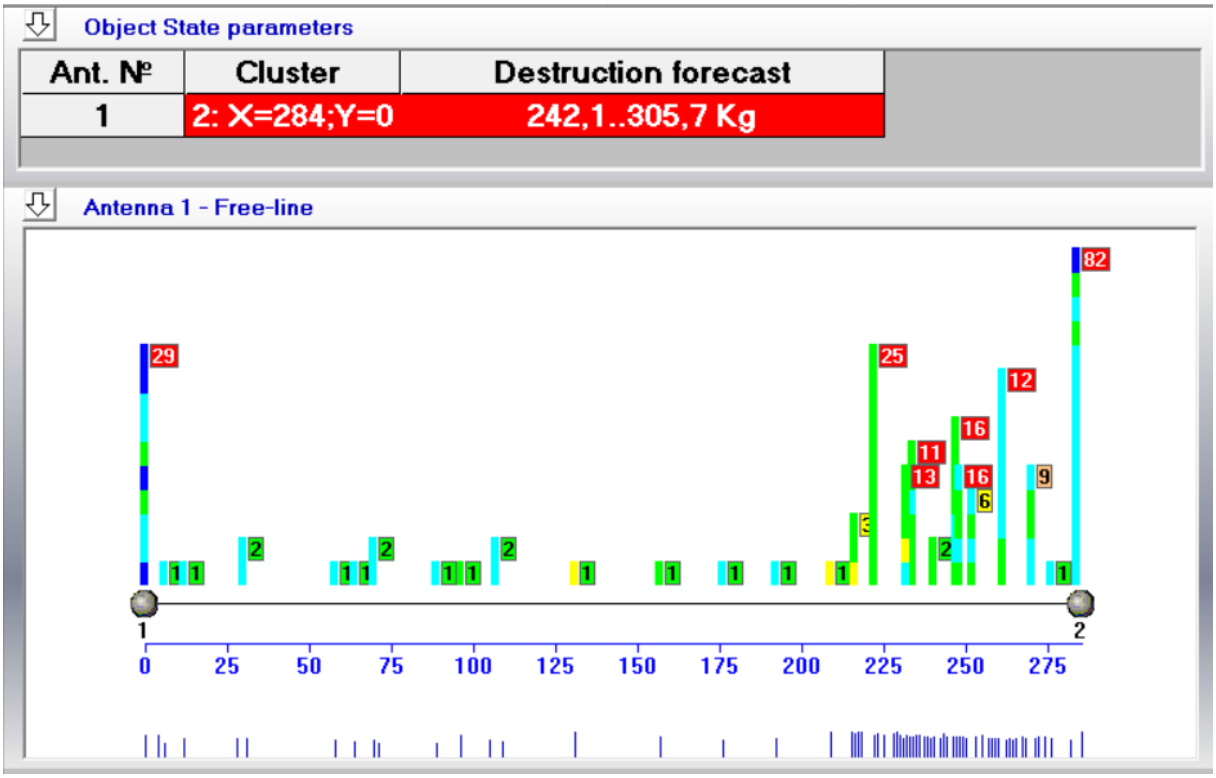

Figure 73. Results of loading the carbon fibre specimen with a built-in AE simulator carbon plate. The prognostic destruction value is shown as 242.1 to 305.7 Kg. The prognostic place of destruction is 284 mm. The centers of acoustic activity are shown by flags

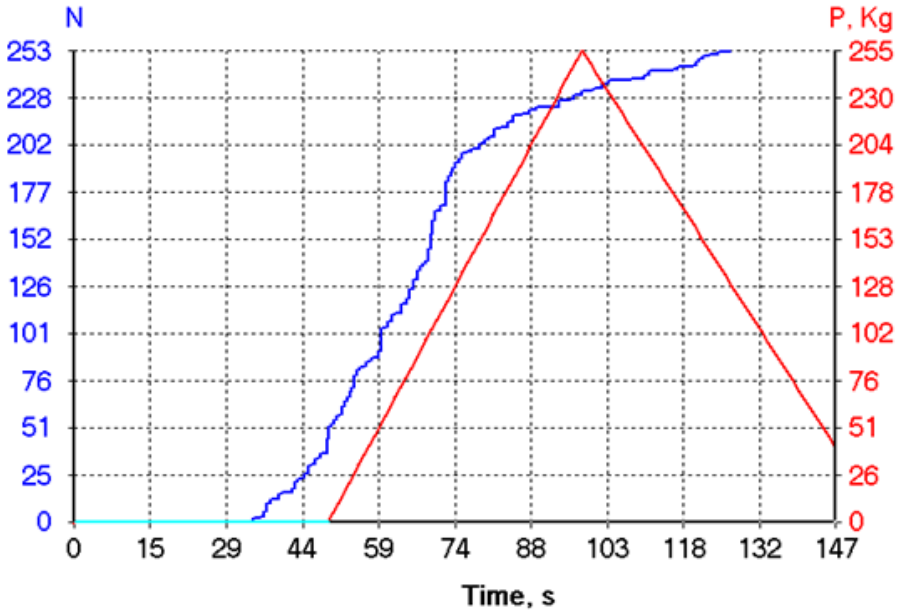

Figure 74. Results of loading of the carbon fibre specimen with a built-in simulator of piezo sensor in time. N – summary curve of AE events, P – loading curve

As we can see the forecast of destruction 242.1 to 305.7 Kg is very close to real destructive load 255 Kg. So, the results for carbon fibre are the same as for fiberglass:

1. The embedded sensor simulators with chosen tested size and position has no influence on strength of main material. So, real PZT sensors of same size can be used in real structures, in particular, in aviation.
2. AE tests conducted shown that acoustic sensitivity and prognostic properties of EMA systems are good both for carbon fibre and fiberglass.

The obtained results suggest that it is possible in principle to create a method of applying the AE technology into practice when monitoring composite materials of tested types, both in standard destructive testing and scanning without loading. This requires further research in this direction and obtaining a set of statistical data that would establish the necessary safety criteria for the operation of structures made of composite materials tested by the AE method.

Resume

1. Research has shown that the glass fiber plastic made of Aeroglass 280 fiberglass and Elan-tech EC157 + Elan-tech W152XLR bonding material and Udo UD CST 150/300 composite material based on the ARALDITE 564 binder are testable from the point of view of the AE method, it allows to determine the coordinates of AE sources with sufficiently high accuracy during test sounding and emits AE waves during deformation and destruction.
2. AE in the course of specimens testing forms two groups of events separated in time. The first occurs shortly after the start of loading. The second is recorded immediately before the destruction and in the process of it, up to the complete separation of the specimen into parts.
3. In the presence of concentrators, the AE method makes it possible to determine their location during specimen loading with enough for practice accuracy.
4. Important for registration of the pre-destructive state and the moment of destruction in the conducted experiments is a sharp, twofold increase in the level of continuous AE.
5. It is shown that with the use of AE systems of the EMA type a prediction of the destructive loading for the studied material is possible.
6. The embedded sensor simulators with chosen tested size and position has no influence on strength of main material. So, real PZT sensors of same size can be used in real structures, in particular, in aviation.
7. Creating a method for composites testing using AE technology and building an algorithm for predicting the destruction of a material based on the EMA series devices is possible but it requires additional research to clearly work out the criteria characterizing the destruction.

Development of smart CFRP structures

Manufacturing of CFRP specimens for tests

For development and testing of the technology for integration of piezoelectric sensors into composite material, KhAI manufactured a number of samples (lay-up scheme $[0_2/90/0/+45/-45/\overline{90}]_s$) made of unidirectional carbon fibre tape + hot curing resin ЭДТ-69У prepreg (in case of hand lay-up) and glass fabric + L285 resin + L287 hardener (in case of RTM technology). Infusion was used to analyse and compare the quality of composite structures with integrated sensors made by two different methods. The samples were cured in accordance with the curing regimes of the resins: ЭДТ-69У (heating up to 80 °C, holding for 1 hour under vacuum + autoclave pressure 2 atm; heating up to 120 °C, holding for 4 hours under vacuum pressure, cooling in an autoclave) and L285 (resin vacuumation, impregnation of the package, curing during 4 hours at 60 °C).

During manufacturing of samples with sensors and wires that were later connected to the equipment, it was necessary to ensure the following requirements:

- to avoid wires damaging during laying up, moulding and, the most important, during removing the panel from the form;
- to provide a dielectric interim layer between the sensor and the panel material carbon fibre. Therefore, the sensors were embedded between two fiberglass prepreg layers and then put into the stack of carbon fibre prepreg layers (Fig. 75).

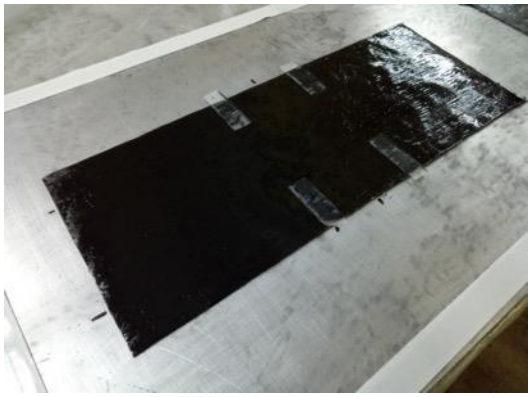
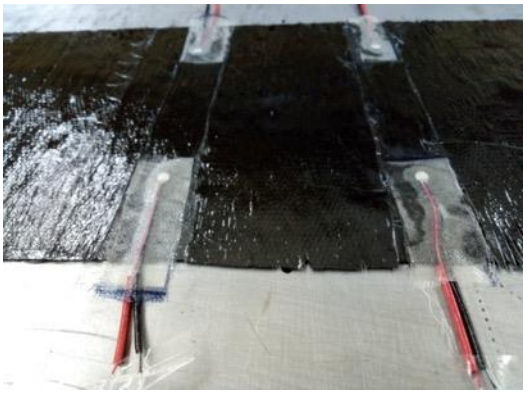

Figure 75. Lay out of sensors on a substrate of fiberglass

The sensors were placed with the side upward, where the wires are soldered in order to avoid their crushing by the excess pressure (Fig. 2).


Figure 76. Panel with sensors, under a vacuum film, prepared for molding

The following defects were observed after the demoulding of the composite panel:

- wires were filled with a resin and their removal from the mould, even with a small effort, could lead to their breakage;
- sensors have changed their position, i.e. "floated" along with the resin during the curing process (Fig. 3).

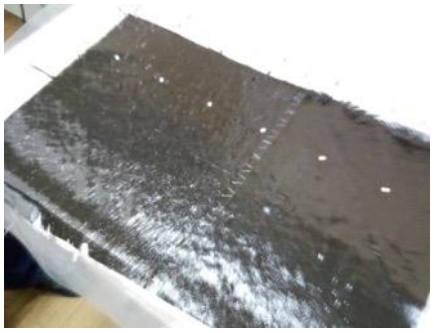


Figure 77. Installation of sensors with the help of grid on samples for shear and bending tests

For future manufacturing of composite structures with embedded sensors, the following is recommended:

- preliminary preparation of the sensors: vacuum curing of a sensor with wires in an envelope made of fiberglass fabric, which further allows more accurate sensor positioning in the composite structure and avoiding its “floating” during the curing process (Fig.78);

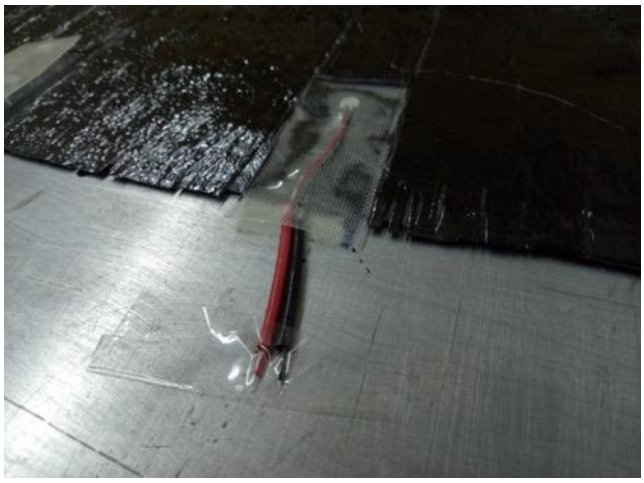

Figure 78. Fixing the sensor wires on the snap

- the wire braid must be heat-resistant, at least to withstand the maximum temperature of composite curing without melting;
- the wire braid must be rigid enough to pierce the prepreg layers, because not always sensors are positioned close to the structure edges. Moreover, location of the wire exit point(s) somewhere on the surface structure provide free access for machining of the structure edges;
- the loose ends of the wires must be long enough for their further stripping and connection with other wires. After going out from the composite structure, the wires should be wrapped in polytetrafluoroethylene (PTFE) film to prevent their sticking to the mould or the structure;
- soft moulding should be used on the solder side of the sensor;
- application of infusion process (Fig. 79) gave positive results in terms of the panel quality, i.e. the sensors do not “float”, remaining on their places, there are no voids between the sensor and composite layers. However, the problem of maintaining the integrity of the wires remains. Wires are completely immersed in the resin and may be broken during their cleaning. It may be proposed to use a combined wire braid, i.e. a part of the braid from the sensor to the exit point from the composite structure to be made of a heat-resistant material with good adhesion to the resin, while another part of the braid is made of PTFE or replaced by a closed silicone form that prevents access of the resin to the wire;

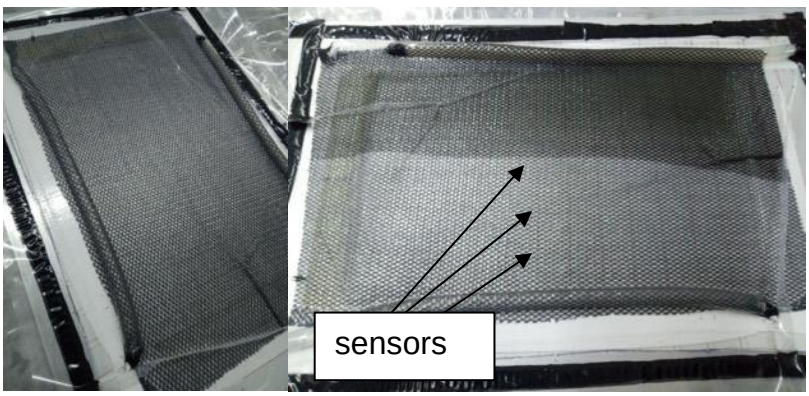

Figure 79. Manufacturing samples by infusion method (to be tested by E. O. Paton Electric Welding Institute)

- to minimize the sensor with wires protrusion on the surface of the composite structure, it is possible to exclude one layer of reinforcing material from the envelope of the sensors (or add layers to the main structure) (Fig. 80).

Figure 80. Installation of the sensors with removal of reinforcing material from the area of sensors installation

Influence of PZT sensors immersion on mechanical properties of CFRP structures

Cured composite panels with sensors were cut into samples to determine the mechanical properties under shear and bending loads. Test samples represented samples with sensors located in the sample central part and the reference samples without sensors. Reference samples were used to analyse the effect of the sensors on the mechanical properties of the composite structure (Fig. 81, Fig. 82).

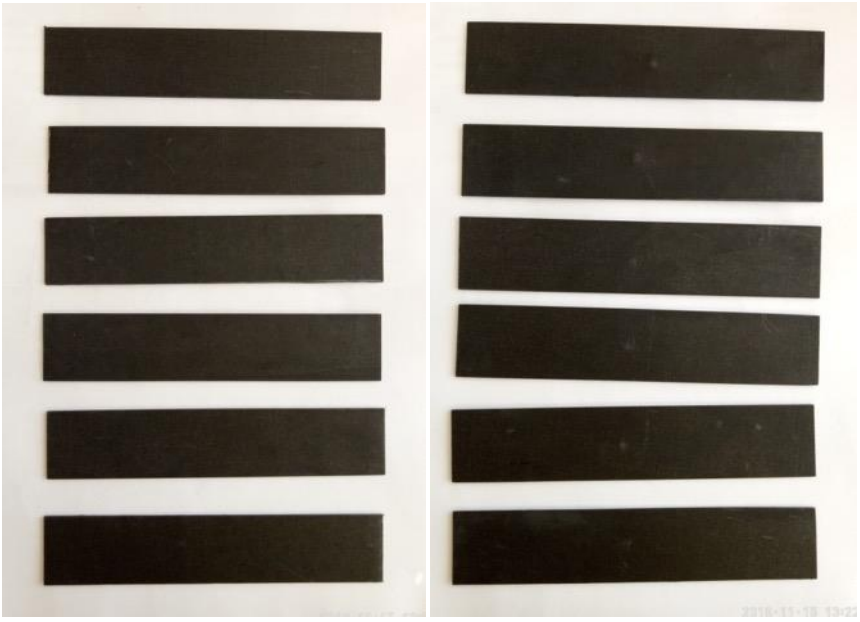

a) b)

Figure 81. Unidirectional CFRP composite samples without sensors (a) and with sensors (b) for bending tests

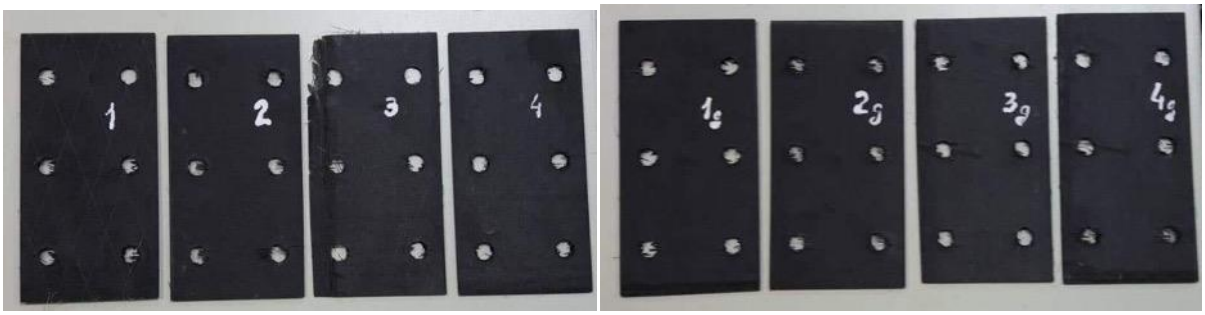

a) b)

Figure 82. Unidirectional CFRP composite samples without sensors (a) and with sensors (b) for shear tests

Shear load tests

Shear tests were performed in accordance with ASTM D4255/D4255M-01. The general view of the samples is shown in Fig. 82. The samples were fixed in the fixture and monotonously loaded until the failure (Fig. 82).

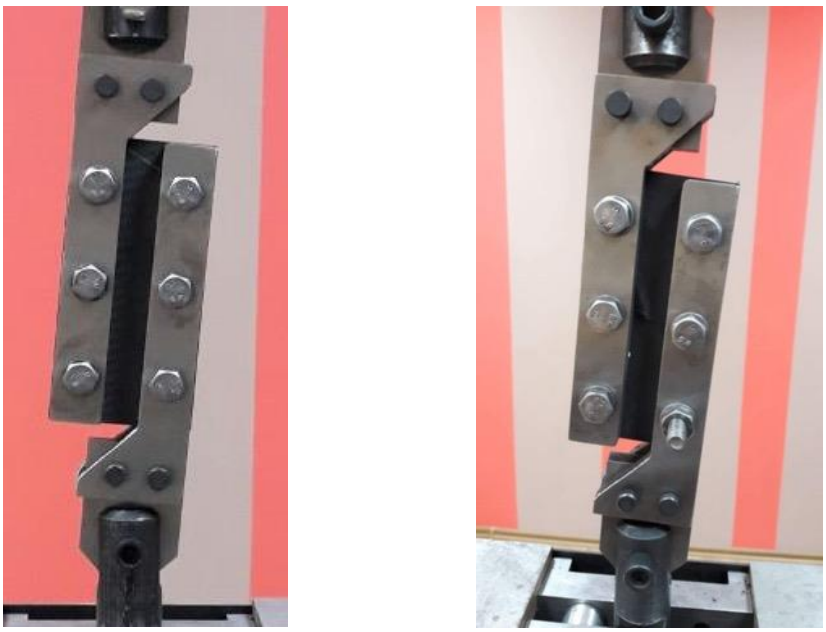

a) b)

Figure 83. Shear tests for the samples without sensors (a) and with sensors (b)

The failure of the samples with embedded sensors under the shear load began immediately above the sensors, and then spread to the rest of the sample area (Fig. 83(b), Fig. 84). Samples without sensors had a uniform field of destruction over the entire surface (Fig. 84, Fig. 85).

Figure 84. ***Samples after shear tests: top – without sensors, bottom – with sensors***

Figure 85. ***Tests under shear samples without a sensor***

The results of the shear tests are presented in table below.

Table 4. Shear test results for samples with sensors and without sensors

Specimen Number	Length, mm	Thickness, mm	Cross-section area, mm^2	Failure load, kN	Shear strength, Mpa	
Samples without sensors						
1	150	1,58	237,0	32,5	137,1	
2	150	1,58	237,0	33,8	142,6	
3	150	1,59	238,5	30,2	excluded	damaged specimen edge
4	150	1,52	228,0	34,7	152,2	
Samples with embedded sensors						
1g	152	1,52	231,0	31,4	135,9	sensor without wire
2g	151	1,55	234,1	31,3	133,7	sensor without wire
3g	149	1,56	232,4	31,7	136,4	sensor with wires
4g	152	1,55	235,6	32,6	138,3	sensor with wires
Results – shear strength (MPa)						
					Without sensors	**With sensors**
Mean value					**143,9**	**136,07**
Standard deviation					**7,64**	**1,89**
Variation, %					**5,3**	**1,4**

Shear tests have demonstrated that the sensor integration reduces the shear strength of the samples by 5.4% in comparison with the reference samples without sensor. It shall be noted that the wires do not introduce additional adverse effect on the structure, i.e. the failure load remains almost at the same level as for the samples with sensors but without wires. Also standard deviation of shear strength is much lower for specimens with embedded PZT. This may be due to the fact that destruction initiated from the sensors in all of the cases, whereas for other specimens the damage initiated from fixture bolts.

Flexural load tests

Flexural load-displacement graphs for both pristine and sensor embedded specimens are shown in Fig. 86 and Fig. 87 respectively. Since the sensor embedded specimens have a thickness variation at the middle of the specimens, recorded load data is normalized with specimen width for each specimen and load-per-width vs cross-head displacement curves is drawn in addition to stress-strain curves. Flexural modulus of elasticity are calculated by using the slope of the stress-strain curve between 0.001 and 0.003 microstrain according to ASTM D- 7264. Also, flexural stiffness is calculated for a displacement range of 2 to 6 mm by dividing the load by displacement. This displacement range is chosen since it adequately corresponds to the strain range used for the calculation of the modulus of elasticity.

The mean values of maximum load-per-width, flexural stiffness and flexural modulus of elasticity are given in the Table 5 with the coefficient of variation. Considering the deviation values given in the brackets, it can be said that the experiments are valid enough to assess the mechanical performance of the tested composite panels for prescribed loading condition. It has clearly seen that the sensor embedment has a minor effect on the maximum load carrying capability and flexural stiffness. However, the calculated modulus of elasticity for sensor embedded specimens is 7.4% lower than the pristine specimens. This is

due to the thicker middle section is used for the calculation of stress values, in other words, the assumption of constant moment of inertia (related to the assumption of uniform cross-section).

Table 5. Flexural test results for samples with sensors and without sensors

	Maximum load-per-width (N/mm)	Flexural stiffness (N/mm)	Flexural modulus of elasticity (GPa)
Pristine specimens	12.78 (8%)	34.74 (10.4%)	84.64 (4.7%)
Sensor embedded specimens	12.23 (6.5%)	34.88 (11.2%)	78.40 (8.6%)

Although the maximum load carrying capability and flexural stiffness values are not significantly changed with the sensor embedment, as can be seen in the cross-head displacement at maximum load is slightly lower for the sensor embedded specimens in comparison to pristine ones. This result may indicate that the sensor embedment is creating a resin rich region at the immediate vicinity of the sensor which reduces the brittleness by introducing an early crack starter. Therefore, the damage propagates in a stable manner after the initiation at the weak resin rich region and a softening behaviour can be observed. Consequently, catastrophic failure occurs at a similar load value with pristine specimens but at a slightly decreased crosshead displacement.

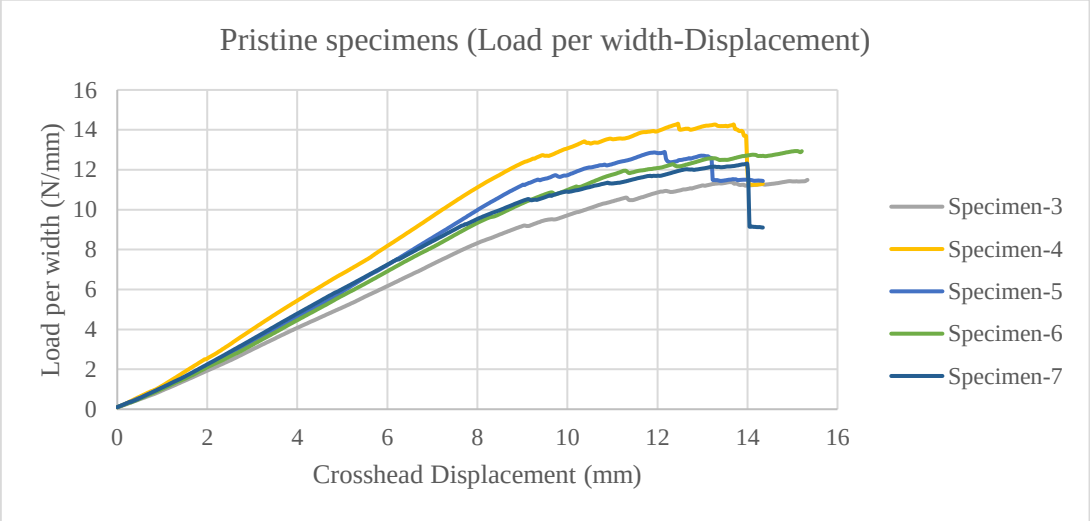

Figure 86. ***Flexural load-displacement graphs for pristine specimens***

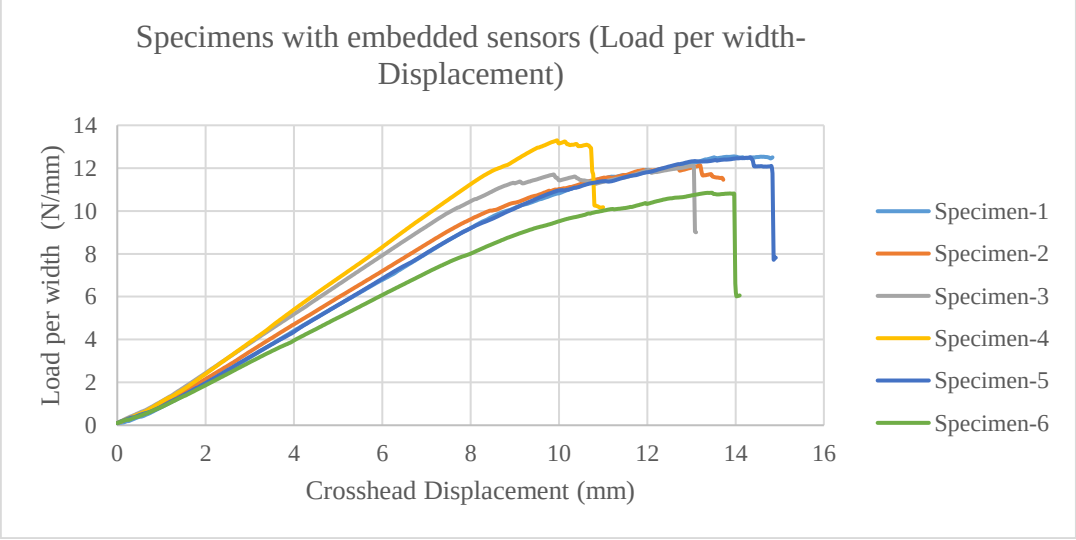

Figure 87. ***Flexural load-displacement graphs for specimens with embedded sensors***

FEM simulations

Material properties for CFRP based on HTS 45 unidirectional carbon fabric and L-285 epoxy resin were set on the base of previously obtained results from standard mechanical tests of CFRP with similar fibers and resin type, and presented in table below.

Table 6. Mechanical properties of CFRP

Property		Symbol	Value
Elasticity modulus, GPa	Along fibres	E1	160
	Transverse to fibres	E2	10.4
Shear modulus, GPa		G12	4.3
Poisson ratio		m12	0.23
Tensile strength, MPa	Along fibres	F1T	1800
	Transverse to fibres	F2T	50
Compressive strength, MPa	Along fibres	F1C	1450
	Transverse to fibres	F2C	110
Shear strength, MPa		F12	45

Material of piezoelectric sensors of type SMD05T04R111WL was assumed as isotropic with elasticity modulus of 86 GPa. Elasticity modulus of used resin is 3.5 GPa. Poisson ration for all isotropic materials were assumed as $\mu = 0.3$.

Laminated shell model

According to this model sensor and resin rich zone simulated as additional plies in the composite laminate with the corresponding material properties. Thickness of the ply which represents sensor is equal to the sensor thickness 0.4 mm and thickness of the ply which represents resin rich zone was assumed as average thickness of this zone 0.2 mm. The outer radius of the resin rich zone was assumed to equal 4 mm according to measurements of manufactured specimens. Laminated shell model is shown in Fig. 88.

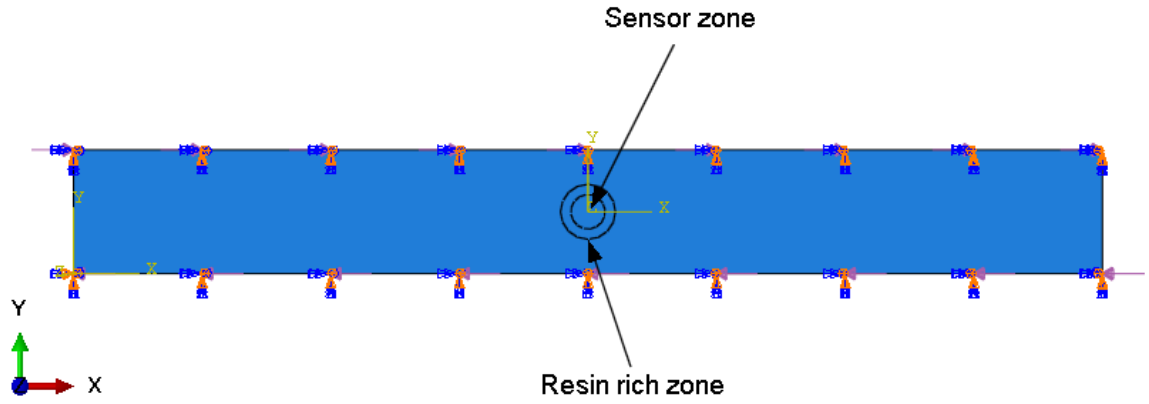

Figure 88. *Laminated shell model of CFRP plate with piezoelectric sensor*

Model represents work zone of the CFRP plate clamped in the shear fixtures. Shell edge load was applied to the longer edges of plate. Boundary conditions at these edges restrict all translations and rotations except the translation along x axis to allow shear deformation of the plate.

Static analysis was performed and failure index was calculated using Tsai – Hill criterion (Fig. 89) to estimate effect of stress concentration, caused by embedded sensor.

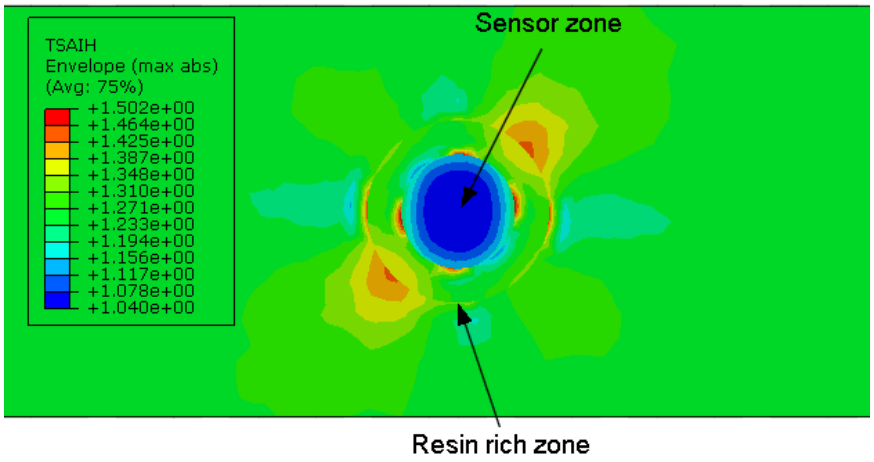

Figure 89. ***Distribution of failure index, calculated using Tsai – Hill criterion***

According to simulation results, failure index in regular zone of plate equals 1.26 and maximum value of failure index in proximity of sensor is 1.5. Thus, first ply failure of plate, according to used model, will occur at 84 % of failure load for plate without sensor.

Solid model

To estimate interlaminar shear and peel stresses in sensor zone solid model was used. Assuming that the middle part of the specimen is in the simple shear condition, the quarter of the middle part of the specimen with dimensions 18 x 18 mm was used for calculation (Fig. 90). This approach justified by the fact that stress-stain state of considered middle part of specimen is symmetrical relative to axes x_1, y_1 (see Fig. 90).

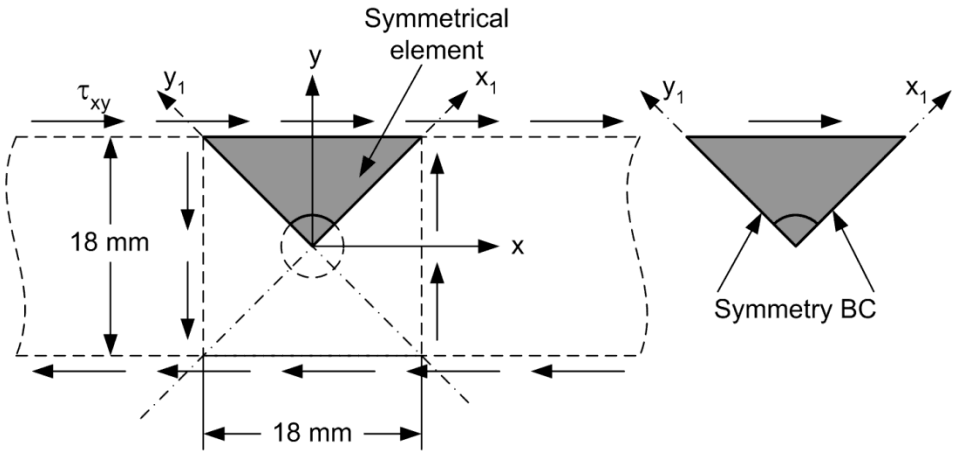

Figure 90. ***Representative for simulation***

Symmetry boundary conditions were applied at the faces coinciding with planes of symmetry, and shear load was applied to the free face of representative element. Solid model of chosen representative element for simulation is shown on the Fig. 91.

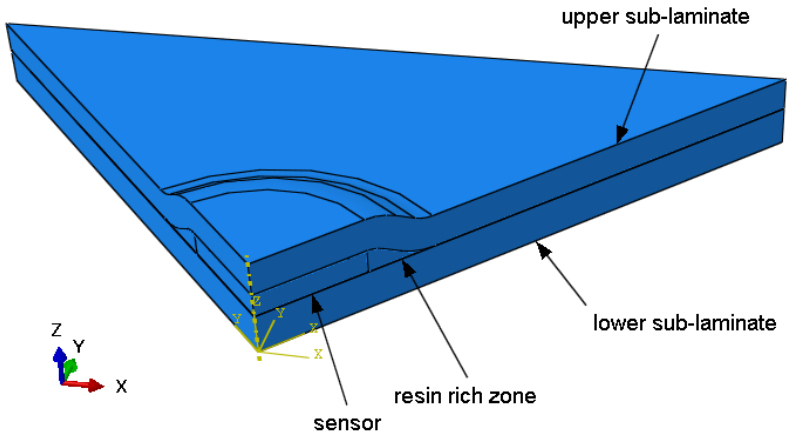

Figure 91. *Solid model of representative element*

Created model consist of four solid bodies which represent two sub-laminates, sensor and resin rich zone. Effective orthotropic material properties were applied to the sub-laminates which were calculated using laminated theory. Material axes for upper sub-laminate were applied using “Discrete” method in Abaqus with top faces of this body as reference surface. Hard contact conditions were applied between all bodies in model. Shear stress which was applied to the faces of representative element is equal to the failure shear stress determined during testing.

Maximum interlaminar shear and peel stresses were observed at the lower sub-laminate face. Results of calculation of these stresses are shown in Fig. 92, 93.

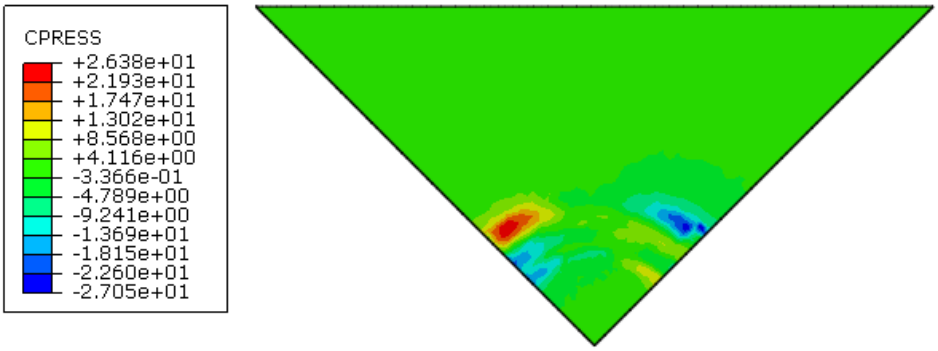

Figure 92. *Contact pressure at the lower sub-laminate top face*

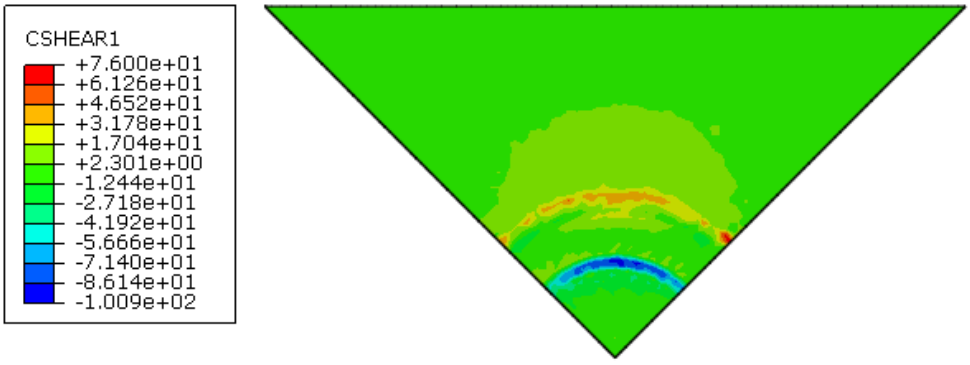

Figure 93. *Interlaminar shear stresses at the lower sub-laminate top face*

As shown by the results, maximum shear stresses of 101 MPa in the proximity of sensor's edge can be greater than interlaminar shear strength of laminate, and can cause debonding. This effect was also observed during testing of specimens.

Conclusions

Simulation results showed that embedding of the piezoelectric sensors can produce significant effect on specimen strength due to stress concentration and interlaminar stresses. But at the same time, results of tests haven't show significant ultimate strength reduction. This can be explained by the fact that initial failure of specimen in sensor zone in the form of matrix failure does not cause ultimate failure of the specimen associated with the fibre brakeage. But embedded sensor can be the source of delamination that was observed during experiment (at the about 70 - 80 % of failure load, Fig. 94) that can propagate under cyclic load. It also can be noted that propagation of delamination during tests was restricted by the fixtures.

Figure 94. ***Delamination at the sensor zone***

Therefore, the simulation results showed that embedding of sensor can have influence on the stress-strain state of specimen, and the most critical factor is interlaminar stresses at the sensor's edges which can cause delamination also observed during experiment. This fact makes it necessary to take it into account at the design of structures with self-sensing capabilities.

Influence of PZT sensors embedment on their artificial damage detection capabilities

CFRP composite panels with integrated PZT sensors

In order to verify how the technology of sensors integration with the structure can impact the performance of PZT sensors in damage detection of composite structures, two CFRP panels (44 cm x 17 cm) has been designed and manufactured. Three type of PZT sensors integration with the structure has been used:

- immersion of sensors in the symmetry plane of the specimen (Panel 1);
- immersion of sensors in a "technological layer" on the surface of the specimen (Panel 2);
- adhesive bonding of sensors to the specimen surface (Panel 1 and Panel 2).

Due to electrical properties of CFRP, a special GFRP coating of PZT sensors has been developed. Cross sections of the two CFRP panels are schematically presented in Fig. 95 and Fig. 96 and the scheme of the panels with indication of sensors positioning is presented in Fig. 97.

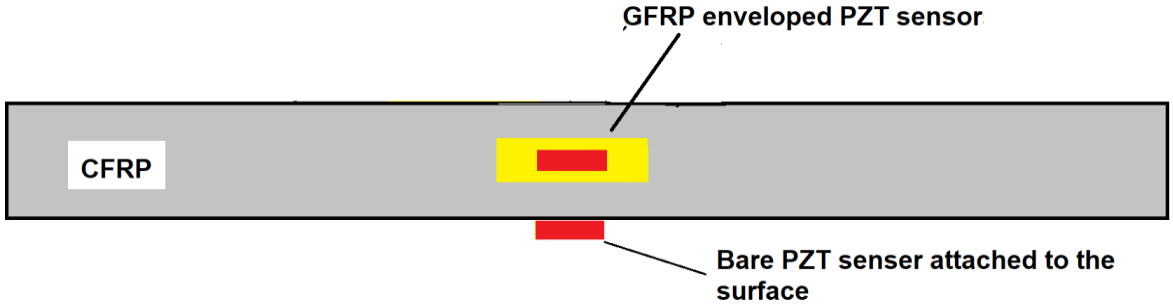

Figure 95. *Cross section of specimen with PZT embedded in the mid-plane and attached to the surface (Panel 1)*

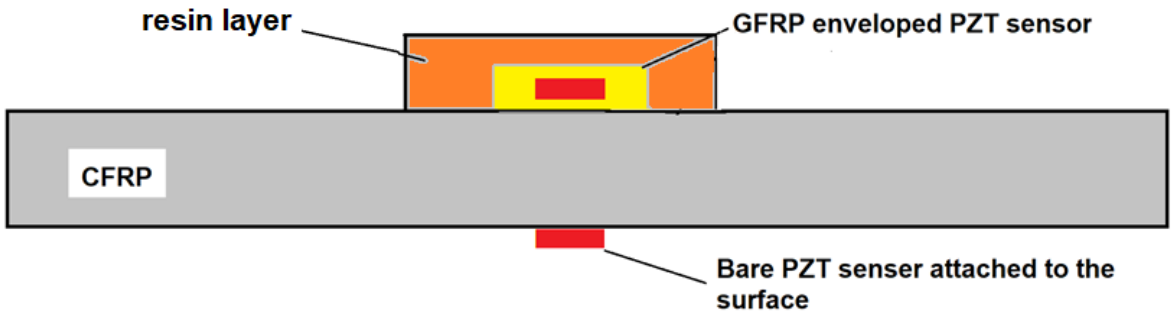

Figure 96. *Cross section of specimen with PZT embedded in surface technological layer and attached to the surface (Panel 2)*

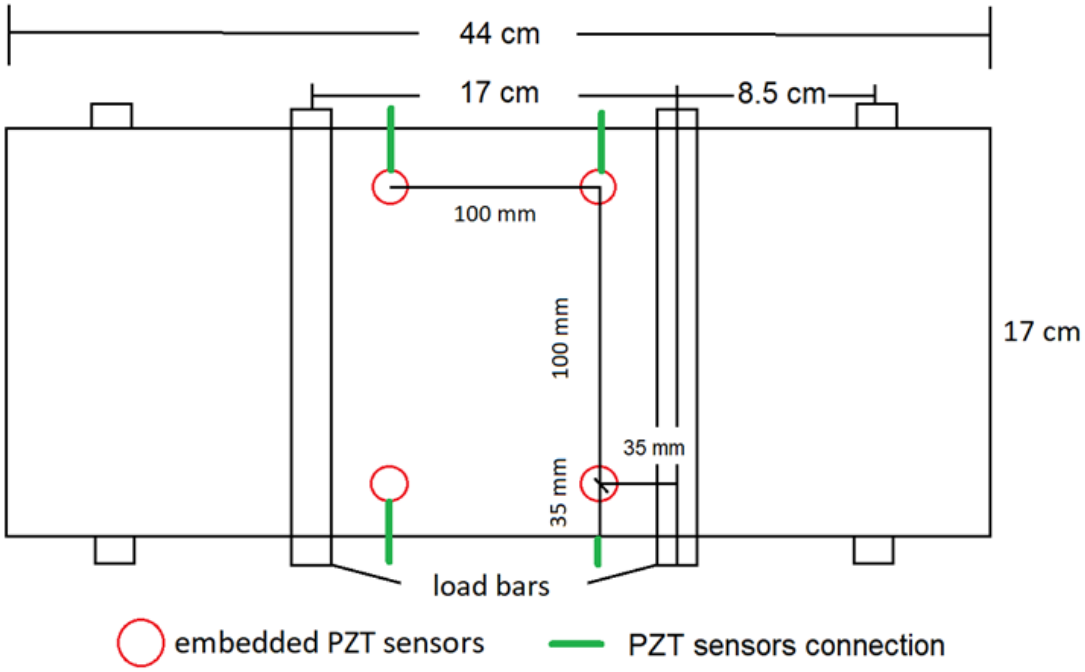

Figure 97. *Scheme of the panels with indication of sensors position and load bars*

Immersion of sensors may improve acoustic coupling between sensors and the structure, therefore it may also improve their performance in damage detection. Also, sensors embedding should have positive effect on their durability, since additional coating lowers the risk of mechanical damage. Contrary, a sensor

embedded in the internal structure of a composite can be considered as a point of stress concentration, adversely affecting the strength of a given component. Therefore two different techniques were proposed for sensors embedding and applied on the two panels:

- immersion of sensors in the symmetry plane of the panel during manufacturing process leads to potentially the strongest improvement of acoustic coupling between sensors and the structure, however it may have negative impact on mechanical properties of the structure;
- immersion of sensors in a “technological layer” near the surface of the specimen may improve acoustic coupling between sensors and the structure and has little or no effect on mechanical performance of the structure.

Both ways of sensor integration provide protection of sensors and improve their durability.

PZT sensors adhesively bonded to panels’ surface were also used in order to compare the two techniques with a common approach to sensors integration in the structure. The two CFRP panels were equipped with two independent PZT networks each composed of 4 single layer PZT discs SMD05T04R111 [1] (Fig. 99, Fig. 99).

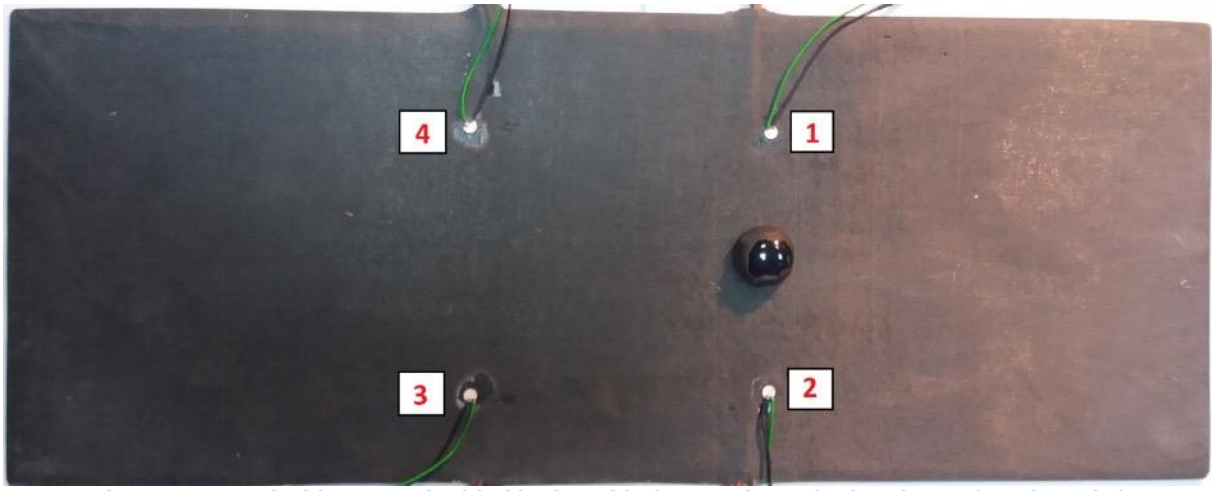

Figure 98. ***Panel with PZT embedded in the mid-plane and attached to the surface (Panel 1)***

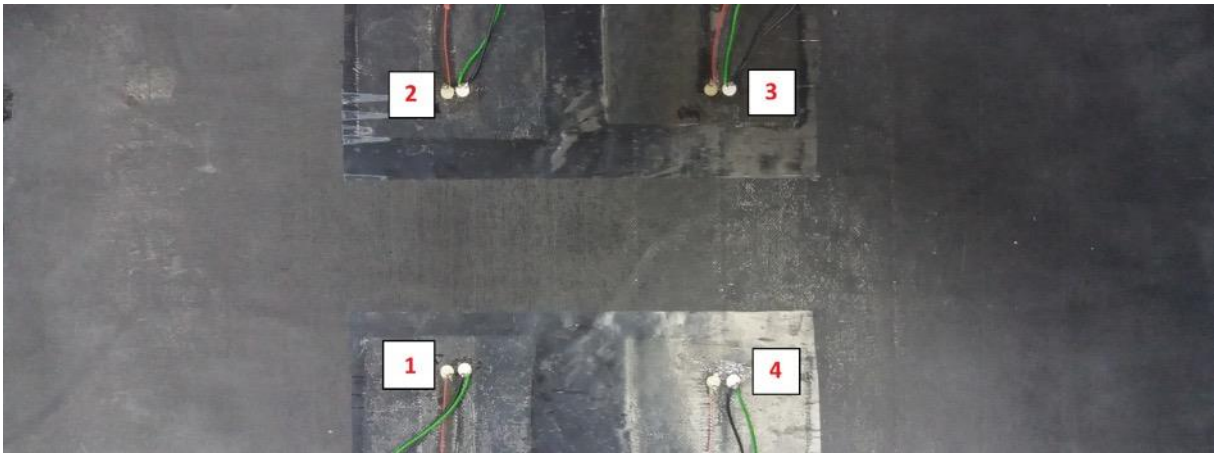

Figure 99. ***Panel with PZT embedded in technological layer and attached to the surface (Panel 2)***

Performance of embedded PZT sensors in artificial damage detection with use of guided waves approach

Pulsed excitation of PZT sensors

An artificial damage has been used as an initial test of damage detection capabilities of embedded PZT sensors.

The damage has been simulated by a mass attached to the specimen surface at predefined positions (Fig. 98):

- on each of the sensing paths, i.e. paths joining a pair of sensors, (1-2, 2-3, 3-4, 1-4);
- in the panel centre (path 1-3, 2-4).

Short burst excitation of PZT actuators has been applied for damage detection. The following set of parameters have been used for PZT excitation:

- excitation frequency: 150, 200, 250 [kHz];
- excitation duration: 3, 8 periods;
- excitation window: Hanning.

An example of the excitation signal is presented in Fig. 100. Elastic waves excited by PZT actuator were received by other PZT sensors of the network, an example of received signal is presented in Fig. 101.

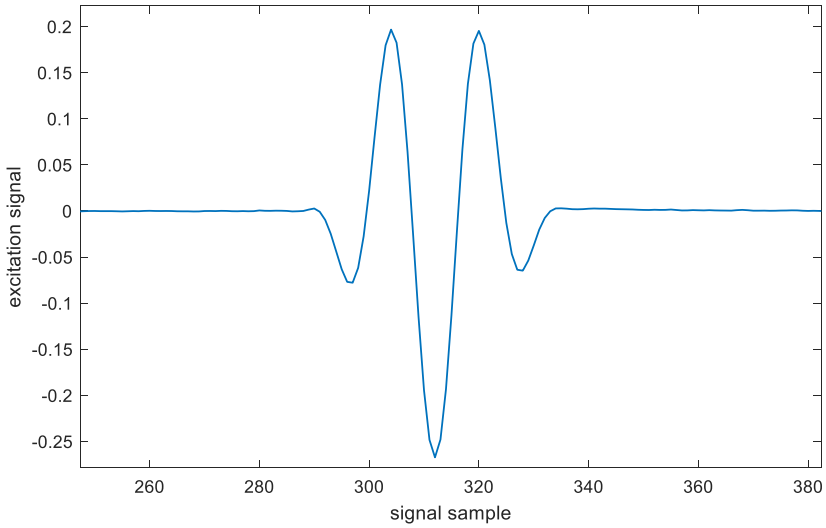

Figure 100. ***An example of signal used for PZT excitation (frequency: 150 kHz, duration: 3 periods)***

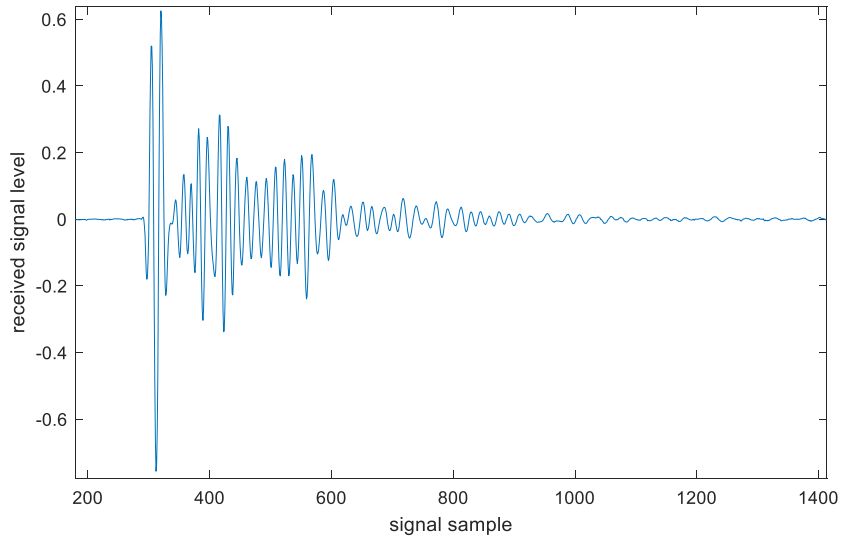

Figure 101. ***An example of signal received by PZT sensor***

Series of measurements have been performed according to the following scheme:

- for a given configuration of artificial damage signals were acquired for embedded and surface attached PZT networks independently;
- data was acquired for every combination of the excitation parameters;

- data was acquired for every sensing path, i.e. pairs of PZT transducers (actuator – receiver) of the network;
- the same excitation signal was applied for structure embedded and surface attached sensors.

For data acquisition PAQ16000D device has been used [2]. Series of measurements were performed for every configuration of artificial damage. Also, two series of reference measurements, without damage presence, in the beginning (before artificial damage was introduced) and at the end of the experiment (after removing artificial damage) have been acquired.

The first of the two acquired reference signals has been adopted as the so called baseline, which is used for signal change detection. The following signal characteristic, i.e. Damage Index (DI), was adopted for signal change assessment:

$$DI(g,s) = 1 - r_{f_{gs}^{env}, f_{gs,b}^{env}} \quad (1)$$

where $r_{f_{gs}^{env}, f_{gs,b}^{env}}$ denotes correlation coefficient between the envelope of the baseline signal $f_{gs,b}^{env}$ acquired for a given pair *g*, *s* of PZT transducers and the envelope of the actual signal f_{gs}^{env} acquired for the same pair of sensors.

Based on the other set of reference measurements, acquired at the end of the experiment reference values of Damage Indices DI_{ref} were obtained. For other series of measurements, i.e. acquired under damage presence, relative DIs values:

$$DI_{rel}(g,s) = {DI(g,s)}\Big/{DI_{ref}(g,s)} \quad (2)$$

were considered, instead of bare values given by the Eq. 1, for easier interpretation of the results.

For assessment of the efficiency of the system it is important to compare indications obtained for damaged state of the structure to indications caused by other factors. In the study, for a given position of artificial damage, relative DIs obtained for the sensing paths for which at least one of the constituent sensor was located far from the damage were considered as barely influenced by damage. In the case shown in Fig. 102, sensing path the most influenced by damage is 1-2 and barely influenced sensing paths are 1-4, 2-3, 3-4. DIs obtained for sensing paths located with respect to damage similar to 1-3, 2-4 were not considered in the study.

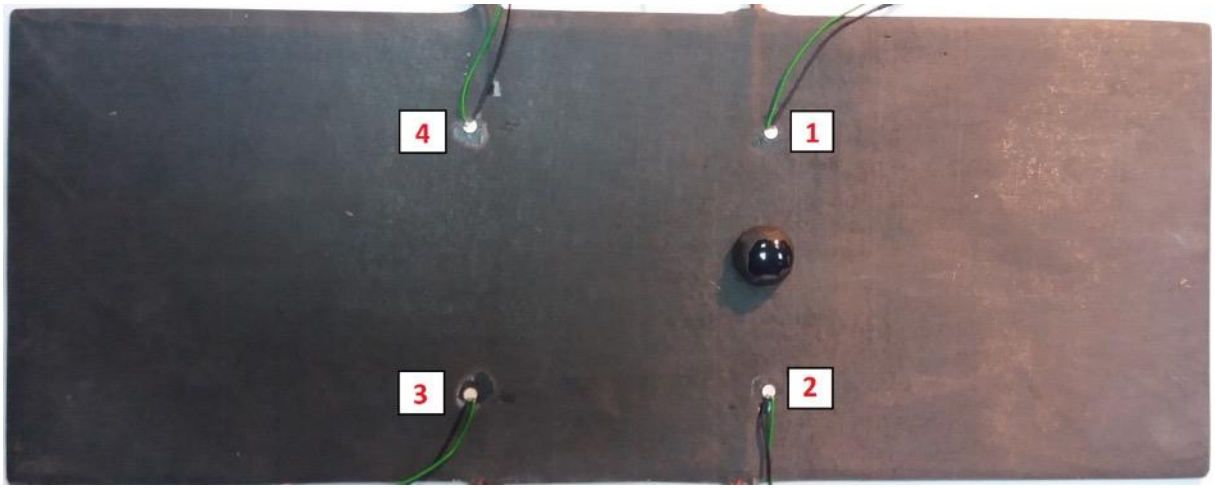

Figure 102. ***An example of artificial damage location***

Based on data collected for all configurations of artificial damage, two sets of relative DIs values for every configuration of the excitation parameters were considered: the set of DIs DI_{rel}^{dam} obtained for sensing paths most influenced by damage (as 1-2 in Fig. 102) and the set DI_{rel}^{other} obtained for sensing

paths which were much less influenced by damage. Based on the set DI_{rel}^{other}, the upper 95% confidence level CI^{other} of non damage related values of DIs has been established. If values DI_{rel}^{dam} are significantly greater than CI^{other}, then damage can be detected and localized within the network with high confidence.

In figures below, the ratio between median value of DI_{rel}^{dam} and confidence level CI^{other} is shown for the panel with sensors embedded in the mid-plane (Fig. 103) and immersed in a technological layer on the panel surface (Fig. 104).

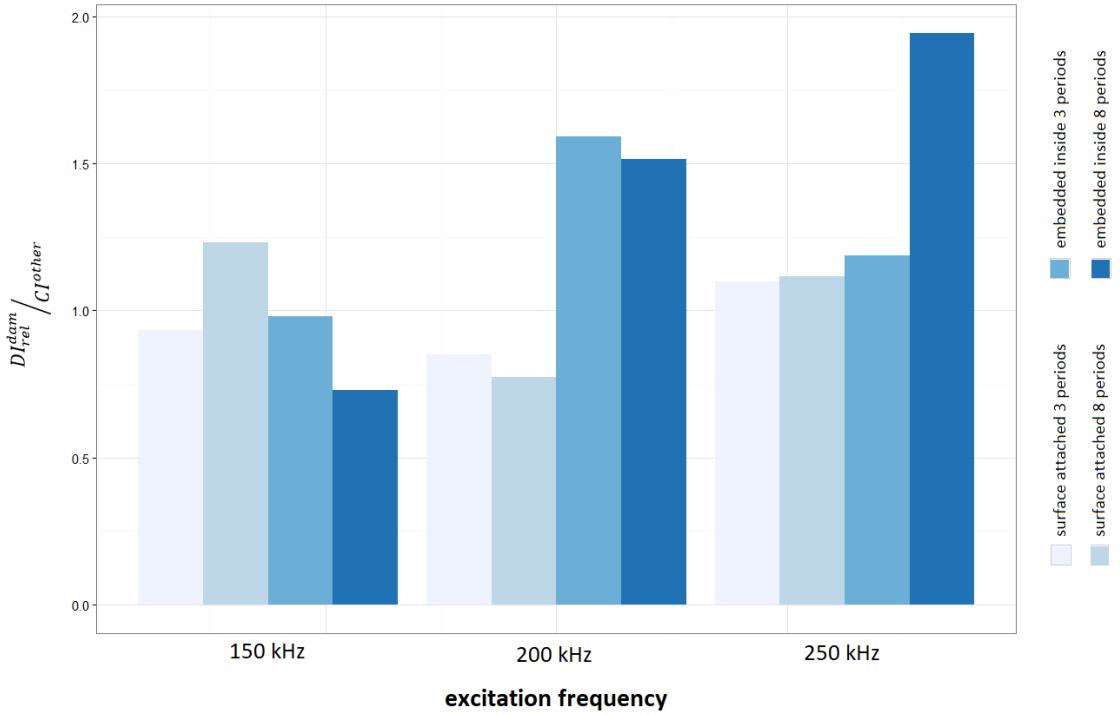

Figure 103. *Comparison of DIs values obtained for panel with PZT sensors embedded in the mid-plane (Panel 1)*

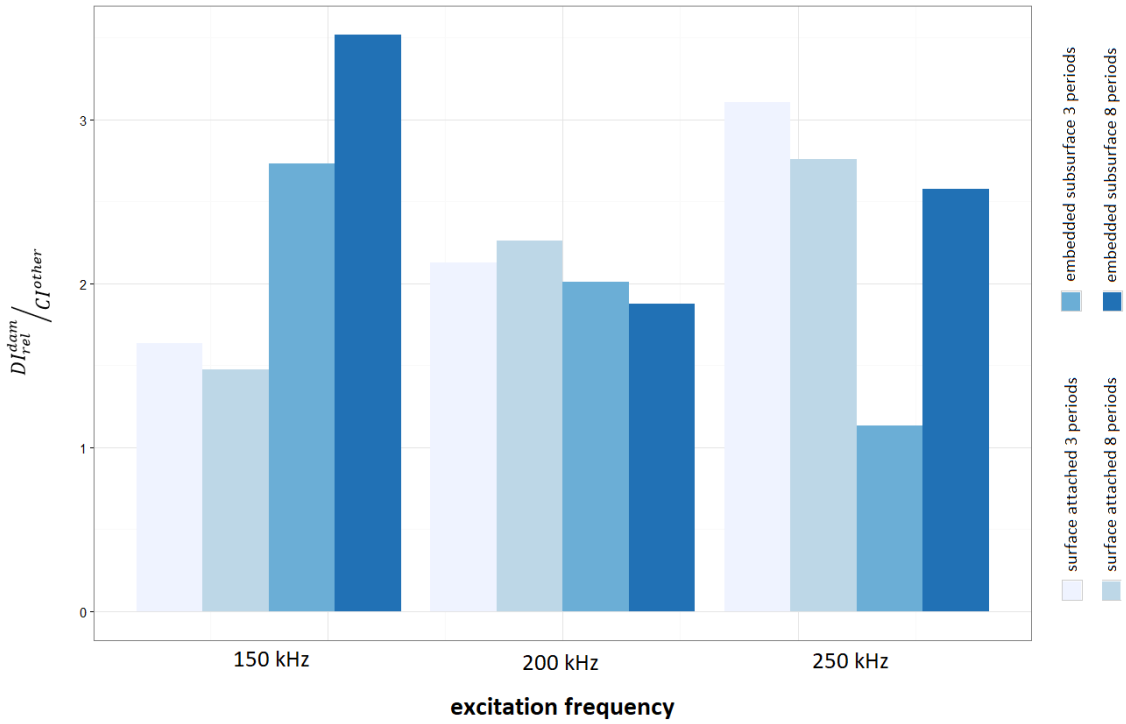

Figure 104. *Comparison of DIs values obtained for panel with PZT sensors immersed in a technological layer on the surface (Panel 2)*

Differences in damage detection capabilities of PZT sensors can be observed for the two panels. For PZT sensors attached to the surface of Panel 1 (Fig. 103), median value of DI_{rel}^{dam} is comparable or less than confidence interval CI^{other} , whereas for Panel 2 the ratio $DI_{rel}^{dam}/CI^{other}$ is significantly greater than 1 for surface attached PZT sensors for all the parameters of the excitation (Fig. 104). This is probably related to structural differences of the two panels. In both cases, improvement of damage detection capabilities for embedded PZT sensors can be observed for different frequency of the excitation:

- for sensors embedded in the mid-plane (Panel 1) the ratio between median value of DI_{rel}^{dam} and confidence level CI^{other} increased by 87% and 96% for 3 and 8 periods of excitation duration respectively at 200 kHz;
- for sensors embedded in technological layer (Panel 2) the ratio between median value of DI_{rel}^{dam} and confidence level CI^{other} increased by 67% and 138% for 3 and 8 periods of excitation duration respectively at 150 kHz.

For other excitation frequencies, incidental changes of damage detection capabilities between embedded and surface attached PZT sensors can be observed, however only for particular duration of the excitation.

Steady excitation of PZT sensors

Damage detection capabilities of embedded and surface attached sensors have been also investigated with use of a variant of Electromechanical Impedance (EMI) approach, called Transfer Impedance (TI) method [3]. In that case PZT actuator is excited with stable sinusoidal voltage. Due to Linear Time Invariant (LTI) systems theory, if a sinusoidal voltage U_{in} is applied to PZT actuator, then the voltage signal U_{out} on the receiver, induced by elastic waves, is also sinusoidal and has the same frequency as U_{in}. Fig. 105 presents an example of signals obtained for PZT sensors receiving elastic waves excited in the structure by PZT actuator excited with sinusoidal voltage.

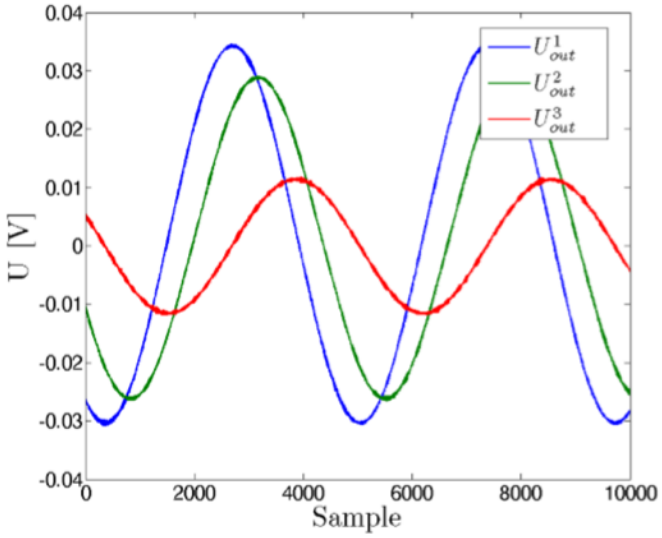

Figure 105. ***Example of signal received by PZT sensors for sinusoidal excitation of PZT***

Therefore the ratio, called the transfer function:

$$TF = \frac{U_{out}}{U_{in}} \quad (3)$$

does not depend on time and can be written in complex form as:

$$TF(\omega)=\frac{U_{out}}{U_{in}}=\frac{|U_{out}|e^{i\omega t+\varphi(\omega)}}{|U_{in}|e^{i\omega t}}=|TF(\omega)|e^{i\varphi(\omega)}\ , \qquad (4)$$

where $|TF(\omega)|$, $\varphi(\omega)$ denote respectively – the amplitude ratio and the phase difference between output and input signals for a given frequency. For damage detection the following Damage Indices (DIs) can be considered:

$$DI(\omega)=\frac{TF(\omega)}{TF_0(\omega)}=\frac{|TF(\omega)|}{|TF_0(\omega)|}e^{i(\varphi(\omega)-\varphi_0(\omega))} \qquad (5)$$

where $TF(\omega)$, $TF_0(\omega)$ denote transfer function based on signals acquired for a given state of the structure and obtained for the reference signals respectively. For structure assessment, it is not necessary to use a single DI calculated at a given frequency. DIs behaviour obtained for a range of frequencies can be better suited for damage detection and classification. For undamaged structure, the DIs should be concentrated in the vicinity of the point *1+i0* in the complex plane, irrespectively of the frequency of the excitation. If damage is present, it can change the output voltage amplitude or its phase, therefore DIs should diverge from the point *1+i0*.

For PZT actuators excitation sinusoidal voltage was applied with the amplitude of 80V peak-to-peak in the frequency range 200 – 350 kHz with 5 kHz step. For both panels transducer no 1 was used as actuator and other sensors of the network as receivers of elastic waves. The damage was simulated by artificial mass attached to the surface on sensing paths 1-2, 1-3, 1-4 (Fig. 98, Fig. 99). As for short burst PZT excitation, the measurements were performed for every artificial damage position and two series of measurements were collected without damage presence, in the beginning and at the end of the experiment.

For structure assessment, 60% of DIs data obtained for a given sensing path, contained in the nearest neighbourhood of estimated median value, were considered. In Fig. 106, Fig. 107 the data corresponding to damaged and undamaged state of the structure for both panels are presented. Unstable behaviour of channel corresponding to sensor no 2 was noticed for Panel 2, therefore only data obtained for sensing paths 1-3 and 1-4 are considered.

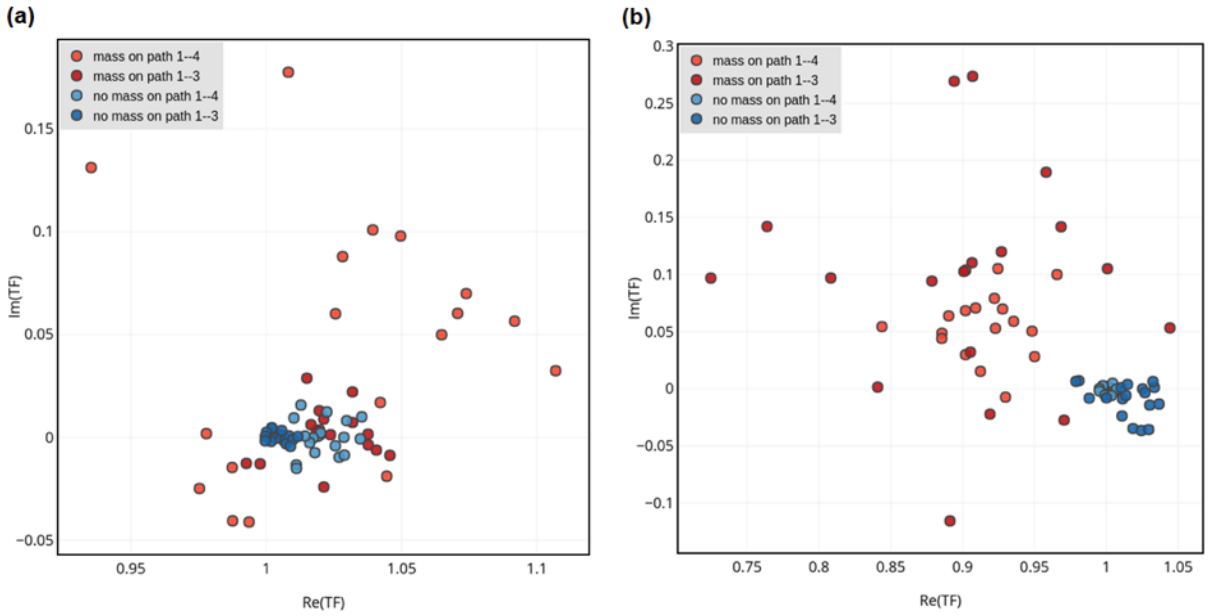

Figure 106. ***Damage Indices obtained for panel 1: (a) surface attached sensors, (b) sensors embedded in the mid-plane (Panel 1)***

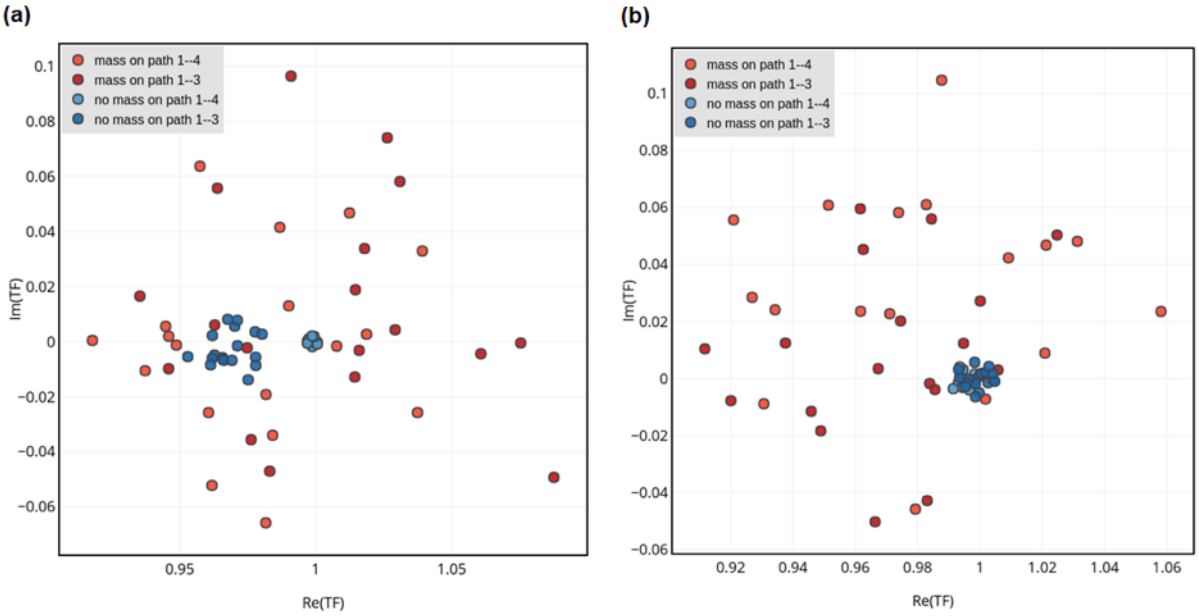

Figure 107. ***Damage Indices obtained for panel 2: (a) surface attached sensors, (b) subsurface embedded sensors (Panel 2)***

Data obtained for surface attached sensors under damage presence are centred around point *1+i0*, where data for undamaged state of the structure are located (Fig. 106a, Fig. 107a) only spread of the data is different for the two states of the structure. Therefore it is hard to detect artificial damage based on surface attached PZT sensors. For embedded sensors, the data obtained for damaged state of the structure are shifted from the point 1+i0 and the reference data (Fig. 106b, Fig. 107b), therefore it is possible to differentiate between the two states of the structure based on DIs values.

The separation of data corresponding to damaged and undamaged state of the structure is better visible for sensors embedded in the mid-plane. The separation of data corresponding to damaged and undamaged state of the structure can be quantified by using Hotelling's T-squared distribution (T2) [4]. It is used for statistical testing of difference between means of multivariate random samples. Higher values of T2 distribution obtained for two groups of multivariate data indicate more significant separation of the two groups. In Fig. 108 values of T2 distribution calculated for DIs obtained for the embedded sensors are presented.

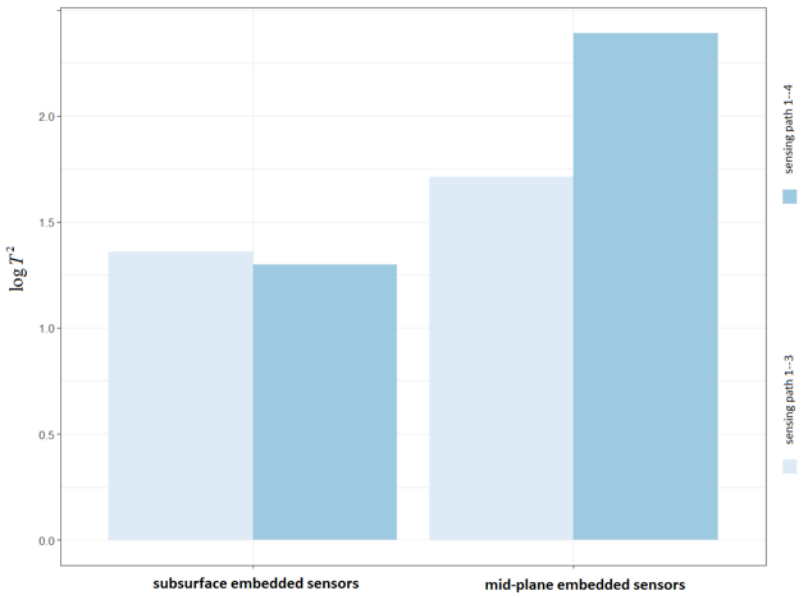

Figure 108. ***Values of T2 statistics obtained for two types of sensors embedding***

Data separation between damaged and undamaged state of the structure was higher for sensors embedded in the mid-plane for both sensing paths. Therefore for this technology of sensors integration with the structure it is possible to achieve better damage detection capabilities with use of Transfer Impedance approach.

References

[1] https://www.steminc.com/PZT/en/piezo-disc-transducer-450-khz

[2] http://www.ec-systems.pl/en/paq-16000d.html

[3] M. Dziendzikowski, P. Niedbala, A. Kurnyta, K. Kowalczyk, K. Dragan, *Structural health monitoring of a composite panel based on PZT sensors and a Transfer Impedance framework*. Sensors, 18(5), 2018, p. 1521.

[4] L. Mujica, J. Rodellar, A. Fernandez, A. Güemes, *Q-statistic and T2-statistic PCA-based measures for damage assessment in structures*. Struct. Health Monit. 2011, 10, p. 539–553.

3.5.4. Summary of the feasibility study and dissemination of the results

Based on identified gaps of SHM technology and demands of aerospace industry, a topic of feasibility study has been established, corresponding to Partners areas of expertise and experience. The main results of joint effort of EU and UA Partners within the Pilot Project 3.1. b are the following:

1. It is possible to apply EMA acoustic emission system developed by NASU-PEWI for composite structures monitoring.
2. Two technologies of PZT sensors integration with composite structures (i.e. *smart structures*) have been developed within the Pilot Project.
3. Both technologies provides protection of PZT sensors which should significantly improve sensors durability.
4. Embedment of sensors in the internal structure of composite is related with slight reduction of shear and flexural strength of the material. Admissibility of this technology of sensors integration depends on particular application and should be related to aircraft component design assumptions.
5. Both the developed technologies of sensors integration improve significantly damage detection capabilities of SHM technology.

The joint effort allowed to bridge some gaps in identified state-of-the-art status of SHM technology by cooperation of EU and UA Partners. Based on experience gained during joint cooperation of EU and UA institutions in the AeroUA project, UA Partners can have significant role in development and application of SHM technology in the aerospace industry, in particular in the following areas:

- development of SHM systems for aerospace structures (also composite) based on Acoustic Emission method;
- design, development and testing of smart composite structures equipped with sensor network technologies providing self-sensing capabilities
- modelling behaviour of smart structures with use of Finite Element Method;
- application and testing of SHM technologies in flight on large scale structures, e.g. Antonov aircrafts.

The abovementioned topics are of great importance for further development of SHM technology and for perspectives of its widespread application in aerospace industry.

Two abstracts of the Pilot Project 3.1.b results have been accepted for oral presentation at the 9th EASN conference in Athens, September 3-6, 2019. The abstracts are provided below.

Techniques for PZT transducers integration with composite structures for enhanced structural health monitoring capabilities

Neha Chandarana[1], Krzysztof Dragan[2,3], Michal Dziendzikowski[2,3], Marina Shevtsova[4], Fedir Gagauz[4], Constantinos Soutis[1]

1 I-Composites Lab, School of Materials, University of Manchester, Manchester M1 3NJ, UK
2 Air Force Institute of Technology, ul. Ks. Boleslawa 6, 01-494 Warszawa, Poland
3 Technology Partners, Pawińskiego 5A, 02-106 Warszawa, Poland
4 National Aerospace University "KhAI", 17 Chkalova str., Kharkiv, Ukraine

*Corresponding author, email address: krzysztof.dragan@itwl.pl

Application of guided waves excited by a network of PZT transducers integrated with a given structure is one of the promising approaches to Structural Health Monitoring (SHM). The performance of a SHM system based on PZT network is a vast area of research including: technology of sensors manufacturing and optimization of their working parameters, development of dedicated electronic units or signal processing methods which would allow for reliable structure assessment. One of the factors which may have significant impact on damage detection capabilities of SHM system based on PZT transducers as well as its durability is technique of sensors integration with a monitored structure.

For composites, beside the possibility of the transducers attachment to a surface of an element, also immersing of PZTs into their internal structure is possible. In the paper three different techniques of sensors integration with CFRP composite structures are presented and the influence of PZT transducers embedding on mechanical properties of the structure is assessed. Furthermore capabilities of structure monitoring is compared for the different techniques of sensors integration. In particular comparison of the efficiency of structure integrated sensors in debonding or impact damage detection as well as damage propagation monitoring with use of acoustic emission signals propagation is delivered in the paper.

Keywords: Structural Health Monitoring of composite structures, PZT transducers, impact damage detection

Active and passive damage monitoring in composites using embedded piezoelectric sensors

Neha Chandarana[1], Kanokporn Tangthana-umrung[1], Marina Shevtsova[2], Fedir Gagauz[2], Krzysztof Dragan[3,4], Michal Dziendzikowski[3,4], Constantinos Soutis[5]

[1]i-Composites Lab, School of Materials, University of Manchester, Manchester, UK
[4]Kharkiv Aviation Institute, KhAI, 17 Chkalova str., Kharkiv, Ukraine
[2]Air Force Institute of Technology, ul. Ks. Boleslawa 6, 01-494 Warsaw, Poland
[3]Technology Partners, Pawińskiego 5A, 02-106 Warsaw, Poland
[5]Aerospace Research Institute, University of Manchester, Manchester, UK

Reliable damage detection and monitoring of composite materials is necessary in facilitating their widespread use in the aerospace industry. The use of active and passive ultrasonic methods is widely accepted for the detection of damage in composites. The anisotropic nature of composites makes identification of different damage mechanisms, such as matrix cracking, delamination, and fibre breakage, more complex to predict and to analyse. The layered structure of composites lends itself to the integration of sensors, which can be used for damage

monitoring. Piezoelectric disc sensors are particularly attractive, due to their low cost, small size, and ability to be used for both the transmission and reception of guided waves. Guided waves can be excited in the structure by two main methods: (i) passive acoustic emission waves, emitted when the structure undergoes a change in response to loading, (ii) active guided waves, transmitted within a network of sensors for on-demand structural health assessment.

In the present work, two carbon fibre/epoxy composite laminates are instrumented with piezoelectric disc sensors, embedded at different through-thickness levels. Glass fibre envelopes isolate the sensors from the surrounding conductive material. Passive and active methods are used to detect and locate damage arising as a result of impact, and progressive damage during flexural loading. A comparison is made between the datasets obtained from embedded and surface mounted sensors, to assess their ability in detecting the damage.

Keywords: structural health monitoring, acoustic emission, guided waves, composite materials, piezoelectric sensors

Also, two papers based on the results obtained within Pilot Project 3.1.b are being prepared which will be submitted to the selected international journals, e.g:

- MDPI Materials (IF 2.972) - https://www.mdpi.com/journal/materials;
- MDPI Journal of Composites Science - https://www.mdpi.com/journal/jcs;
- IOP Smart Materials and Structures (IF 3.543) - https://iopscience.iop.org/journal/0964-1726/page/about-the-journal;
- Sage Journal of Intelligent Material Systems and Structures (IF 2.582) - https://uk.sagepub.com/en-gb/eur/journal/journal-intelligent-material-systems-and-structures.

4. Progress with respect to WP3 performance indicators

Work Package (High-Level Objective)	Performance indicators	Amount achieved by the end of the project	Target by end of project (M36)
WP3. EU-UA aviation research knowledge transfer pilot projects ***(High-Level Objective 3)***	• No. of short term staff exchanges about advanced design of aerospace composite structures	17	> 8
	• No. of trainings on advanced design of aerospace composite structures	24	> 5
	• No. of short term staff exchanges about aerospace composite structural health monitoring system	58	> 8
	• Feasibility study on aerospace composite structural health monitoring system	1	1

Completed visits:

- 11-12.10.2016, Hamburg - AERO-UA Project Kick-off Meeting
- 10.12.2016, Manchester - Meeting between KhAI and UoM, as part of a visit funded by the British Council in Ukraine
- 19-20.04.2017, Kyiv - AERO-UA Project Meeting, tour of Antonov
- 21.04.2017, Kyiv - UoM representative visited NASU institutes: Frantsevich Institute for Problems of Materials Science, Pisarenko Institute for Problems of Strength, Paton Electric Welding Institute
- 3-4.07.2017, Manchester - Working Meeting hosted by UoM
- 21-22.09.2017, Warsaw - AERO-UA Project Meeting, visit to ITWL, WZL-4, Warsaw University of Technology
- 29.05-1.06.2018, Kharkiv - AERO-UA Project Meeting and visit to KhAI lab
- 18-25.11.2018, Manchester - “Composites in Action” workshop
- 4-7.12.2018, Toulouse - AERO-UA Project Meeting;
- 24-26.04.2019, Zaporizhia - AERO-UA Project Meeting
- 1-2.09.2019, Athens - AERO-UA Final Project Meeting